A Thesis for the Degree of Doctor of Philosophy

Genomic and Functional Analyses of EnvZ/OmpR Two-Component System Modulating Virulence and Antibiotic Resistance of *Salmonella enterica* Serovar Enteritidis

살모넬라 엔테리티디스균의 병원성 및 항생제 내성을 조절하는 EnvZ/OmpR two-component system 의 유전적 특성 및 기능 연구

August, 2022

Duhyun Ko

Department of Agricultural Biotechnology

The Graduate School

Seoul National University

Genomic and Functional Analyses of EnvZ/OmpR Two-Component System Modulating Virulence and Antibiotic Resistance of *Salmonella enterica* Serovar Enteritidis

살모넬라 엔테리티디스균의 병원성 및 항생제 내성을 조절하는 EnvZ/OmpR two-component system 의 유전적 특성 및 기능 연구

지도교수 최 상 호

이 논문을 농학박사학위논문으로 제출함

2022 년 5 월

서울대학교 대학원

농생명공학부

고 두 현

고두현의 박사학위논문을 인준함

2022 년 6 월

위 원 장 _____(인)

부위원장 _____(인)

위 원 _____(인)

위 원 _____(인)

위 원 _____(인)

Abstract

Genomic and Functional Analyses of EnvZ/OmpR Two-Component System Modulating Virulence and Antibiotic Resistance of *Salmonella enterica* Serovar Enteritidis

Duhyun Ko

Department of Agricultural Biotechnology

The Graduate School

Seoul National University

Pathogenic bacteria encounter various environmental conditions during their infection cycle. Under certain environments, genetic mutations occur naturally and often enhance bacterial survival and virulence. In the present study, the function of specific genetic mutation in the *envZ* gene, which encodes a sensor kinase of EnvZ/OmpR two-component system, has been identified in a food-borne pathogen *Salmonella enterica* serovar Enteritidis. A phylogenetic analysis of the *S.* Enteritidis strains showed that 8 strains of *S.* Enteritidis isolated in South Korea, including FORC_075 and FORC_078, have almost identical genome sequences. Interestingly, however, the abilities of FORC_075 to form biofilms and red, dry, and rough (RDAR)

colonies were significantly impaired, resulting in phenotypic differences among the 8 strains. Comparative genomic analyses revealed that one of the non-synonymous single nucleotide polymorphisms (SNPs) unique to FORC_075 has occurred in *envZ*. The SNP in *envZ* leads to an amino acid change from Pro248 (CCG) in other strains including FORC_078 to Leu248 (CTG) in FORC_075. Allelic exchange of *envZ* between FORC_075 and FORC_078 identified that the SNP in *envZ* is responsible for the impaired biofilm- and RDAR colony-forming abilities of *S.* Enteritidis. Biochemical analyses demonstrated that the SNP in *envZ* significantly increases the phosphorylated status of OmpR in *S.* Enteritidis and alters the expression of the OmpR regulon. Phenotypic analyses further identified that the SNP in *envZ* decreases motility of *S.* Enteritidis but increases its adhesion and invasion to both human epithelial cells and murine macrophage cells. In addition, survival under acid stress is also elevated by the SNP in *envZ*. Altogether, these results suggest that the natural occurrence of the SNP in *envZ* could contribute to phenotypic diversity of *S.* Enteritidis, possibly improving its fitness and pathogenesis. Meanwhile, little is known about the role of EnvZ/OmpR in antibiotic resistance, except that it regulates the expression of OmpC and OmpF, two outer membrane porins (OMPs) permeable to small hydrophilic antibiotics. To determine the role of EnvZ/OmpR in antibiotic resistance, two mutant strains of *S.* Enteritidis expressing different phosphorylated status of OmpR were first generated. The mutant strains showing high and low cellular level of phosphorylated OmpR (OmpR-P) represent active and inactive

states of EnvZ/OmpR, respectively. Interestingly, it was found that resistance to various antibiotics, especially β-lactams, in *S.* Enteritidis is elevated by the active state of EnvZ/OmpR. Transcriptome analysis newly discovered that the active state of EnvZ/OmpR induces a differential expression of multiple OMP genes besides *ompC* and *ompF*, including SEN1522, SEN2875, *ompD*, and *ompW*. Biochemical analyses demonstrated that OmpR alters the OMP composition in *S.* Enteritidis by directly activating SEN1522 and SEN2875 but repressing *ompD* and *ompW*. Non-canonically, a high cellular level of OmpR caused by the active state of EnvZ/OmpR is required for the regulation of the four OMP genes. In particular, phosphorylation of OmpR is not necessary for the repression of *ompD* and *ompW*. Phenotypic analysis revealed that among the four OMP genes, the decreased expression of *ompD*, in addition to *ompF*, is responsible for the EnvZ/OmpR-mediated resistance to β-lactams in *S.* Enteritidis. Notably, EnvZ/OmpR specifically responds to β-lactams and provides *S.* Enteritidis with benefits for survival upon exposure to the antibiotics. Taken to together, these results suggest that EnvZ/OmpR remodels the OMP composition in response to β-lactams and thereby contributes to the enhanced resistance in *S*. Enteritidis to the antibiotics. In conclusion, this study demonstrated the phenotypic diversity of *S.* Enteritidis attributed to specific genetic mutation in *envZ* and the mechanism by which the active state of EnvZ/OmpR improves antibiotic resistance in *S.* Enteritidis.

Keywords: *Salmonella enterica* serovar Enteritidis, EnvZ/OmpR two-component system, SNP, Phenotypic diversity, Virulence, Antibiotic resistance

Student number: 2019-36715

Contents

List of Figures

List of Tables

Chapter I.

Background

I-1. *Salmonella enterica* serovar Enteritidis

Salmonella enterica is a Gram-negative, rod-shaped, and motile bacterium with peritrichous flagella, which belongs to *Enterobacteriaceae*. *S. enterica* is divided into six subspecies identified by DNA-DNA hybridization: subsp. *enterica* (I), subsp. *salamae* (II), subsp. *arizonae* (IIIa), subsp. *diarizonae* (IIIb), subsp. *houtenae* (IV), and subsp. *indica* (VI) (Achtman et al., 2012). *S. enterica* subsp. *enterica* (I) is highly associated with infections in human and warm-blooded animals, while the other five subspecies of *S. enterica* are usually isolated from cold-blooded animals and environments (Baumler et al., 1998; Brenner et al., 2000). *S. enterica* is also classified into more than 2,600 different serovars by a Kauffman-White method which identifies serologic variations of somatic (O) and flagellar (H) antigens, and the majority of the *S. enterica* serovars belongs to *S. enterica* subsp. *enterica* (I) (Brenner et al., 2000; Kauffmann, 1966).

S. enterica is a major food-borne pathogen worldwide. The *S. enterica* serovars differ in their host range and the ability to cause diseases, called salmonellosis. Based on the symptoms of salmonellosis, the *S. enterica* serovars are divided into typhoidal *Salmonella* and non-typhoidal *Salmonella* (NTS). Typhoidal *Salmonella* including *S. enterica* serovar Typhi and *S. enterica* serovar Paratyphi A is a human-restricted pathogen that causes enteric fever, an invasive disease leading to about 136,000 deaths globally in 2017 (Stanaway et al., 2019). In contrast, NTS which comprises

most of the *S. enterica* serovars has a broad host range and usually causes mild gastroenteritis. However, some NTS strains are also responsible for the invasive diseases inducing bacteremia and systemic infections (Gal-Mor et al., 2014). It has been reported that the NTS strains cause 93.8 million illnesses with 155,000 deaths each year worldwide (Majowicz et al., 2010).

Among the NTS, *S. enterica* serovar Enteritidis is one of the frequently isolated serovars in many countries, accounting for most cases of human salmonellosis (Braden, 2006). Infection by *S.* Enteritidis usually occurs through the ingestion of contaminated food products. Because *S.* Enteritidis has a superior ability to survive in egg white compared with other *S. enterica* serovars, eggs are the most important source for its transmission to humans (De Vylder et al., 2013; Sher et al., 2021). Upon ingested, *S.* Enteritidis encounters extremely acidic condition at the stomach. The survived pathogen adheres to the intestinal epithelial cells and invades them by promoting bacterial-mediated endocytosis (Ohl & Miller, 2001). When the epithelial barrier is disrupted, *S.* Enteritidis is engulfed by phagocytic cells such as macrophages and dendritic cells. Within the phagocytic cells, *S.* Enteritidis forms *Salmonella*-containing vacuoles (SCVs), a niche to evade the immune responses and successfully replicate (Steele-Mortimer, 2008). As the infected phagocytic cells migrate to other organs, the pathogen is disseminated, resulting in systemic infection (Ohl & Miller, 2001). These pathological features of *S.* Enteritidis infection are multifactorial and complex phenomena requiring numerous virulence factors to

interact with host cells.

I-1-1. Virulence factors of *S*. Enteritidis

Fimbriae

Fimbriae are filamentous polymeric proteins located at the bacterial surface (Mol & Oudega, 1996). In general, *S.* Enteritidis carries 13 fimbrial gene clusters (*csg*, *bcf*, *lpf*, *peg*, *saf*, *sef*, *stb*, *std*, *ste*, *stf*, *sth*, *sti*, and *fim*) which consist of more than 4 genes encoding fimbrial subunits, chaperones, and regulatory proteins. *S.* Enteritidis uses fimbriae to interact with specific receptor of host cells, which results in adhesion and colonization (Rehman et al., 2019). For example, FimH binds to glycoprotein 2 of M cell, a modified intestinal cell found in mucosa-associated lymphoid tissue, leading to efficient invasion of *S. enterica* (Ohno & Hase, 2010). In addition, the fimbrial structure are important for bacterial aggregation and biofilm formation (Rehman et al., 2019).

Type III secretion systems (T3SSs)

T3SS is a needle-like apparatus that translocates effector proteins into the cytosol of host cells. *S.* Enteritidis has two T3SSs, T3SS-1 and T3SS-2, which are encoded by *Salmonella* pathogenicity island-1 (SPI-1) and SPI-2, respectively. T3SS-1 and T3SS-2 function at different times during the course of infection. T3SS-1 is activated

upon contact with host cell and essential for *S.* Enteritidis to invade intestinal epithelial cells and to induce inflammation (Gerlach & Hensel, 2007). The effector proteins translocated through T3SS-1 such as SopE, SopB, and SipA interact with Rho-family GTPases, leading to actin cytoskeletal disruption and bacterial internalization (Boyle et al., 2006; Gerlach & Hensel, 2007). SopB also activates chloride secretion of the epithelial cells, inducing diarrhea (Norris et al., 1998). Furthermore, SipA promotes not only actin polymerization but also transepithelial migration of leukocytes, leading to intestinal inflammation (Wall et al., 2007).

T3SS-2 is activated inside the phagocytic cells and translocates effector proteins to form and maintain SCVs (Gerlach & Hensel, 2007). SpiC is the first reported effector protein translocated by T3SS-2 to inhibit formation of phagolysosome (Uchiya et al., 1999). The SseF and SseG proteins interact with each other and contribute to *Salmonella*-induced filaments (Sifs) formation as well as intracellular replication (Deiwick et al., 2006). Accordingly, T3SS-2 of *S.* Enteritidis plays a critical role in the development of systemic infection.

Magnesium uptake systems

Magnesium (Mg^{2+}), the second-most abundant cation in living cells, is an essential micronutrient as a cofactor for many enzymatic reactions (Flatman, 1991). After phagocytosis, macrophages lower the Mg^{2+} concentration of the phagosome to inhibit bacterial growth (Blanc-Potard & Groisman, 2021). To overcome this

nutritional deprivation inside the phagosome, *S.* Enteritidis has several magnesium transporters: CorA, MgtA, and MgtB. CorA is the primary Mg^{2+} channel expressed constitutively, and its energy source for Mg^{2+} transport is a membrane potential (Groisman et al., 2013). The *corA* mutant of *S. enterica* shows decreased invasion and intracellular replication and attenuated virulence in mouse model (Papp-Wallace et al., 2008). MgtA and MgtB are P-type ATPases which obtain energy from ATP hydrolysis for Mg^{2+} uptake (Groisman et al., 2013). The expression of *mgtA* and *mgtB* is inducible in response to low Mg^{2+} concentration (Snavely et al., 1991). MgtB is a specific Mg^{2+} uptake system of *S. enterica*, encoded by the *mgtCB* operon located in SPI-3.

I-1-2. Antibiotic resistance of *S.* Enteritidis

The discovery of antimicrobial agents to treat infections by pathogenic microorganisms is one of the greatest advances of the 20th century (Katz & Baltz, 2016). Especially, antibiotics enable the development of modern medical approahces including organ transplantation and cancer management (Munita & Arias, 2016). Because antibiotics inhibit bacterial growth, antibiotic resistance is a natural and inevitable consequene. However, misuses and abuses of antibiotics have accelerated the emergence of bacteria resistant to multiple antibiotics (French, 2010). As a result, antibiotic reisistance has now been considered as one of the biggest threats to public health (Lushniak, 2014).

Bacteria exhibit three types of antibiotic resistance: intrinsic, acquired, and adaptive resistance (Fernandez & Hancock, 2012). Intrinsic resistance is a natural property of bacterial species to resist particular antibiotics (Fernandez & Hancock, 2012). For example, *Vibrio cholerae* carries unique lipid A modification system in its chromosome responsible for polymyxin B resistance (Herrera et al., 2014). In addition, the efflux pump systems conserved in *Pseudomonas aeruginosa* contribute to resistant to multiple antibiotics including tetracycline and erythromycin (Masuda et al., 2000). Acquired resistance is provided by acquisition of genetic materials or spontaneous mutations, which allows antibiotic susceptible bacteria to be resistant (Fernandez & Hancock, 2012). Finally, adaptive resistance is a temporary property that decreases the antibiotic susceptibility of bacteria by altering the expression of genes upon exposure to specific environments (Fernandez & Hancock, 2012). Through these three types of antibiotic resistance, *S.* Enteritidis has developed diverse mechanisms to survive in the antibiotic treatments. This section will describe three major mechanisms by which *S.* Enteritidis shows antibiotic resistance.

Enzymatic inactivation of antibiotics

One of the mechanisms of antibiotic resistance is a production of enzymes that inactivate antibiotics. As many antibiotics have chemical bonds susceptible to hydrolytic cleavage, several enzymes have evolved to hydrolyze the bonds and eliminate the antibiotic activity. β-lactamase is the most well-known enzyme

hydrolyzing β-lactam ring of antibiotics belonging to penicillins and cephalosporins (Poole, 2004). Some enzymes transfer chemical moieties to the antibiotics rather than degrade them, inducing steric hindrance and decreasing the access of antibiotics to their intracellular targets (Munita & Arias, 2016). For example, aminoglycoside acetyltransferases transfer an acetyl group to the aminoglycosides that bind to ribosomal proteins and inhibit protein biosynthesis. Due to this structural modification, the binding affinity of aminoglycosides to the ribosomal proteins is reduced, and thus the antibiotic activity is also reduced (Disney, 2012).

Alteration of target sites for antibiotics

To inhibit bacterial growth, antibiotics target essential cellular processes including DNA replication and cell wall and protein biosynthesis. Fluoroquinolones interfere DNA replication by inhibiting the activity of DNA gyrase encoded by *gyrA* and *gyrB* and topoisomerase IV encoded by *parC* and *parE* (Blondeau, 2004). Chromosomal mutations in these genes possibly decrease affinity of gyrase or topoisomerase IV to fluoroquinolones, leading to antibiotic resistance (Kumar et al., 2015). In addition, mutations in 16S rRNA confer resistance to several antibiotics belonging to aminoglycosides (Recht & Puglisi, 2001).

Limitation of influx in antibiotics

For Gram-negative bacteria, outer membrane is the first-line of defense against the

influx of toxic compounds including antibiotics. Indeed, vancomycin is inactive against Gram-negative bacteria because the antibiotic can not penetrate their outer membrane (Fernandes et al., 2017). Hydrophilic antibiotics such as β-lactams, tetracyclines, and some fluoroquinolones enter into the cells through the water-filled outer membrane porins (OMPs). Thus, reduction in the number of porins or modification of porin selectivity leads to a decrease in outer membrane permeability and thus reduces the influx in antibiotics. OmpC and OmpF are the most abundant OMPs in *S. enterica*. Accordingly, mutations in *ompC* and *ompF* increase bacterial resistance to β-lactams or fluoroquinolones (Futoma-Koloch et al., 2019; Medeiros et al., 1987). In addition to OMPs, overexpression of efflux pump systems, which consist of outer membrane protein TolC and inner membrane and periplasmic proteins such as AcrAB, confers mutidrug resistance to many bacteria (Blair et al., 2015).

I-1-3. Two-component systems of *S.* Enteritidis

Two-component system (TCS) is a signal transduction system of bacteria to sense and respond to various environments. TCS consists of a sensor kinase and its cognate response regulator. Generally, the sensor kinase contains the dimerization and histidine phosphotransfer (DHp) domain and catalytic and ATP binding (CA) domain, and the response regulator contains an N-terminal receiver domain and a C-terminal DNA-binding domain (Capra & Laub, 2012). Under the specific environmental

condition, a histidine residue conserved in the DHp domain of sensor kinase is autophosphorylated, and a phosphoryl group is transferred to an aspartate residue conserved in the receiver domain of response regulator (Capra & Laub, 2012). When the response regulator is phosphorylated, its conformation is changed, facilitating DNA-binding and gene regulation. Mostly, the sensor kinase has both kinase and phosphatase activities to modulate the phosphorylated status of its cognate response regulator (Gao & Stock, 2009). TCSs play important roles in cellular processes such as nutrient uptake, chemotaxis, pathogenesis, and antibiotic resistance. This section will describe several TCSs and their physiological roles in *S.* Enteritidis.

SsrA/SsrB

SsrA/SsrB TCS consists of sensor kinase SsrA and response regulator SsrB. The *ssrA* and *ssrB* genes are located in the SPI-2 region, and thus, uniquely found in *S. enterica*. Although environmental signals directly sensed by SsrA are still unknown, it is speculated that SCV-like condition is possibly associated with the activation of SsrA/SsrB TCS (Lee et al., 2000). SsrB is a NarL/FixJ-type of response regulator. The C-terminal domain of SsrB comprises four α-helices containing helix-turn-helix DNA binding domain (Carroll et al., 2009). SsrB regulates the expression of the SPI-2 genes as well as other non-SPI-2 genes but acquired by horizontal gene transfer (Worley et al., 2000). Furthermore, recent studies suggested that SsrB represses the

SPI-1 genes, playing a key transcriptional regulator that helps transition of *S. enterica* from extracellular to intracellular lifestyle (Perez-Morales et al., 2017).

EnvZ/OmpR

EnvZ/OmpR TCS consists of sensor kinase EnvZ and response regulator OmpR. The *envZ* and *ompR* genes are widely conserved in many bacteria including *Escherichia coli, S. enterica,* and *Yersinia* species. EnvZ/OmpR has been reported to regulate the expression of two OMPs OmpC and OmpF in response to the external osmolarity (Slauch et al., 1988). High osmolarity induces conformational change of EnvZ to be more stable, leading to increased autophosphorylation of EnvZ and phosphotransfer to OmpR (Wang et al., 2012). In *S. enterica,* the EnvZ activity is also responsive to changes in pH (Mideros-Mora et al., 2020). OmpR has a winged helix-turn-helix motif in its DNA-binding domain and interacts more with the phosphate backbone of DNA than with specific bases. Thus, OmpR recognizes DNA regions less specifically than other response regulators (Quinn et al., 2014). This property would allow OmpR to act as a global regulator that controls various phenotypes of *S.* Enteritidis. For example, OmpR directly activates the *ssrA* and *ssrB* genes which are critical for the pathogenesis of *S. enterica* (Lee et al., 2000). OmpR also controls biofilm formation of *S. enterica* by regulating the expression of *csgD* which encodes

a master regulator of curli and cellulose biosynthesis (Gerstel et al., 2006; Gerstel et al., 2003).

PhoQ/PhoP

PhoQ/PhoP TCS consists of sensor kinase PhoQ and response regulator PhoP. It has been demonstrated that PhoQ is activated by a variety of environmental signals similar to intracellular conditions, such as low Mg^{2+} concentration, mildly acidic pH, and the presence of cationic antimicrobial peptides (CAMPs) (Groisman et al., 2021). PhoP is a OmpR/PhoB-type of response regulator with a winged helix-turn-helix motif for DNA binding. PhoP activates the expression of Mg^{2+} transporters MgtA and MgtB, and thus mutant of *phoP* shows impaired growth in extremely low Mg^{2+} concentration (Vescovi et al., 1996). PhoP also activates the *pagP* gene related to lipopolysaccharide modification and confers resistance to CAMPs (Groisman, 2001). Recently, it has been reported that PhoQ senses high osmolarity independently of EnvZ and induces phosphorylation of PhoP, accelerating the resumption of bacterial growth under the osmotic stress (Yuan et al., 2017).

I-2. Objective of this study

Acquisition of accessory genes as well as spontaneous chromosomal mutation such as single nucleotide polymorphism (SNP) have a great potential to lead to the evolution of pathogenic bacteria. With the development of next-generation sequencing technology, a number of whole genome sequences of bacteria have been accumulated, which enables comprehensive identification of genetic variations within the bacterial species. A major food-borne pathogen *S.* Enteritidis usually induces mild gastroenteritis but often causes systemic infection which should be treated with antibiotics. Genomic analysis of *S.* Enteritidis would provide insights into the genetic basis for its ability to survive and develop food-borne diseases. In the present study, I compared whole genome sequences of the *S.* Enteritidis strains and found a unique non-synonymous SNP in the *envZ* gene encoding the sensor kinase of EnvZ/OmpR two-component system. I demonstrated that the SNP in *envZ* is a key genetic determinant for virulence-related phenotypes of *S.* Enteritidis including biofilm formation, motility, infectivity to host cells, and acid resistance. Furthermore, it was found that the *envZ* gene carrying the SNP enhances the antibiotic resistance of *S.* Enteritidis, and its molecular mechanism was identified.

Chapter II.

An SNP in *envZ* potentially leading to phenotypic diversity of *Salmonella enterica* serovar Enteritidis

II-1. Introduction

Bacterial pathogens have evolved genetically to adapt to various environmental conditions (Arber, 2000). Many studies have revealed that genetic mutations occur naturally in bacteria for their optimal fitness and successful pathogenesis during the course of infection (Lieberman et al., 2011; Yang et al., 2011). Horizontal gene transfer, one of the possible mechanisms for genetic evolution, results in the acquisition of novel genes and enables non-pathogenic bacteria to be pathogenic (Kelly et al., 2009). Alternatively, small genetic changes such as single nucleotide polymorphisms (SNPs) have potential to modify the function of original genes and to induce phenotypic diversity of pathogens, leading to their pathoadaptive evolution (Sokurenko et al., 1999). Along with the rapid development of next-generation sequencing technologies, comparative genomic analysis has discovered a number of SNPs occurring in many pathogenic bacteria including *Clostridium difficile*, *Mycobacterium tuberculosis,* and *Salmonella enterica* (Collery et al., 2017; Mikheecheva et al., 2017; Scaltriti et al., 2015). However, studies on the association of each SNP with bacterial pathogenesis are still limited.

S. enterica serovar Enteritidis is a major food-borne pathogen, which causes diseases ranging from mild gastroenteritis to severe systemic infection (Authority et al., 2018; Chen et al., 2013). *Salmonella* has multiple two-

component systems to recognize diverse environmental changes and to respond appropriately (Capra & Laub, 2012). The EnvZ/OmpR two-component system is well-studied in *Salmonella*. The sensor kinase EnvZ phosphorylates itself and transfers the phosphoryl group to its cognate response regulator OmpR in response to specific environmental signals such as osmolarity and pH change (Chakraborty et al., 2017; Delgado et al., 1993; Wang et al., 2012). Phosphorylation induces conformational changes of OmpR, which enhances its DNA binding affinity (Head et al., 1998), and thus, the expression of the OmpR regulon is mostly dependent on the amount of phosphorylated OmpR (OmpR-P). The OmpR regulon includes *ompF* and *ompC*, which encode outer membrane porins, and regulation of their expression is well characterized. A low level of OmpR-P is enough to activate the transcription of *ompF*, but not of *ompC* (Aiba & Mizuno, 1990). In contrast, a high level of OmpR-P activates *ompC* transcription, while repressing *ompF* transcription (Aiba & Mizuno, 1990).

The EnvZ/OmpR two-component system also regulates virulence-related genes and plays an essential role in the pathogenesis of *Salmonella* (Dorman et al., 1989; Quinn et al., 2014). For example, the EnvZ/OmpR system controls the expression of *csgD*, which encodes a master regulator activating the biosynthesis of curli fimbriae and cellulose (Gerstel et al., 2003; Hammar et al., 1995; Romling et al., 2000). Curli fimbriae and cellulose are major biofilm

components and contribute to the development of a red, dry, and rough (RDAR) colony morphology (Austin et al., 1998; Romling, 2005; Solano et al., 2002). In addition, the EnvZ/OmpR system represses expression of flagellar genes such as *fljB* and *fliC*, which are associated with the motility of *Salmonella* (Xu et al., 2010). The EnvZ/OmpR system positively regulates the expression of *hilA*, encoding a major activator of virulence genes located in the *Salmonella* pathogenicity island 1 (SPI-1), and the expression of *ssrA* and *ssrB*, encoding a master activator of the SPI-2 genes (Ellermeier et al., 2005; Feng et al., 2003; Lee et al., 2000). The SPI-1 and SPI-2 encode type III secretion systems and enable the efficient invasion to host cells and intracellular replication (Galan, 1996; Groisman & Ochman, 1993, 1997; Shea et al., 1996). Furthermore, OmpR itself is an acid shock protein and regulates the expression of genes that are necessary for acid resistance (Bang et al., 2000; Chakraborty & Kenney, 2018; Chakraborty et al., 2015; Chakraborty et al., 2017).

In the present study, we conducted a phylogenetic analysis of 241 strains of *S.* Enteritidis and revealed that 8 strains isolated in South Korea, including FORC_075 and FORC_078, have almost identical genome sequences. Interestingly, however, distinct phenotypes were observed in FORC_075 which showed an impaired biofilm formation and a smooth and white (SAW) colony morphology. We identified that 9 non-synonymous SNPs have occurred exclusively in FORC_075, and one of which is in *envZ* resulting in an amino

acid change from Pro248 in other strains including FORC_078 to Leu248 in FORC_075. By exchanging the SNP allele in *envZ* between FORC_075 and FORC_078, we demonstrated that the SNP in *envZ* determines the biofilm formation and colony morphology. The SNP in *envZ* induces functional modification of EnvZ, increasing the cellular level of OmpR-P in *S.* Enteritidis and altering the expression of the OmpR regulon. Further phenotypic analyses revealed that the SNP in *envZ* decreases motility, but increases both adhesion and invasion to host cells and elevates survival under acid stress. Taken together, these results suggest that the natural occurrence of the SNP in *envZ* plays a critical role in differentiating the virulence-related phenotypes of *S.* Enteritidis and thus, contributes to its phenotypic diversity.

II-2. Materials and Methods

II-2-1. Strains, plasmids, and culture conditions

The strains and plasmids used in this study are listed in Table II-1. Unless otherwise noted, all strains were grown aerobically in Luria-Bertani (LB) medium at 37°C. When required, antibiotics were added to the medium at the following concentrations: ampicillin, 100 μg/ml; kanamycin, 100 μg/ml; chloramphenicol, 20 μg/ml. Bacterial growth was monitored spectrophotometrically at 600 nm (A_{600}).

Table II-1. Bacterial strains and plasmids used in this study

Strain or plasmid	Relevant characteristics[a]	Reference or source[b, c]
Bacterial strains		
S. Enteritidis		
FORC_007	Environmental isolate; Gm^s	MFDS
FORC_019	Clinical isolate; Gm^r	NCCP
FORC_051	Clinical isolate; Gm^r	MFDS
FORC_052	Clinical isolate; Gm^s	MFDS
FORC_056	Environmental isolate; Gm^r	MFDS
FORC_074	Clinical isolate; Gm^r	NCCP
FORC_075	Clinical isolate; Gm^r	NCCP
FORC_078	Clinical isolate; Gm^s	NCCP
FORC_078-*zirT*::*kan*	FORC_078 with *zirT::kan*; Gm^s; Km^r	This study
FORC_075-*envZ*::*cat*	FORC_075 with *envZ::cat*; Gm^r; Cm^r	This study
FORC_078-*envZ*::*kan*	FORC_078 with *envZ::kan*; Gm^s; Km^r	This study
FORC_075-$EnvZ_{L248P}$	FORC_075 with *envZ* encoding $EnvZ_{L248P}$; Gm^r	This study
FORC_078-$EnvZ_{P248L}$	FORC_078 with *envZ* encoding $EnvZ_{P248L}$; Gm^s	This study
ATCC 13076	Standard strain	Laboratory collection
ATCC 13076-$EnvZ_{P248L}$	ATCC 13076 with *envZ* encoding $EnvZ_{P248L}$	This study
envZ::*cat*	ATCC 13076 with *envZ*::*cat*	This study
ompR::*cat*	ATCC 13076 with *ompR*::*cat*	This study
ATCC 13076-$EnvZ_{H243A}$	ATCC 13076 with *envZ* encoding $EnvZ_{H243A}$	This study
ATCC 13076-$OmpR_{D55A}$	ATCC 13076 with *ompR* encoding $OmpR_{D55A}$	This study
Δ*ompR*	ATCC 13076 with Δ*ompR*	This study
Δ*ompR envZ*$_{P248L}$	ATCC 13076-$EnvZ_{P248L}$ with Δ*ompR*	This study

Δ*ompF*	ATCC 13076 with Δ*ompF*	This study
Δ*ompF envZ*$_{P248L}$	ATCC 13076-EnvZ$_{P248L}$ with Δ*ompF*	This study
ΔSEN1522	ATCC 13076 with ΔSEN1522	This study
ΔSEN2875	ATCC 13076 with ΔSEN2875	This study
Δ*ompD*	ATCC 13076 with Δ*ompD*	This study
Δ*ompD envZ*$_{P248L}$	ATCC 13076-EnvZ$_{P248L}$ with Δ*ompD*	This study
Δ*ompW*	ATCC 13076 with Δ*ompW*	This study
Δ*ompD* Δ*ompF*	ATCC 13076 with Δ*ompD* and Δ*ompF*	This study
Δ*ompR* Δ*ompD* Δ*ompF*	ATCC 13076 with Δ*ompR*, Δ*ompD*, and Δ*ompF*	This study
E. coli		
S17-1 λ*pir*	λ-*pir* lysogen; *thi pro hsdR hsdM*$^{+}$ *recA* RP4-2 Tc::Mu-Km::Tn7;Tp^{r} Sm^{r}; host for π-requiring plasmids	(Simon et al., 1983)
BL21(DE3)	*F*$^{-}$, *ompT*, *hsdS* (r$_{B}^{-}$, m$_{B}^{-}$), *gal dcm* (DE3)	Laboratory collection
Plasmids		
pKD46	P$_{BAD}$-*gam-beta-exo oriA101 repA101*^{ts}; Ap^{r}	(Datsenko & Wanner, 2000)
pKD3	FRT *cat* FRT PS1 PS2 *oriR6K*γ; Ap^{r} Cm^{r}	(Datsenko & Wanner, 2000)
pKD13	FRT *aph* FRT PS1 PS4 *oriR6K*γ; Ap^{r} Km^{r}	(Datsenko & Wanner, 2000)
pCVD442	Suicide vector; *oriR6K*γ *sacB oriT* of RP4; Ap^{r}	(Donnenberg & Kaper, 1991)
pDH1903	pCVD442 with *envZ* of FORC_078	This study
pDH1904	pCVD442 with *envZ* of FORC_075	This study
pET-28a(+)	His$_{6}$-tag fusion expression vector; Km^{r}	Novagen
pDH2003	pET-28a(+) with *ompR*; Km^{r}	This study
pDH1907	pCVD442 with *envZ*$_{H243A}$; Ap^{r}	This study

pDH1906	pCVD442 with $ompR_{D55A}$; Ap^r	This study
pDH2014	pCVD442 with Δ*ompR*; Ap^r	This study
pDH2107	pCVD442 with Δ*ompF*; Ap^r	This study
pDH2103	pCVD442 with ΔSEN1522; Ap^r	This study
pDH2015	pCVD442 with ΔSEN2875; Ap^r	This study
pDH2101	pCVD442 with Δ*ompD*; Ap^r	This study
pDH2110	pCVD442 with Δ*ompW*; Ap^r	This study
pJK1113	pKS1101 with *nptI*; Ap^r; Km^r	(Lim et al., 2014)
pDH2104	pJK1113 with wild-type *ompR*; Ap^r, Km^r	This study
pDH2108	pJK1113 with $ompR_{D55A}$; Ap^r, Km^r	This study
pRKΩlacZ	pRK415 derivative containing promoterless *lacZ*; Tc^r	(Park et al., 2006)
pDH2105	pRKΩlacZ with P_{ompR}; Tc^r	This study

[a]Gm^s, gentamicin-sensitive; Gm^r, gentamicin-resistant; Km^r, kanamycin-resistant; Cm^r, chloramphenicol-resistant; Tp^r, trimethoprim-resistant; Sm^r, streptomycin-resistant; Ap^r, ampicillin-resistant; Tc^r, tetracycline-resistant.

[b]MFDS, Ministry of Food and Drug Safety, https://www.mfds.go.kr/

[c]NCCP, National Culture Collection for Pathogens, http://www.cdc.go.kr/

II-2-2. Comparative genomic analysis

The 8 whole genome sequences of the *S.* Enteritidis strains, FORC_007, FORC_019, FORC_051, FORC_052, FORC_056, FORC_074, FORC_075, and FORC_078, were retrieved from the NCBI RefSeq database (https://www.ncbi.nlm.nih.gov/). Additionally, the 233 whole genome sequences, which were analyzed at "complete" and "chromosomal" levels and named as "*Salmonella enterica* subsp. enterica serovar Enteritidis" were retrieved from the NCBI RefSeq database. All accession numbers used in this study are listed in Table II-2. For average nucleotide identity (ANI) analysis, ANI values were calculated by the JSpecies program with the BLAST algorithm comparing 1,020-bp fragmented whole genome sequences of the 8 FORC strains (Richter & Rossello-Mora, 2009). For phylogenetic analysis, each genome of a total of 241 strains of *S.* Enteritidis was mapped to the genome of *S.* Enteritidis P125109 (reference genome) by the Snippy program (https://github.com/tseemann/snippy). The recombinant region was removed from the resulting alignment by the Gubbins program (Croucher et al., 2015), and then core SNPs were extracted by the SNP-sites program (Page et al., 2016). The extracted SNPs were used to calculate SNP distances between the *S.* Enteritidis strains by the snp-dists program (https://github.com/tseemann/snp-dists). A total of 7,154 SNP sites of 241 strains were used to construct a phylogenetic tree by the RAxML program with a gamma distribution and a general time-reversible model under 500 bootstrap repeats (Stamatakis, 2006).

For pangenome analysis, the whole genomes of the 8 FORC strains were annotated by the Prokka program (Seemann, 2014), and their pangenome was built by the Roary program (Page et al., 2015) using the resulting annotations. For SNP analysis, the whole genome sequences of FORC_007, FORC_019, FORC_051, FORC_052, FORC_056, FORC_074, and FORC_075 were aligned to that of FORC_078 by the NUCmer program (Kurtz et al., 2004). SNP positions were inferred by show-snps programs (Kurtz et al., 2004), and insertions and deletions were excluded. The effect of non-synonymous SNPs on protein function was predicted by the PROVEAN (Protein variation effect analyzer, http://provean.jcvi.org/) (Choi & Chan, 2015), SNAP2 (Screening for non-acceptable polymorphisms 2, https://www.rostlab.org/services/snap/) (Hecht et al., 2015), and SIFT (Sorting intolerant from tolerant, https://sift.bii.a-star.edu.sg/) (Sim et al., 2012) programs.

Table II-2. List of the *S.* Enteritidis strains in Figure II-1.

Name	Strain	Assembly accession number	Level	Region of isolation	Source of isolation
Salmonella enterica subsp. enterica serovar Enteritidis str. P125109	P125109	GCF_000009505.1	Complete Genome	Missing	Missing
Salmonella enterica subsp. enterica serovar Enteritidis str. 77-1427	77-1427	GCF_000280315.2	Complete Genome	USA:RI	Clinical
Salmonella enterica subsp. enterica serovar Enteritidis str. CDC_2010K_0968	CDC_2010K-0968	GCF_000329365.2	Complete Genome	USA:OH	Clinical
Salmonella enterica subsp. enterica serovar Enteritidis str. 18569	18569	GCF_000335875.2	Complete Genome	Mexico	Poultry
Salmonella enterica subsp. enterica serovar Enteritidis	Durban	GCF_000612325.1	Complete Genome	South Africa: Durban	Blood
Salmonella enterica subsp. enterica serovar Enteritidis str. EC20121175	EC20121175	GCF_000623055.1	Complete Genome	Canada: Manitoba	Chick Paper
Salmonella enterica subsp. enterica serovar Enteritidis str. EC20121176	EC20121176	GCF_000623075.1	Chromosome	Canada: Quebec	Food
Salmonella enterica subsp. enterica serovar Enteritidis str. EC20121178	EC20121178	GCF_000623095.1	Complete Genome	Canada: Quebec	Environmental-Chicken
Salmonella enterica subsp. enterica serovar Enteritidis str. EC20121179	EC20121179	GCF_000623115.2	Complete Genome	Canada: Quebec	Environmental-Quail
Salmonella enterica subsp. enterica serovar Enteritidis str. EC20121180	EC20121180	GCF_000623135.1	Complete Genome	Canada: Quebec	Environmental-Chicken
Salmonella enterica subsp. enterica serovar Enteritidis str. SA20093266	SA20093266	GCF_000623155.2	Chromosome	Canada: Ontario	Animal - Chicken-Feces
Salmonella enterica subsp. enterica	EC20110223	GCF_000623175.2	Chromosome	Canada: Ontario	Human- Mung

serovar Enteritidis str. EC20110223					Bean-Outbreak
Salmonella enterica subsp. enterica serovar Enteritidis str. EC20120005	EC20120005	GCF_000623195.2	Complete Genome	Canada: Ontario	Broiler
Salmonella enterica subsp. enterica serovar Enteritidis str. EC20120544	EC20120544	GCF_000623215.2	Chromosome	Canada: British Columbia	Food
Salmonella enterica subsp. enterica serovar Enteritidis str. EC20120548	EC20120548	GCF_000623235.2	Chromosome	Canada: British Columbia	Food
Salmonella enterica subsp. enterica serovar Enteritidis str. EC20120555	EC20120555	GCF_000623255.2	Chromosome	Canada: British Columbia	Food-Porcine
Salmonella enterica subsp. enterica serovar Enteritidis str. EC20110361	EC20110361	GCF_000623275.1	Complete Genome	Canada: Alberta	Human-Sporadic
Salmonella enterica subsp. enterica serovar Enteritidis str. EC20110360	EC20110360	GCF_000623295.1	Complete Genome	Canada: Alberta	Human-Sporadic
Salmonella enterica subsp. enterica serovar Enteritidis str. EC20110359	EC20110359	GCF_000623315.1	Complete Genome	Canada: Alberta	Human-Sporadic
Salmonella enterica subsp. enterica serovar Enteritidis str. EC20110358	EC20110358	GCF_000623335.1	Complete Genome	Canada: Alberta	Human-Sporadic
Salmonella enterica subsp. enterica serovar Enteritidis str. EC20110357	EC20110357	GCF_000623355.1	Complete Genome	Canada: Alberta	Human-Sporadic
Salmonella enterica subsp. enterica serovar Enteritidis str. EC20110356	EC20110356	GCF_000623375.1	Complete Genome	Canada: Alberta	Human-Outbreak
Salmonella enterica subsp. enterica serovar Enteritidis str. SA19981857	SA19981857	GCF_000623395.2	Complete Genome	Canada: Quebec	Animal - Avian
Salmonella enterica subsp. enterica serovar Enteritidis str. SA19982831	SA19982831	GCF_000623415.2	Chromosome	Canada: Quebec	Animal - Chicken-Environment Swab
Salmonella enterica subsp. enterica	SA19983126	GCF_000623435.2	Chromosome	Canada: Ontario	Animal - Chicken

serovar Enteritidis str. SA19983126					
Salmonella enterica subsp. enterica serovar Enteritidis str. SA19992322	SA19992322	GCF_000623455.2	Complete Genome	Canada: Quebec	Human-Stool
Salmonella enterica subsp. enterica serovar Enteritidis str. SA19994216	SA19994216	GCF_000623475.1	Complete Genome	Canada: Alberta	Animal - Porcine-Feces
Salmonella enterica subsp. enterica serovar Enteritidis str. SA20083456	SA20083456	GCF_000623495.2	Chromosome	Canada: Ontario	Animal - Chicken Broiler
Salmonella enterica subsp. enterica serovar Enteritidis str. SA20083636	SA20083636	GCF_000623515.2	Chromosome	Canada: Ontario	Environment - Litter/Manure
Salmonella enterica subsp. enterica serovar Enteritidis str. SA20084384	SA20084384	GCF_000623535.2	Chromosome	Canada: Ontario	Food
Salmonella enterica subsp. enterica serovar Enteritidis str. SA19930684	SA19930684	GCF_000623555.2	Chromosome	Canada: Ontario	Animal - Chicken
Salmonella enterica subsp. enterica serovar Enteritidis str. SA19942384	SA19942384	GCF_000623575.2	Chromosome	Canada: Ontario	Food - Turkey
Salmonella enterica subsp. enterica serovar Enteritidis str. SA19943269	SA19943269	GCF_000623595.2	Chromosome	Canada: Ontario	Food - Turkey
Salmonella enterica subsp. enterica serovar Enteritidis str. SA19960848	SA19960848	GCF_000623615.2	Complete Genome	Canada: Ontario	Animal - Chicken-Litter
Salmonella enterica subsp. enterica serovar Enteritidis str. SA19961622	SA19961622	GCF_000623635.2	Chromosome	Canada: British Columbia	Animal - Avian
Salmonella enterica subsp. enterica serovar Enteritidis str. SA19970510	SA19970510	GCF_000623655.2	Complete Genome	Canada: Quebec	Animal - Chicken-Environment Swab
Salmonella enterica subsp. enterica serovar Enteritidis str. SA19970769	SA19970769	GCF_000623675.2	Complete Genome	Canada: Quebec	Animal - Chicken-Egg
Salmonella enterica subsp. enterica	SA19971331	GCF_000623695.2	Chromosome	Canada: British	Animal - Avian

serovar Enteritidis str. SA19971331				Columbia	
Salmonella enterica subsp. enterica serovar Enteritidis str. SA19980677	SA19980677	GCF_000623715.2	Complete Genome	Canada: Quebec	Animal - Chicken-Environment Swab
Salmonella enterica subsp. enterica serovar Enteritidis str. SA19981522	SA19981522	GCF_000623735.2	Complete Genome	Canada: Quebec	Animal - Avian-Environment Swab
Salmonella enterica subsp. enterica serovar Enteritidis str. EC20090135	EC20090135	GCF_000623755.2	Chromosome	Canada: Ontario	Chicken
Salmonella enterica subsp. enterica serovar Enteritidis str. EC20090193	EC20090193	GCF_000623775.2	Chromosome	Canada: Ontario	Chicken
Salmonella enterica subsp. enterica serovar Enteritidis str. EC20090332	EC20090332	GCF_000623795.2	Chromosome	Canada: Ontario	Chicken
Salmonella enterica subsp. enterica serovar Enteritidis str. SA20090877	SA20090877	GCF_000623815.2	Chromosome	Canada: Saskatchewan	Food
Salmonella enterica subsp. enterica serovar Enteritidis str. SA20091739	SA20091739	GCF_000623835.2	Chromosome	Canada: Saskatchewan	Food
Salmonella enterica subsp. enterica serovar Enteritidis str. SA20093421	SA20093421	GCF_000623855.2	Chromosome	Canada: Ontario	Animal - Chicken
Salmonella enterica subsp. enterica serovar Enteritidis str. SA20093430	SA20093430	GCF_000623875.2	Chromosome	Canada: British Columbia	Animal - Chicken
Salmonella enterica subsp. enterica serovar Enteritidis str. SA20093538	SA20093538	GCF_000623895.2	Chromosome	Canada: Saskatchewan	Food
Salmonella enterica subsp. enterica serovar Enteritidis str. SA20093543	SA20093543	GCF_000623915.2	Chromosome	Canada: Saskatchewan	Food
Salmonella enterica subsp. enterica serovar Enteritidis str. SA20093784	SA20093784	GCF_000623935.2	Chromosome	Canada: British Columbia	Food

Salmonella enterica subsp. enterica serovar Enteritidis str. SA20093788	SA20093788	GCF_000623955.2	Chromosome	Canada: British Columbia	Food
Salmonella enterica subsp. enterica serovar Enteritidis str. SA20093950	SA20093950	GCF_000623975.2	Chromosome	Canada: Saskatchewan	Food
Salmonella enterica subsp. enterica serovar Enteritidis str. SA20093977	SA20093977	GCF_000623995.2	Chromosome	Canada: British Columbia	Animal - Chicken
Salmonella enterica subsp. enterica serovar Enteritidis str. SA20094079	SA20094079	GCF_000624015.2	Chromosome	Canada: Saskatchewan	Food
Salmonella enterica subsp. enterica serovar Enteritidis str. SA20094350	SA20094350	GCF_000624035.2	Chromosome	Canada: Ontario	Animal - Chicken Brooder
Salmonella enterica subsp. enterica serovar Enteritidis str. SA20094352	SA20094352	GCF_000624055.2	Complete Genome	Canada: Ontario	Animal - Chicken Broiler Growers
Salmonella enterica subsp. enterica serovar Enteritidis str. SA20094383	SA20094383	GCF_000624075.2	Chromosome	Canada: Ontario	Food
Salmonella enterica subsp. enterica serovar Enteritidis str. SA20094389	SA20094389	GCF_000624095.2	Chromosome	Canada: Ontario	Food
Salmonella enterica subsp. enterica serovar Enteritidis str. SA20094521	SA20094521	GCF_000624115.2	Chromosome	Canada: British Columbia	Food
Salmonella enterica subsp. enterica serovar Enteritidis str. SA20094642	SA20094642	GCF_000624135.2	Chromosome	Canada: Quebec	Animal - Chicken
Salmonella enterica subsp. enterica serovar Enteritidis str. EC20120916	EC20120916	GCF_000624155.2	Chromosome	Canada: Ontario	Animal-Chicken
Salmonella enterica subsp. enterica serovar Enteritidis str. EC20121177	EC20121177	GCF_000624175.1	Complete Genome	Canada: Ontario	Food
Salmonella enterica subsp. enterica serovar Enteritidis str. SA20092320	SA20092320	GCF_000624195.2	Chromosome	missing	Animal - Chicken
Salmonella enterica subsp. enterica serovar Enteritidis str. SA20094803	SA20094803	GCF_000624215.2	Chromosome	Canada: Ontario	Animal - Chicken-Fluff

Salmonella enterica subsp. enterica serovar Enteritidis str. SA20095309	SA20095309	GCF_000624235.2	Chromosome	Canada: Ontario	Environment - Water-River
Salmonella enterica subsp. enterica serovar Enteritidis str. SA20095440	SA20095440	GCF_000624255.1	Chromosome	Canada: Ontario	Animal - Chicken Growers
Salmonella enterica subsp. enterica serovar Enteritidis str. EC20110222	EC20110222	GCF_000624275.2	Chromosome	Canada: Ontario	Food- Mung Bean-Outbreak
Salmonella enterica subsp. enterica serovar Enteritidis str. EC20111514	EC20111514	GCF_000624295.2	Chromosome	Canada: Alberta	Animal-Chicken
Salmonella enterica subsp. enterica serovar Enteritidis str. EC20111515	EC20111515	GCF_000624315.2	Chromosome	Canada: Alberta	Animal-Chicken
Salmonella enterica subsp. enterica serovar Enteritidis str. EC20111554	EC20111554	GCF_000624335.2	Chromosome	Canada: British Columbia	Animal-Chicken
Salmonella enterica subsp. enterica serovar Enteritidis str. EC20111561	EC20111561	GCF_000624355.2	Chromosome	Canada: Ontario	Animal-Chicken
Salmonella enterica subsp. enterica serovar Enteritidis str. EC20111576	EC20111576	GCF_000624375.2	Chromosome	Canada: Ontario	Animal-Chicken
Salmonella enterica subsp. enterica serovar Enteritidis str. EC20120002	EC20120002	GCF_000624395.2	Complete Genome	Canada: Ontario	Broiler
Salmonella enterica subsp. enterica serovar Enteritidis str. EC20120003	EC20120003	GCF_000624415.2	Chromosome	Canada: Ontario	Cattle
Salmonella enterica subsp. enterica serovar Enteritidis str. EC20120007	EC20120007	GCF_000624435.2	Chromosome	Canada: Ontario	Broiler
Salmonella enterica subsp. enterica serovar Enteritidis str. EC20120213	EC20120213	GCF_000624455.2	Chromosome	Canada: British Columbia	Food
Salmonella enterica subsp. enterica serovar Enteritidis str. EC20120219	EC20120219	GCF_000624475.2	Chromosome	Canada: Quebec	Food
Salmonella enterica subsp. enterica serovar Enteritidis str. EC20120229	EC20120229	GCF_000624495.2	Chromosome	Canada: Saskatchewan	Food

Salmonella enterica subsp. enterica serovar Enteritidis str. EC20120240	EC20120240	GCF_000624515.2	Chromosome	Canada: British Columbia	Food
Salmonella enterica subsp. enterica serovar Enteritidis str. EC20120356	EC20120356	GCF_000624535.2	Chromosome	Canada: Ontario	Animal-Domestic Cattle
Salmonella enterica subsp. enterica serovar Enteritidis str. EC20120469	EC20120469	GCF_000624555.2	Chromosome	Canada: Ontario	Food
Salmonella enterica subsp. enterica serovar Enteritidis str. EC20120496	EC20120496	GCF_000624575.2	Chromosome	Canada: British Columbia	Food
Salmonella enterica subsp. enterica serovar Enteritidis str. EC20120497	EC20120497	GCF_000624595.2	Chromosome	Canada: British Columbia	Food
Salmonella enterica subsp. enterica serovar Enteritidis str. EC20120498	EC20120498	GCF_000624615.2	Chromosome	Canada: Saskatchewan	Food
Salmonella enterica subsp. enterica serovar Enteritidis str. EC20120505	EC20120505	GCF_000624635.2	Chromosome	Canada: British Columbia	Food
Salmonella enterica subsp. enterica serovar Enteritidis str. EC20120528	EC20120528	GCF_000624655.2	Chromosome	Canada: Nova Scotia	Food
Salmonella enterica subsp. enterica serovar Enteritidis str. EC20120994	EC20120994	GCF_000624675.1	Chromosome	Canada: Ontario	Food
Salmonella enterica subsp. enterica serovar Enteritidis str. EC20121004	EC20121004	GCF_000624695.1	Chromosome	Canada: Ontario	Food
Salmonella enterica subsp. enterica serovar Enteritidis str. EC20121541	EC20121541	GCF_000624715.1	Chromosome	Canada: Ontario	Food
Salmonella enterica subsp. enterica serovar Enteritidis str. EC20121542	EC20121542	GCF_000624735.2	Chromosome	Canada: Ontario	Food
Salmonella enterica subsp. enterica serovar Enteritidis str. EC20121671	EC20121671	GCF_000624755.2	Chromosome	Canada: Ontario	Food
Salmonella enterica subsp. enterica serovar Enteritidis str. EC20121672	EC20121672	GCF_000624775.2	Chromosome	Canada: Ontario	Food

Salmonella enterica subsp. enterica serovar Enteritidis str. EC20121689	EC20121689	GCF_000624795.2	Chromosome	Canada: Ontario	Food
Salmonella enterica subsp. enterica serovar Enteritidis str. SA20121703	SA20121703	GCF_000624815.2	Chromosome	Canada: Ontario	Food
Salmonella enterica subsp. enterica serovar Enteritidis str. EC20121744	EC20121744	GCF_000624835.2	Chromosome	Canada: British Columbia	Food
Salmonella enterica subsp. enterica serovar Enteritidis str. EC20121746	EC20121746	GCF_000624855.2	Chromosome	Canada: British Columbia	Food
Salmonella enterica subsp. enterica serovar Enteritidis str. EC20121748	EC20121748	GCF_000624875.2	Chromosome	Canada: British Columbia	Food
Salmonella enterica subsp. enterica serovar Enteritidis str. EC20121750	EC20121750	GCF_000624895.2	Chromosome	Canada: Ontario	Food
Salmonella enterica subsp. enterica serovar Enteritidis str. EC20121751	EC20121751	GCF_000624915.2	Chromosome	Canada: British Columbia	Food
Salmonella enterica subsp. enterica serovar Enteritidis str. EC20121753	EC20121753	GCF_000624935.2	Chromosome	Canada: British Columbia	Food
Salmonella enterica subsp. enterica serovar Enteritidis str. EC20120734	EC20120734	GCF_000624955.2	Chromosome	Canada: Ontario	Food
Salmonella enterica subsp. enterica serovar Enteritidis str. EC20120738	EC20120738	GCF_000624975.2	Chromosome	Canada: Ontario	Food
Salmonella enterica subsp. enterica serovar Enteritidis str. EC20120765	EC20120765	GCF_000624995.2	Chromosome	Canada: British Columbia	Animal-Chicken
Salmonella enterica subsp. enterica serovar Enteritidis str. EC20120773	EC20120773	GCF_000625015.2	Chromosome	Canada: Ontario	Food
Salmonella enterica subsp. enterica serovar Enteritidis str. EC20120774	EC20120774	GCF_000625035.2	Chromosome	Canada: Ontario	Food
Salmonella enterica subsp. enterica serovar Enteritidis str. EC20120775	EC20120775	GCF_000625055.2	Chromosome	Canada: Ontario	Food

Salmonella enterica subsp. enterica serovar Enteritidis str. EC20120776	EC20120776	GCF_000625075.2	Chromosome	Canada: Ontario	Food
Salmonella enterica subsp. enterica serovar Enteritidis str. EC20120917	EC20120917	GCF_000625095.2	Chromosome	Canada: Ontario	Animal-Chicken
Salmonella enterica subsp. enterica serovar Enteritidis str. EC20120918	EC20120918	GCF_000625115.2	Chromosome	Canada: Ontario	Animal-Chicken
Salmonella enterica subsp. enterica serovar Enteritidis str. EC20120925	EC20120925	GCF_000625135.2	Chromosome	Canada: Ontario	Animal-Domestic Cattle
Salmonella enterica subsp. enterica serovar Enteritidis str. EC20120927	EC20120927	GCF_000625155.2	Chromosome	Canada: Ontario	Animal-Chicken
Salmonella enterica subsp. enterica serovar Enteritidis str. EC20120963	EC20120963	GCF_000625175.2	Chromosome	Canada: Ontario	Food
Salmonella enterica subsp. enterica serovar Enteritidis str. EC20120968	EC20120968	GCF_000625195.2	Chromosome	Canada: Ontario	Food
Salmonella enterica subsp. enterica serovar Enteritidis str. EC20120969	EC20120969	GCF_000625215.2	Chromosome	Canada: Ontario	Food
Salmonella enterica subsp. enterica serovar Enteritidis str. EC20120970	EC20120970	GCF_000625235.2	Chromosome	Canada: Ontario	Food
Salmonella enterica subsp. enterica serovar Enteritidis str. EC20121812	EC20121812	GCF_000625255.2	Chromosome	Canada: British Columbia	Food
Salmonella enterica subsp. enterica serovar Enteritidis str. EC20121825	EC20121825	GCF_000625275.2	Chromosome	Canada: British Columbia	Food
Salmonella enterica subsp. enterica serovar Enteritidis str. EC20121826	EC20121826	GCF_000625295.2	Chromosome	Canada: British Columbia	Food
Salmonella enterica subsp. enterica serovar Enteritidis str. EC20121969	EC20121969	GCF_000625315.2	Chromosome	Canada: Ontario	Food
Salmonella enterica subsp. enterica serovar Enteritidis str. EC20121970	EC20121970	GCF_000625335.2	Chromosome	Canada: Ontario	Food

Salmonella enterica subsp. enterica serovar Enteritidis str. SA20090419	SA20090419	GCF_000625355.1	Chromosome	Canada: Ontario	Animal - Chicken
Salmonella enterica subsp. enterica serovar Enteritidis str. SA20090435	SA20090435	GCF_000625375.2	Chromosome	Canada: British Columbia	Animal - Chicken
Salmonella enterica subsp. enterica serovar Enteritidis str. EC20090530	EC20090530	GCF_000625395.2	Chromosome	Canada: Ontario	Animal-Chicken
Salmonella enterica subsp. enterica serovar Enteritidis str. EC20100088	EC20100088	GCF_000625415.2	Chromosome	Canada: Ontario	Animal
Salmonella enterica subsp. enterica serovar Enteritidis str. EC20100089	EC20100089	GCF_000625435.2	Chromosome	Canada: Ontario	Animal
Salmonella enterica subsp. enterica serovar Enteritidis str. EC20120580	EC20120580	GCF_000625455.2	Chromosome	missing	Animal-Chicken
Salmonella enterica subsp. enterica serovar Enteritidis str. EC20120581	EC20120581	GCF_000625475.2	Chromosome	missing	Animal-Chicken
Salmonella enterica subsp. enterica serovar Enteritidis str. EC20120590	EC20120590	GCF_000625495.2	Chromosome	Canada: Nova Scotia	Animal-Chicken
Salmonella enterica subsp. enterica serovar Enteritidis str. EC20120597	EC20120597	GCF_000625515.2	Chromosome	Canada: Ontario	Animal-Chicken
Salmonella enterica subsp. enterica serovar Enteritidis str. EC20120685	EC20120685	GCF_000625535.1	Chromosome	Canada: British Columbia	Animal-Chicken
Salmonella enterica subsp. enterica serovar Enteritidis str. EC20120686	EC20120686	GCF_000625555.2	Chromosome	Canada: British Columbia	Animal-Chicken
Salmonella enterica subsp. enterica serovar Enteritidis str. EC20120687	EC20120687	GCF_000625575.2	Chromosome	Canada: British Columbia	Animal-Chicken
Salmonella enterica subsp. enterica serovar Enteritidis str. EC20120697	EC20120697	GCF_000625595.1	Chromosome	missing	Animal-Chicken
Salmonella enterica subsp. enterica serovar Enteritidis str. EC20120722	EC20120722	GCF_000625615.2	Chromosome	Canada: Ontario	Food

Salmonella enterica subsp. enterica serovar Enteritidis str. EC20121976	EC20121976	GCF_000625635.2	Chromosome	Canada: Ontario	Food
Salmonella enterica subsp. enterica serovar Enteritidis str. SA20085285	SA20085285	GCF_000625655.1	Chromosome	Canada: Ontario	Environment - Litter/Manure
Salmonella enterica subsp. enterica serovar Enteritidis str. EC20090195	EC20090195	GCF_000625675.2	Chromosome	Canada: Saskatchewan	Food
Salmonella enterica subsp. enterica serovar Enteritidis str. SA20094682	SA20094682	GCF_000625695.2	Chromosome	Canada: Manitoba	Animal - Chicken-Cecum
Salmonella enterica subsp. enterica serovar Enteritidis str. EC20100131	EC20100131	GCF_000625715.2	Chromosome	Canada: Ontario	Animal-Chicken
Salmonella enterica subsp. enterica serovar Enteritidis str. SA20100239	SA20100239	GCF_000625735.1	Chromosome	Canada: Ontario	Animal - Bovine-Liver
Salmonella enterica subsp. enterica serovar Enteritidis str. EC20120677	EC20120677	GCF_000625755.1	Chromosome	Canada: Alberta	Animal-Chicken
Salmonella enterica subsp. enterica serovar Enteritidis str. EC20121765	EC20121765	GCF_000625775.2	Chromosome	Canada: British Columbia	Food-Pig
Salmonella enterica subsp. enterica serovar Enteritidis str. EC20121986	EC20121986	GCF_000625795.2	Chromosome	Canada: Ontario	Food
Salmonella enterica subsp. enterica serovar Enteritidis str. EC20121989	EC20121989	GCF_000625815.2	Chromosome	Canada: Ontario	Food
Salmonella enterica subsp. enterica serovar Enteritidis str. EC20120051	EC20120051	GCF_000625835.2	Chromosome	Canada: Ontario	Animal-Domestic Cattle
Salmonella enterica subsp. enterica serovar Enteritidis str. SA20082034	SA20082034	GCF_000625855.1	Complete Genome	Canada: Ontario	Environment - Litter/Manure
Salmonella enterica subsp. enterica serovar Enteritidis str. EC20121990	EC20121990	GCF_000625875.2	Chromosome	Canada: Ontario	Food
Salmonella enterica subsp. enterica serovar Enteritidis str. EC20122022	EC20122022	GCF_000625895.2	Chromosome	Canada: Ontario	Food

Salmonella enterica subsp. enterica serovar Enteritidis str. EC20122026	EC20122026	GCF_000625915.2	Chromosome	Canada: Ontario	Food
Salmonella enterica subsp. enterica serovar Enteritidis str. EC20122031	EC20122031	GCF_000625935.2	Chromosome	Canada: Ontario	Food
Salmonella enterica subsp. enterica serovar Enteritidis str. EC20122033	EC20122033	GCF_000625955.2	Chromosome	Canada: Ontario	Food
Salmonella enterica subsp. enterica serovar Enteritidis str. EC20122045	EC20122045	GCF_000625975.2	Chromosome	Canada: Ontario	Food
Salmonella enterica subsp. enterica serovar Enteritidis str. SA20123395	SA20123395	GCF_000625995.2	Chromosome	Canada: Alberta	Animal - Rodent
Salmonella enterica subsp. enterica serovar Enteritidis str. EC20130345	EC20130345	GCF_000626015.2	Chromosome	Canada: Ontario	Animal-Chicken
Salmonella enterica subsp. enterica serovar Enteritidis str. EC20130346	EC20130346	GCF_000626035.2	Chromosome	Canada: Ontario	Animal-Chicken
Salmonella enterica subsp. enterica serovar Enteritidis str. EC20130347	EC20130347	GCF_000626055.1	Chromosome	Canada: Ontario	Animal-Chicken
Salmonella enterica subsp. enterica serovar Enteritidis str. EC20130348	EC20130348	GCF_000626075.2	Chromosome	Canada: Ontario	Animal-Chicken
Salmonella enterica subsp. enterica serovar Enteritidis str. EC20120200	EC20120200	GCF_000626095.2	Complete Genome	Canada: Nova Scotia	Food
Salmonella enterica subsp. enterica serovar Enteritidis str. EC20100103	EC20100103	GCF_000626115.2	Chromosome	Canada: Ontario	Chicken
Salmonella enterica subsp. enterica serovar Enteritidis str. EC20090884	EC20090884	GCF_000626135.2	Chromosome	Canada: Ontario	Chicken
Salmonella enterica subsp. enterica serovar Enteritidis str. EC20090531	EC20090531	GCF_000626155.2	Chromosome	Canada: Ontario	Chicken
Salmonella enterica subsp. enterica serovar Enteritidis str. EC20110354	EC20110354	GCF_000626175.1	Complete Genome	Canada: Alberta	Human (Hospitalized)-

					Outbreak
Salmonella enterica subsp. enterica serovar Enteritidis str. EC20120008	EC20120008	GCF_000626195.1	Complete Genome	Canada: Ontario	Reptile
Salmonella enterica subsp. enterica serovar Enteritidis str. EC20100101	EC20100101	GCF_000626215.1	Complete Genome	Canada: Ontario	Chicken
Salmonella enterica subsp. enterica serovar Enteritidis str. EC20110221	EC20110221	GCF_000626235.1	Complete Genome	Canada: Ontario	Food- Mung Bean-Outbreak
Salmonella enterica subsp. enterica serovar Enteritidis str. EC20090698	EC20090698	GCF_000626255.1	Complete Genome	Canada: Alberta	Chicken-Abbatoir-Sporadic
Salmonella enterica subsp. enterica serovar Enteritidis str. EC20090641	EC20090641	GCF_000626275.2	Complete Genome	Canada: Alberta	Chicken-Abbatoir-Sporadic
Salmonella enterica subsp. enterica serovar Enteritidis str. EC20110355	EC20110355	GCF_000626295.1	Complete Genome	Canada: Alberta	Food Breast-Outbreak
Salmonella enterica subsp. enterica serovar Enteritidis str. EC20111175	EC20111175	GCF_000626335.1	Complete Genome	Canada: Quebec	Environmental (Chicken Fluff)-Outbreak
Salmonella enterica subsp. enterica serovar Enteritidis str. EC20111174	EC20111174	GCF_000626355.1	Complete Genome	Canada: Quebec	Environmental (Chicken Fluff)-Outbreak
Salmonella enterica subsp. enterica serovar Enteritidis str. EC20111095	EC20111095	GCF_000626375.1	Complete Genome	Canada: Quebec	Human-Outbreak
Salmonella enterica subsp. enterica serovar Enteritidis str. EC20120009	EC20120009	GCF_000626395.1	Chromosome	Canada: Ontario	Rodent
Salmonella enterica subsp. enterica serovar Enteritidis str. EC20120929	EC20120929	GCF_000626415.2	Chromosome	Canada: Ontario	Animal-Chicken
Salmonella enterica subsp. enterica serovar Enteritidis str. EC20121747	EC20121747	GCF_000626435.2	Chromosome	Canada: British Columbia	Food-Turkey
Salmonella enterica subsp. enterica	SA19940857	GCF_000626455.1	Chromosome	Canada: Ontario	Animal -

serovar Enteritidis str. SA19940857					Chicken-Environment Swab
Salmonella enterica subsp. enterica serovar Enteritidis str. SA20084644	SA20084644	GCF_000626475.1	Chromosome	Canada: Ontario	Animal - Avian
Salmonella enterica subsp. enterica serovar Enteritidis str. SA20084824	SA20084824	GCF_000626495.1	Chromosome	Canada: Ontario	Animal - Chicken-Fluff (Hatchery)
Salmonella enterica subsp. enterica serovar Enteritidis str. SA20094177	SA20094177	GCF_000626515.1	Chromosome	Canada: Ontario	Food
Salmonella enterica subsp. enterica serovar Enteritidis str. SA20094301	SA20094301	GCF_000626535.1	Chromosome	Canada: Newfoundland	Animal - Chicken-Fluff
Salmonella enterica subsp. enterica serovar Enteritidis str. EC20111510	EC20111510	GCF_000626555.2	Chromosome	Canada: British Columbia	Animal-Chicken
Salmonella enterica subsp. enterica serovar Enteritidis str. EC20100325	EC20100325	GCF_000626695.2	Complete Genome	Canada: Ontario	Food
Salmonella enterica subsp. enterica serovar Enteritidis	OLF-SE7-100819	GCF_000750215.1	Complete Genome	Canada	Environment
Salmonella enterica subsp. enterica serovar Enteritidis	OLF-SE8-1021710	GCF_000750255.1	Complete Genome	Canada	Chicken
Salmonella enterica subsp. enterica serovar Enteritidis	OLF-SE9-10012	GCF_000750295.1	Complete Genome	Canada	Shellfish Monitoring Program
Salmonella enterica subsp. enterica serovar Enteritidis	OLF-SE10-10052	GCF_000750335.1	Complete Genome	Canada	Environment
Salmonella enterica subsp. enterica serovar Enteritidis	OLF-SE11-10058	GCF_000750375.1	Complete Genome	Canada	Environment
Salmonella enterica subsp. enterica	OLF-SE3-	GCF_000750395.2	Complete	Canada	Environment

serovar Enteritidis	98983-4		Genome		
Salmonella enterica subsp. enterica serovar Enteritidis	OLF-SE2-98984-6	GCF_000750415.2	Complete Genome	Canada	Environment
Salmonella enterica subsp. enterica serovar Enteritidis	OLF-SE4-0317-8	GCF_000750435.1	Complete Genome	Canada	Environment
Salmonella enterica subsp. enterica serovar Enteritidis	OLF-SE5-1104-2	GCF_000750455.1	Complete Genome	Canada	Environment
Salmonella enterica subsp. enterica serovar Enteritidis	OLF-SE1-1019-1	GCF_000750475.1	Complete Genome	Canada	Environment
Salmonella enterica subsp. enterica serovar Enteritidis	OLF-SE6-00219-16	GCF_000750495.1	Complete Genome	Canada	Environment
Salmonella enterica subsp. enterica serovar Enteritidis	SEJ	GCF_000754375.1	Complete Genome	Missing	Missing
Salmonella enterica subsp. enterica serovar Enteritidis str. EC20100134	EC20100134	GCF_000831025.2	Chromosome	Canada: Ontario	Chicken
Salmonella enterica subsp. enterica serovar Enteritidis str. EC20100130	EC20100130	GCF_000831045.2	Chromosome	Canada: Ontario	Chicken
Salmonella enterica subsp. enterica serovar Enteritidis str. EC20100100	EC20100100	GCF_000968775.2	Chromosome	Canada: Saskatchewan	Food
Salmonella enterica subsp. enterica serovar Enteritidis str. SA20100349	SA20100349	GCF_000968795.1	Chromosome	Canada: Manitoba	Animal - Avian-Yolk Sac
Salmonella enterica subsp. enterica serovar Enteritidis	SEE1	GCF_001185215.1	Complete Genome	USA: Pennsylvania	Missing
Salmonella enterica subsp. enterica serovar Enteritidis	SEE2	GCF_001185245.1	Complete Genome	USA: Pennsylvania	Missing
Salmonella enterica subsp. enterica serovar Enteritidis	FORC_007	GCF_001305235.1	Complete Genome	South Korea: Gyeongbuk	Steamed Conch
Salmonella enterica subsp. enterica	CMCC50041	GCF_001484025.1	Complete	Denmark	Missing

serovar Enteritidis			Genome		
Salmonella enterica subsp. enterica serovar Enteritidis	OLF-00D98987-1	GCF_001647045.1	Complete Genome	Canada	Poultry Environment
Salmonella enterica	FORC_019	GCF_001705055.1	Complete Genome	South Korea	Blood
Salmonella enterica subsp. enterica serovar Enteritidis	CFSAN051873	GCF_001973275.2	Complete Genome	USA: PA	Spleen
Salmonella enterica subsp. enterica serovar Enteritidis	CFSAN033543	GCF_002128365.1	Complete Genome	USA:OH	Product Egg Raw Whole
Salmonella enterica subsp. enterica serovar Enteritidis	CFSAN033541	GCF_002128385.1	Complete Genome	USA:PA	Product Egg Raw White
Salmonella enterica subsp. enterica serovar Enteritidis	FORC_052	GCF_002220345.1	Complete Genome	South Korea: Seoul	Lettuce
Salmonella enterica	FORC_051	GCF_002313085.1	Complete Genome	Korea: Seoul	Blood
Salmonella enterica	FORC_056	GCF_002313105.1	Complete Genome	South Korea: Seoul	Fish
Salmonella enterica subsp. enterica serovar Enteritidis	56-3991	GCF_002760915.1	Complete Genome	USA	Human
Salmonella enterica subsp. enterica serovar Enteritidis	70-1605	GCF_002760935.1	Complete Genome	USA	Human
Salmonella enterica subsp. enterica serovar Enteritidis	74-1357	GCF_002760955.1	Complete Genome	USA	Human
Salmonella enterica subsp. enterica serovar Enteritidis	77-2980	GCF_002760975.1	Complete Genome	USA	Human
Salmonella enterica subsp. enterica serovar Enteritidis	79-2359	GCF_002760995.1	Complete Genome	USA	Human
Salmonella enterica subsp. enterica	81-1435	GCF_002761015.1	Complete	USA	Human

serovar Enteritidis			Genome		
Salmonella enterica subsp. enterica serovar Enteritidis	81-1706	GCF_002761035.1	Complete Genome	USA	Human
Salmonella enterica subsp. enterica serovar Enteritidis	93-0639	GCF_002761075.1	Complete Genome	USA	Human
Salmonella enterica subsp. enterica serovar Enteritidis	95-0621	GCF_002761095.1	Complete Genome	USA	Human
Salmonella enterica subsp. enterica serovar Enteritidis	49-2444	GCF_002761115.1	Complete Genome	USA	Human
Salmonella enterica subsp. enterica serovar Enteritidis	69-3861	GCF_002761135.1	Complete Genome	USA	Human
Salmonella enterica subsp. enterica serovar Enteritidis	81-1607	GCF_002761155.1	Complete Genome	USA	Human
Salmonella enterica subsp. enterica serovar Enteritidis	81-1705	GCF_002763415.1	Complete Genome	USA	Human
Salmonella enterica subsp. enterica serovar Enteritidis	SJTUF10978	GCF_002813975.1	Complete Genome	China: Shanghai	Chicken
Salmonella enterica subsp. enterica serovar Enteritidis	SJTUF10984	GCF_002813995.1	Complete Genome	China: Shanghai	Chicken
Salmonella enterica subsp. enterica serovar Enteritidis	SE86	GCF_002982095.1	Complete Genome	Brazil: Rio Grande do Sul	Missing
Salmonella enterica subsp. enterica serovar Enteritidis	ATCC BAA-708	GCF_003031995.1	Complete Genome	missing	Missing
Salmonella enterica subsp. enterica serovar Enteritidis	PIR00532	GCF_003032035.1	Complete Genome	missing	Missing
Salmonella enterica subsp. enterica serovar Enteritidis	RM4283	GCF_003184325.1	Complete Genome	Canada: Vancouver	Feces
Salmonella enterica subsp. enterica	RM2968	GCF_003184425.1	Complete	USA:California	Raw Almonds

serovar Enteritidis str. RM2968			Genome		
Salmonella enterica subsp. enterica serovar Enteritidis	FORC_075	GCF_003429365.1	Complete Genome	South Korea	Human Stool
Salmonella enterica	FORC_074	GCF_003515965.1	Complete Genome	South Korea	Human Stool
Salmonella enterica subsp. enterica serovar Enteritidis	NCM 61	GCF_003663765.1	Complete Genome	China: Anhui	Chicken Meat And Conveyer Belt
Salmonella enterica subsp. enterica serovar Enteritidis	CFSAN076214	GCF_003710165.1	Complete Genome	Canada	Raw Almonds
Salmonella enterica	FORC_078	GCF_004135835.1	Complete Genome	South Korea	Stool
Salmonella enterica subsp. enterica serovar Enteritidis	SAP18-0432	GCF_005889955.1	Complete Genome	USA:GA	Missing
Salmonella enterica subsp. enterica serovar Enteritidis	SAP18-H9654	GCF_005889975.1	Complete Genome	USA:GA	Missing
Salmonella enterica subsp. enterica serovar Enteritidis	SJTUF12519v2	GCF_006517015.1	Complete Genome	China:Shanghai	Human Feces
Salmonella enterica subsp. enterica serovar Enteritidis	SJTUF12367v2	GCF_006517055.1	Complete Genome	China:Shanghai	Human Feces
Salmonella enterica subsp. enterica serovar Enteritidis	PT1	GCF_008313815.1	Complete Genome	Denmark: Roskilde	Missing
Salmonella enterica subsp. enterica serovar Enteritidis	K12SE001	GCF_008369645.1	Chromosome	South Korea: Chungcheongnam-do	Chicken
Salmonella enterica subsp. enterica serovar Enteritidis	NCCP 16206	GCF_009884355.1	Complete Genome	South Korea: Gyeongnam	Stool

II-2-3. Biofilm formation

Biofilms of the *S.* Enteritidis strains were formed as described previously (Neiger et al., 2019) with minor modifications. Briefly, the overnight cultures of the *S.* Enteritidis strains were diluted to an A_{600} of 0.01 in tryptic soy broth (1:20 diluted TSB), and 200 μl of the resulting culture was used to form biofilms on each well of 96-well polystyrene microtiter plates (Nunc, Roskilde, Denmark). After static incubation at 30°C for 24 or 48 h, the planktonic cells were removed, and the remaining biofilms were stained with 1% crystal violet (CV) solution (Sigma-Aldrich, St. Louis, MO) and quantified as described previously (Park et al., 2015).

II-2-4. Colony morphology assay

For analysis of colony morphology, 1 μl of overnight cultures of the *S.* Enteritidis strains was used to spot onto LB agar plates without salt, containing 40 μg/ml of Congo red (Sigma) and 20 μg/ml of Coomassie brilliant blue (Sigma) (CR agar plates) or 200 μg/ml of calcofluor white (Sigma) (CFW agar plates). The resulting colonies were grown at 26°C for 96 h and visualized using a Stemi 305 stereomicroscope (Zeiss, Oberkochen, Germany) equipped with an Axiocam 105 color camera (Zeiss) or photographed using a digital camera (PowerShot G7X Mark II, Canon, Tokyo, Japan).

II-2-5. Generation of a *zirT* mutant

The *zirT* gene (FORC78_1136) was inactivated by deletion (1,465-bp of 1,983-bp) of the coding region using the lambda red recombination method (Datsenko & Wanner, 2000). Briefly, a linear DNA fragment containing kanamycin resistance (Km^r) cassette was amplified from pKD13 using ZIRT01-F and ZIRT01-R which were designed to carry 5'- and 3'- flanking regions of *zirT* (Table II-3). The resulting fragment was introduced into the *zirT* coding region of FORC_078 carrying pKD46 to generate FORC_078-*zirT*::*kan* (Table II-1).

Table II-3. Oligonucleotides used in this study

Name	Oligonucleotide sequence (5'→3')[a, b]	Use
For mutant construction		
ZIRT01-F	GGAAAAATAAAGGCGTTACCAGGGCAGGCCGCTAATCATCGTGTAGGCTGGAGCTGCTTC	Deletion of *zirT* ORF
ZIRT01-R	GCTTCCGTTGGCTTCTTCAGTACCCGGCGTAAAAAGCACCCTGTCAAACATGAGAATTAA	
ENVZ01-F	GAGGTCAACAAAAGCTCGCCCGTCGTGTGGCTCAAAACCTGTGTAGGCTGGAGCTGCTTC	
ENVZ01-R1	CGATGCGACTCGGTGCCGCTGCTGACCTTAATCCAGCCGTCTGTCAAACATGAGAATTAA	
ENVZ01-R2	CGATGCGACTCGGTGCCGCTGCTGACCTTAATCCAGCCGTATGGGAATTAGCCATGGTCC	Amplification of antibiotic resistance cassettes
pKD3-OMPR-F	GAGCTTTTTTAAGAATACACACTTACATTTGTTGCGAACCTTTGGGAGTACAGACAGTGTAGGCTGGAGCTGCTTC	
pKD3-OMPR-R	CGATGAGCAACAGCGTGCGGGCAAATGAACTTCGCGGCGAGAAGCGCATTCGCCTCATCATATGAATATCCTCCTTAG	
ENVZ02-F	ACGTGCATGCATCGTCACCTTGCTGTTCGT	Amplification of *envZ* region containing SNP allele
ENVZ02-R	ACGTGAGCTCCCTCTTTTGTCGTCCCCTGG	
ENVZPM-F1	ACGTGCATGCATCGTCACCTTGCTGTTCGT	
ENVZPM-R1	CGCAAGTCGGCGCTGACGCCC	Point mutation of *envZ* ORF
ENVZPM-F2	GGCGTCAGCGCCGACTTGC	
ENVZPM-R2	ACGTGAGCTCCCTCTTTTGTCGTCCCCTGG	
OMPRPM-F1	ACGTGCATGCTTTGAGTGTTTCGTACCCTT	
OMPRPM-R1	CATTAAAGCCAGTACCATGAGATGG	Point mutation of *ompR* ORF
OMPRPM-F2	GGTACTGGCTTTAATGCTGCC	
OMPRPM-R2	ACGTGAGCTCGATAGATTTCCCGACGAAAC	

OMPRD-F1	GAATTCCCGGGAGAGCTGAATTTGCTGGTGACTCAC	Deletion of *ompR* ORF
OMPRD-R1	CCACCATACGATGGAAAGATTCACGGGTC	
OMPRD-F2	ATCTTTCCATCGTATGGTGGAAGAAGATCC	
OMPRD-R2	TCTAGAGGTACCGCATGCTTCGTTGGTGTAGAGAGAG	
OMPFD-F1	GAATTCCCGGGAGAGCTATATTTGTAGCACTTTCACG	Deletion of *ompF* ORF
OMPFD-R1	TTTACTCTGCTCCCCTTTAAAACCAATCTG	
OMPFD-F2	TTAAAGGGGAGCAGAGTAAAGGTAAGCAGT	
OMPFD-R2	TCTAGAGGTACCGCATGGGTAAGTAATACCGACAGC	
SEN1522D-F1	GAATTCCCGGGAGAGCTTGACTTGATTATGATTCCGT	Deletion of SEN1522 ORF
SEN1522D-R1	TATAGTTTGCCAAATCCAGTTTATTGCCATC	
SEN1522D-F2	ACTGGATTTGGCAAACTATACCCGTACTTA	
SEN1522D-R2	TCTAGAGGTACCGCATGGGTGTTGTCTGTATTAGGAT	
SEN2875D-F1	GAATTCCCGGGAGAGCTAGTTGCTTATGTGTTGGCTA	Deletion of SEN2875 ORF
SEN2875D-R1	CCTTACTGTCTGTACTGGCATTATCGTCTG	
SEN2875D-F2	TGCCAGTACAGACAGTAAGGTCGGATATGG	
SEN2875D-R2	TCTAGAGGTACCGCATGATACAGATTCCAGTCAGTGC	
OMPDD-F1	GAATTCCCGGGAGAGCTAAAAATAGTCTGCCATTGAC	Deletion of *ompD* ORF
OMPDD-R1	GGTTTTATTCAACTGATCGTTGATCTGAGTTTCGC	
OMPDD-F2	ACGATCAGTTGAATAAAACCCAGAACTTTGAAG	
OMPDD-R2	TCTAGAGGTACCGCATGCTTATGACCGAGTCTACATC	
OMPWD-F1	GAATTCCCGGGAGAGCTTAATCTGTCCCGCAGTGTTC	Deletion of *ompW* ORF
OMPWD-R1	AATCCTTAAATTTTCATACCCGCTCCATCG	
OMPWD-F2	GGTATGAAAATTAAGGATTCCTGGGGCG	
OMPWD-R2	TCTAGAGGTACCGCATGAATCCGTGTGTCATGTCCTT	
For protein overexpression		
OMPR01-F	GTTTAACTTTAAGAAGGAGATATACCATGCAAGAGAATTATAAGATTCTG	Amplification of *ompR* ORF
OMPR01-R	CAGTGGTGGTGGTGGTGGTGTGCTTTAGAACCGTCCG	

For qRT-PCR		
OMPF-qRT-F	TTCTTTGGTCTGGTGGACGG	Quantification of *ompF* expression
OMPF-qRT-R	CTTGCTGTTGCTGTACGCTG	
OMPC-qRT-F	CTGAAATTCGCTGACGCAGG	Quantification of *ompC* expression
OMPC-qRT-R	TCGGTGTTACGGTAAGTGGC	
CSGD-qRT-F	GCAGGATAATTTAAGCCGCA	Quantification of *csgD* expression
CSGD-qRT-R	TAATCCGCTGACCACGTGTTC	
FLIC-qRT-F	AAGCGACAGTGGGTGATCTG	Quantification of *fliC* expression
FLIC-qRT-R	CAGTCACTACAGCACCGGAA	
SEN1522-qRT-F	ATCAGGTCAACGCCAATCGT	Quantification of SEN1522 expression
SEN1522-qRT-R	CAACAGACCCCATATCGGCA	
SEN2875-qRT-F	TGGATACGCCCAGTCCCATA	Quantification of SEN2875 expression
SEN2875-qRT-R	GCAAATGAGGTTGTCAGCCC	
OMPD-qRT-F	AACCGTACTGAAAGCCAGGG	Quantification of *ompD* expression
OMPD-qRT-R	TCTGAGTCCAGGTATCGCCA	
OMPW-qRT-F	CGACGGACAATATCGGGGTT	Quantification of *ompW* expression
OMPW-qRT-R	TGGAATCGCCGAAGTACCAC	
16S-qRT-F	TGCCTGATGGAGGGGGATAA	Quantification of 16S rRNA expression
16S-qRT-R	TGAGCCGTTACCTCACCAAC	
For EMSA		
PSEN1522-F	CACGAAGCGAAGAAGTGCTA	Amplification of $P_{SEN1522}$ regulatory region
PSEN1522-R	ACCGCAGATAACACCACTAC	
PSEN2875-F	CCCGTTATATATCCTTCATACTTC	Amplification of $P_{SEN2875}$ regulatory region
PSEN2875-R	GCATTTTGTTCATCTTCTTCTC	
PompD-F	GTGCTCCTCCTGCGCCATAC	Amplification of P_{ompD} regulatory region
PompD-R	GTCACTGCCACTGCCACTAA	
PompW-F	TAATCTGTCCCGCAGTGTTC	Amplification of P_{ompW} regulatory region
PompW-R	CCTTCTGTAGGTCTGACGGT	

For manipulation of OmpR expression		
OMPRP-F	GCAGGAGGAATTCACCATGCAAGAGAATTATAAGATTC	Amplification of *ompR* ORF
OMPRP-R	CAGCCAAGCTTGCATGTCATGCTTTAGAACCGTC	
For reporter construction		
PompR-F	ACGTCTGCAGGTTTGAGTGTTTCGTACCC	Amplification of P_{ompR} regulatory region
PompR-R	ACGTGGATCCCTTATAATTCTCTTGCATTGTC	

[a]The oligonucleotides were designed using the genomic sequences of *S.* Enteritidis ATCC 13076 (GenBank accession number GCA_001643395.1), *S.* Enteritidis FORC_075 (RefSeq assembly accession number GCF_003429365.1), and *S.* Enteritidis FORC_078 (RefSeq assembly accession number GCF_004135835.1).

[b]Regions of oligonucleotides not complementary to the corresponding genes are underlined.

II-2-6. Generation of single nucleotide substitution mutants

For single nucleotide substitutions (C → T in *envZ* of FORC_078 and T → C in *envZ* of FORC_075), the *envZ* genes of FORC_078 and FORC_075 were first replaced with Km^r cassette and chloramphenicol resistance (Cm^r) cassette, respectively, using lambda red recombination method (Datsenko & Wanner, 2000). Briefly, pairs of primers, ENVZ01-F and ENVZ01-R1 or ENVZ01-F and ENVZ01-R2, which were designed to carry 5'- and 3'- flanking regions of *envZ*, were used for amplification of linear DNA fragments containing Km^r cassette from pKD13 and Cm^r cassette from pKD3, respectively (Table II-3). The resulting Km^r cassette was introduced into the *envZ* gene of FORC_078 carrying pKD46 to generate FORC_078-*envZ*::*kan*, and the resulting Cm^r cassette was introduced into the *envZ* gene of FORC_075 carrying pKD46 to generate FORC_075-*envZ*::*cat* (Table II-1).

Then, the *envZ* region of FORC_078 containing the SNP allele (C) and that of FORC_075 containing the SNP allele (T) were amplified using ENVZ02-F and ENVZ02-R (Table S2), and the resulting fragments were ligated into SphI-SacI-digested pCVD442 to generate pDH1903 and pDH1904, respectively (Table S1). *E. coli* S17-1 λ*pir* containing pDH1903 was used as a conjugal donor to FORC_075-*envZ*::*cat* to generate FORC_075-$EnvZ_{L248P}$ (Table II-1). *E. coli* S17-1 λ*pir* containing pDH1904 was used as a conjugal donor to FORC_078-*envZ*::*kan* to generate FORC_078-$EnvZ_{P248L}$ (Table II-1). The conjugation and isolation of the transconjugants were conducted using the method described previously (Philippe et

al., 2004). The single nucleotide substitution was confirmed by DNA sequencing. Same experimental procedures were adopted for single nucleotide substitution (C → T) in *envZ* of ATCC 13076 to generate ATCC 13076-EnvZ$_{P248L}$ (Table II-1).

II-2-7. Purification of OmpR and Western blot analysis

The *ompR* gene was amplified using OMPR01-F and OMPR01-R (Table S2), and the resulting fragment was subcloned into pET-28a(+) (Novagen, Madison, WI) to generate pDH2003 (Table II-1). The His$_6$-tagged OmpR was expressed in *E. coli* BL21(DE3) and purified by affinity chromatography (Qiagen, Valencia, CA). The purified His$_6$-tagged OmpR was used to raise mouse anti-OmpR polyclonal antibody (AbClon, Seoul, South Korea).

For Western blot analysis, the *S.* Enteritidis strains grown to an A_{600} of 2.5 were harvested by centrifugation, and the cells were lysed using B-PER Bacterial Protein Extraction Reagent with Enzymes (Thermo Fisher Scientific, Waltham, MA). The cell debris was removed by centrifugation to obtain clear cell lysates. OmpR and DnaK in the clear cell lysates were detected by Western blot analysis using mouse anti-*S.* Enteritidis OmpR antibody and mouse anti-*E. coli* DnaK antibody (Enzo Life Science, Farmingdale, NY) as described previously (Lee et al., 2020). Phosphorylated status of OmpR was detected by Western blot analysis using 10% SuperSep Phos-tag precast gels (Wako, Osaka, Japan). After electrophoresis, the precast gels were washed three times with transfer buffer (25 mM Tris, 192 mM

glycine, 20% methanol, and 5 mM EDTA) to remove Zn^{2+} and further washed once with transfer buffer without EDTA. The phosphorylated- and unphosphorylated-OmpR were detected using the same mouse anti-*S.* Enteritidis OmpR antibody.

II-2-8. RNA purification and transcript analysis

Total RNAs were isolated from the *S.* Enteritidis strains grown to an A_{600} of 2.5 by using an RNeasy mini kit (Qiagen). For quantitative reverse transcription-PCR (qRT-PCR), cDNA was synthesized from 1 μg of the total RNAs by using an iScript™ cDNA synthesis kit (Bio-Rad, Hercules, CA). Real-time PCR amplification of the cDNA was performed by using a CFX96 real-time PCR detection system (Bio-Rad) with pairs of specific primers (Table II-3) as described previously (Kim et al., 2012). Relative expression levels of each gene were calculated by using the 16S rRNA expression level as the internal reference for normalization.

II-2-9. Motility, adhesion, invasion, and acid resistance assay

For motility assay, 2 μl of the *S.* Enteritidis strains grown to an A_{600} of 2.5 was used to stab into LB semisolid medium containing 0.3% agar. The plates were incubated at 37°C for 7 h, and the migration area of cells was visualized by the Gel Doc EZ Imager (Bio-rad).

For adhesion assay, HeLa human epithelial cells and RAW 264.7 murine macrophage cells were grown in Dulbecco modified Eagle medium (DMEM) (Gibco-BRL,

Gaithersburg, MD) supplemented with 10% fetal bovine serum, 100 U/ml penicillin, and 100 μg/ml streptomycin. One day before bacterial infection, the HeLa cells and RAW 264.7 cells were seeded into 24-well tissue culture plates at a concentration of 2.5×10^5 cells/well and incubated at 37°C under 5% CO_2. Each well was infected with the *S*. Enteritidis strains grown to an A_{600} of 2.5 at a multiplicity of infection (MOI) of 10, centrifuged immediately at 500×g for 5 min, and then incubated for 30 min. The wells were washed three times with phosphate buffered saline (PBS) to remove non-adherent bacteria and then lysed in 1% Triton X-100 for 30 min. For invasion assay, the wells were further incubated for 30 min with DMEM supplemented with 100 μg/ml gentamicin to kill extracellular bacteria before lysis with 1% Triton X-100. The adhered and intracellular bacteria were diluted in PBS and plated on LB agar to enumerate the CFU.

For acid resistance assay, the *S.* Enteritidis strains grown to an A_{600} of 2.5 were washed once with PBS (acid-unadapted bacteria) or further incubated in M9 minimal medium containing 10 mM glucose (M9G) (pH 4.3) at 37°C for 2 h (acid-adapted bacteria). Then, the acid-unadapted and –adapted bacteria were incubated in M9G (pH 3.0) at 37°C for 2 h. The pH of M9G was adjusted with HCl. The aliquots of the resulting cultures were diluted in PBS and plated on LB agar to enumerate the CFU.

II-2-10. Sequence analysis

The protein ID of FORC_075 EnvZ (WP_080165161.1) was submitted to the NCBI

Identical Protein Groups database, and a list of *Salmonella* strains expressing the same FORC_075 EnvZ was retrieved. The isolation information of each strain was retrieved from the NCBI BioSample database, and its serovar was predicted by the SISTR (*Salmonella in silico* typing resource) program (Yoshida et al., 2016) using the whole genome sequences.

II-2-11. Data analysis

Data analyses were performed as indicated in the figure legends using GraphPad Prism 7.0 (GraphPad Software, San Diego, CA, United States). Significance of differences between experimental groups was accepted at a p value < 0.05.

II-3. Results

II-3-1. The *S.* Enteritidis strains isolated in South Korea have a close genetic relationship

Previously, 8 strains of *S.* Enteritidis isolated from different sources in South Korea were collected and designated as FORC_007, FORC_019, FORC_051, FORC_052, FORC_056, FORC_074, FORC_075, and FORC_078, and then, their whole genomes were completely sequenced and deposited in the NCBI GenBank database under the accession numbers GCA_001305235.1, GCA_001705055.1, GCA_002313085.1, GCA_002220345.1, GCA_002313105.1, GCA_003515965.1, GCA_003429365.1, and GCA_004135835.1, respectively. To examine their genetic similarity, ANI values were first calculated. Remarkably, the ANI values between each genome were very high ranging from 99.98% to even 100%, which indicates that the 8 FORC strains possess almost identical genome sequences. Then, to determine their evolutionary relationship in the context of the *S.* Enteritidis strains isolated in different countries, an SNP-based phylogenetic analysis was performed. Although all FORC strains were isolated from different sources or in different years (Table II-4), they were clustered very closely in the phylogenetic tree (Fig. II-1), indicating again that their genetic backgrounds are highly similar. In more detail, the FORC_052, FORC_056, FORC_075, and FORC_078 strains were located in the same branch (Cluster-A in Fig. II-1), and the other FORC strains, FORC_007,

FORC_019, FORC_051, and FORC_074, were clustered together with 7 strains isolated in Asia (2 for South Korea and 5 for China) (Cluster-B in Fig. II-1). As can be inferred from the phylogenetic tree, the maximum SNP distances within Cluster-A, within Cluster-B, and between the two cluster were 49, 84, and 94, respectively (Fig. II-2). The close phylogenetic relationship between the 8 FORC strains and the 7 Asian strains may result from their relative geographical proximity. Together, these results indicate that the 8 FORC strains share their genomic features and have highly similar genetic backgrounds.

Table II-4. General information of the *S.* Enteritidis strains isolated in South Korea

Strain	Year of isolation (Region of isolation[a])	Source of isolation	Sequencing technology	Assembly level	Genome	Size (bp)
FORC_007	2014 (Gyeongsangbuk-do)	Steamed conch	Illumina; PacBio	Complete genome	Chromosome Plasmid	4,680,477 101,428
FORC_019	2014 (ND)	Human blood	Illumina; PacBio	Complete genome	Chromosome Plasmid	4,680,751 116,939
FORC_051	2016 (ND)	Human blood	PacBio	Complete genome	Chromosome Plasmid	4,679,637 96,999
FORC_052	2014 (Seoul)	Lettuce	PacBio	Complete genome	Chromosome	4,686,254
FORC_056	2015 (Seoul)	Fish	PacBio	Complete genome	Chromosome Plasmid	4,686,230 59,371
FORC_074	2002 (ND)	Human stool	PacBio	Complete genome	Chromosome Plasmid-I Plasmid-II	4,682,412 60,923 51,931
FORC_075	2017 (ND)	Human stool	PacBio	Complete genome	Chromosome Plasmid	4,707,598 34,661
FORC_078	2002 (ND)	Human stool	PacBio	Complete genome	Chromosome Plasmid	4,686,022 59,333
K12SE001	2011 (Chungcheongnam-do)	Chicken	PacBio	Chromosome	Chromosome	4,680,830
NCCP 16206	2011 (ND)	Stool	IonTorrent; PacBio	Complete genome	Chromosome Plasmid	4,690,706 83,299

[a]The isolation region of clinical strain was indicated as ND.

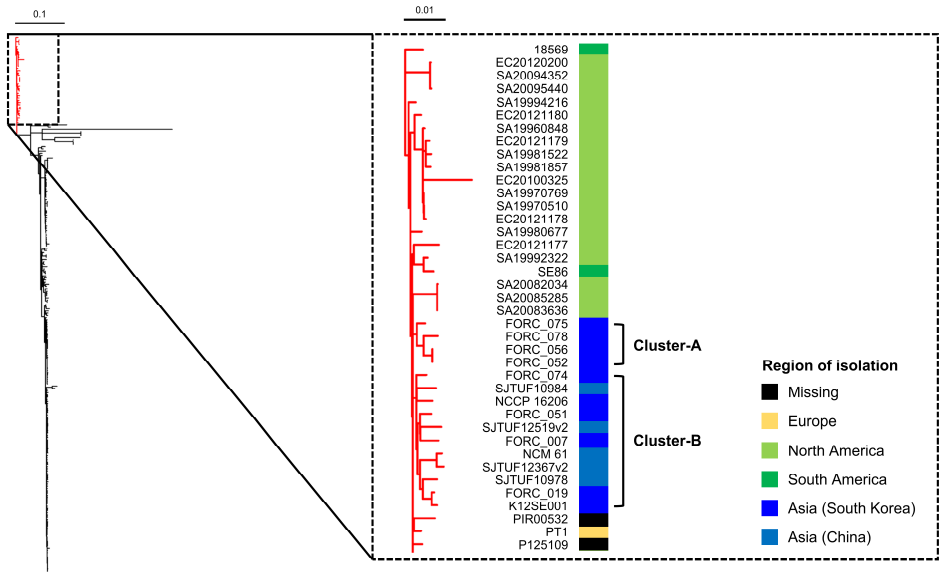

Figure II-1. Phylogenetic tree of the *S.* Enteritidis strains. The phylogenetic relationships were calculated by the RAxML program (Stamatakis, 2006) and visualized using the iTOL program (https://itol.embl.de/) (Letunic & Bork, 2016). The branch containing the *S.* Enteritidis strains isolated in South Korea is shown in a dashed box on the right at the finer scale resolution. Regions of isolation are indicated in different color. Scale bars represent the nucleotide substitutions per site.

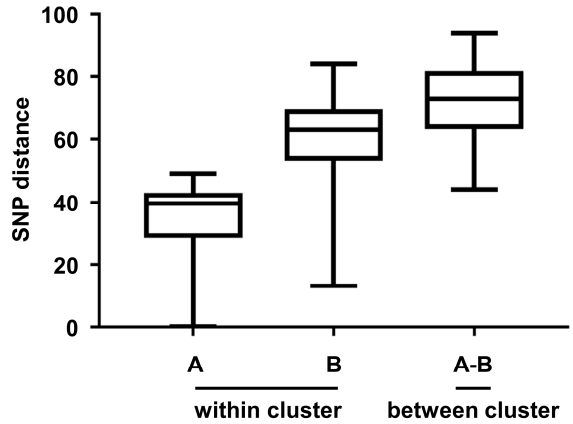

Figure II-2. Pairwise SNP distances between the *S.* Enteritidis strains. The pairwise SNP distances between each *S.* Enteritidis strain were calculated by snp-dists program (https://github.com/tseemann/snp-dists), and their variations were shown in a box plot. A, Cluster-A in Figure II-1; B, Cluster-B in Figure II-1.

II-3-2. FORC_075 exhibits an impaired biofilm formation and a SAW colony morphology

Because the ability of *Salmonella* to form biofilms is important for persistence and survival under environmental stresses (Desai & Kenney, 2017, 2019; Desai et al., 2016; MacKenzie et al., 2017), the biofilm-forming abilities of the 8 FORC strains were evaluated. Interestingly, the biofilm-forming ability of FORC_075 was extremely lower than those of other FORC strains (Fig. II-3). Especially, the amount of biofilms formed by FORC_075 was approximately 20-fold lower than that formed by FORC_078, a strain phylogenetically closest to FORC_075 (Fig. II-1 and II-3A). One possible hypothesis for the impaired biofilm formation is that FORC_075 has lost the ability to produce the major biofilm components such as curli fimbriae and cellulose. Because both curli fimbriae and cellulose contribute to the development of the RDAR colony morphology (Romling, 2005), the *S.* Enteritidis strains were grown on agar plates containing Congo red (CR agar plates), and their colony morphologies were also compared. FORC_007 formed red and dry colony with concentric rings (Fig. II-3B), which indicates the production of curli fimbriae only (Serra et al., 2013). While FORC_019, FORC_051, FORC_052, FORC_056, FORC_074, and FORC_078 formed RDAR colonies, FORC_075 formed SAW colony, displaying significantly distinct colony morphology from those of other FORC strains (Fig. II-3B). These results support our hypothesis that FORC_075 produces low levels of curli fimbriae and cellulose. To further confirm the cellulose production, the *S.* Enteritidis strains were grown on agar plates containing calcofluor

white (CFW agar plates), and their colonies were observed under UV light (Solano et al., 2002). Consistent with the results of Fig. II-3B, low fluorescence intensities were observed in the colonies of FORC_007 and FORC_075 compared with those of other FORC strains forming RDAR colonies (Fig. II-4), indicating that FORC_007 and FORC_075 produce a small amount of cellulose. Taken together, these results suggest that the impaired biofilm formation of FORC_075 is attributed to low levels of both curli fimbriae and cellulose production. Because the genome sequences of the 8 FORC strains were almost identical, the significantly different phenotypes of biofilm formation and colony morphology of FORC_075 were unexpected.

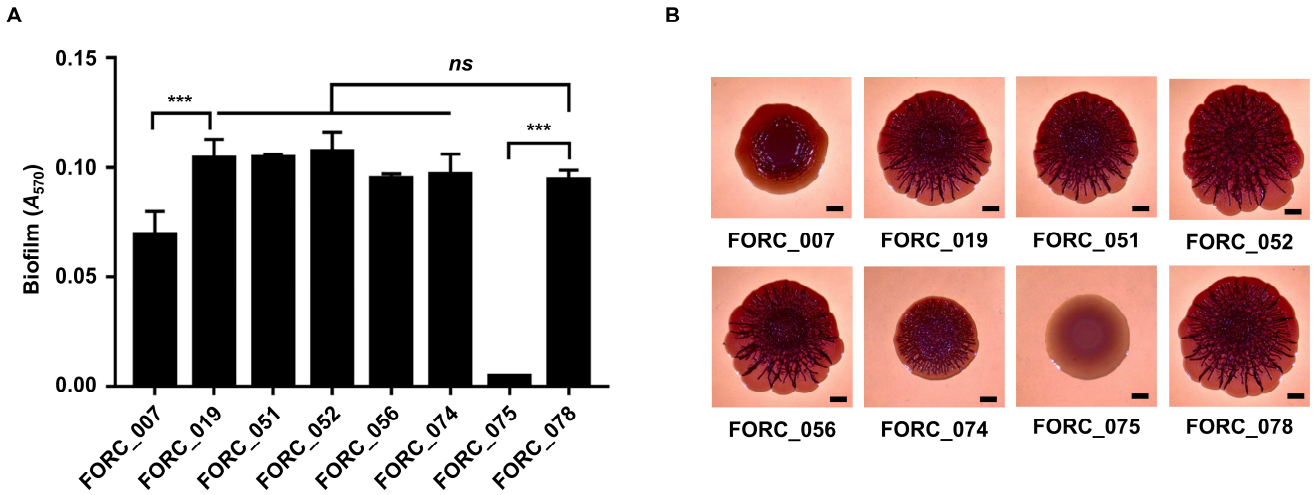

Figure II-3. Distinct biofilm formation and colony morphology of FORC_075. (A) Biofilms of the *S.* Enteritidis strains were grown on 96-well microtiter plates for 48 h and quantified using CV staining. Error bars represent the standard deviation (SD) from three independent experiments. Statistical significance was determined by multiple comparisons after one-way analysis of variance (ANOVA). ***, $p<0.001$; *ns*, not significant. (B) The *S.* Enteritidis strains were spotted onto CR agar plates and incubated for 96 h. The colony morphology was visualized using a stereomicroscope (Stemi 305, Zeiss) at 4 × magnification. Scale bars, 2 mm.

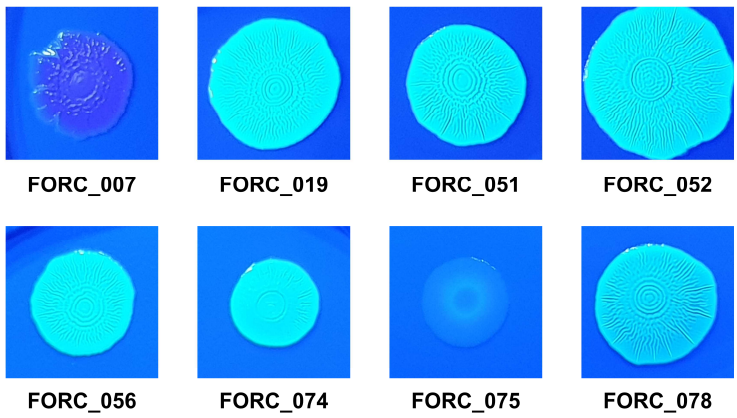

Figure II-4. Colony morphologies of the *S.* Enteritidis strains on CFW agar plates. The *S.* Enteritidis strains were spotted onto CFW agar plates and incubated for 96 h. The colony morphology was photographed using a digital camera (PowerShot G7X Mark II, Canon).

II-3-3. A single SNP in *envZ* is responsible for the distinct phenotypes of FORC_075

To elucidate the genetic basis for the unexpected phenotypes of FORC_075, whole genome sequence of FORC_075 was compared with those of the other FORC strains including FORC_078 using various bioinformatics tools. First, the pangenome of the 8 FORC strains was built to identify genes carried differently in the FORC strains. The size of the pangenome was 4,767 genes, of which about 91% (4,364 genes) constitute the core genome with a length of 4,052,928-bp, indicating again that the 8 FORC strains have similar genetic backgrounds. Among the accessory genome, the *zir* operon (FORC78_1133~FORC78_1142) was not detected only in FORC_075 (Fig. II-5A). This region belongs to a genomic island known as GEI 1664/1678 (Klumpp & Fuchs, 2007), suggesting that genomic rearrangement may have occurred in FORC_075 genome. Especially, the *zir* operon (FORC78_1134~FORC78_1137; *zirRTSU*) is conserved throughout the *Salmonella* serovars (Gal-Mor et al., 2008). The *zirT* gene encodes a membrane transporter ZirT, which mediates a secretion of ZirS and ZirU, and this secretion system plays a role of antivirulence modulator during infection (Gal-Mor et al., 2008; Prehna et al., 2012). Because the previous study suggested that the ZirT-dependent secretion system may play a potential role in biofilm formation (Prehna et al., 2012), the *zirT* gene was deleted in the FORC_078 genetic background, and the biofilm- and RDAR colony-forming abilities were determined. However, the biofilm formation and

colony morphology of the isogenic *zirT* mutant of FORC_078 were similar to those of the parent strain (Fig. II-5B and C). This result indicates that the loss of the *zir* operon in the FORC_075 genome is not responsible for its impaired biofilm formation and SAW colony morphology.

Next, the whole genome sequences of the 8 FORC strains were compared at the single nucleotide level. Among a total of 198 SNPs detected in the 8 strains, 9 non-synonymous SNPs were unique to the FORC_075 strain (Table II-5). Especially, the two genes containing SNPs, *dps* and *envZ*, are related to biofilm formation (Prigent-Combaret et al., 2001; Theoret et al., 2012). The SNP in *dps* resulted in an amino acid change from Glu142 to Ala142 in Dps, and the SNP in *envZ* resulted in an amino acid change from Pro248 to Leu248 in EnvZ (Table II-5). When the effect of each SNP on protein function was predicted *in silico*, the SNP in *dps* was predicted not to have significant effects on the function of Dps (Table II-5). In contrast, the SNP in *envZ* was predicted to affect the function of EnvZ (Table II-5). Accordingly, the SNP in *envZ* rather than the SNP in *dps* was considered as the most likely candidate responsible for the impaired biofilm formation and SAW colony morphology of FORC_075.

To verify the effects of the SNP in *envZ* on the distinct phenotypes of FORC_075, the SNP alleles of FORC_078 and FORC_075 were exchanged with each other to express $EnvZ_{P248L}$ in FORC_078 and $EnvZ_{L248P}$ in FORC_075, and their biofilm formation and colony morphology were evaluated. The substitution of Pro248 of

FORC_078 EnvZ with Leu (P248L) reduced the biofilm-forming ability to the level even lower than that of FORC_075 (Fig. II-6A). In addition, the P248L substitution abolished the RDAR colony morphology of FORC_078 and led to the SAW colony morphology similar to that of FORC_075 (Fig. II-6B). Although the substitution of Leu248 of FORC_075 EnvZ with Pro (L248P) did not completely restore the ability of FORC_075 to form RDAR colony to the level comparable to that of FORC_078, the L248P substitution dramatically increased biofilm- and RDAR colony-forming abilities of FORC_075 (Fig. II-6). Thus, the combined results indicate that the SNP in *envZ* is a major genetic change determining the ability of biofilm formation and the type of colony morphology of *S.* Enteritidis.

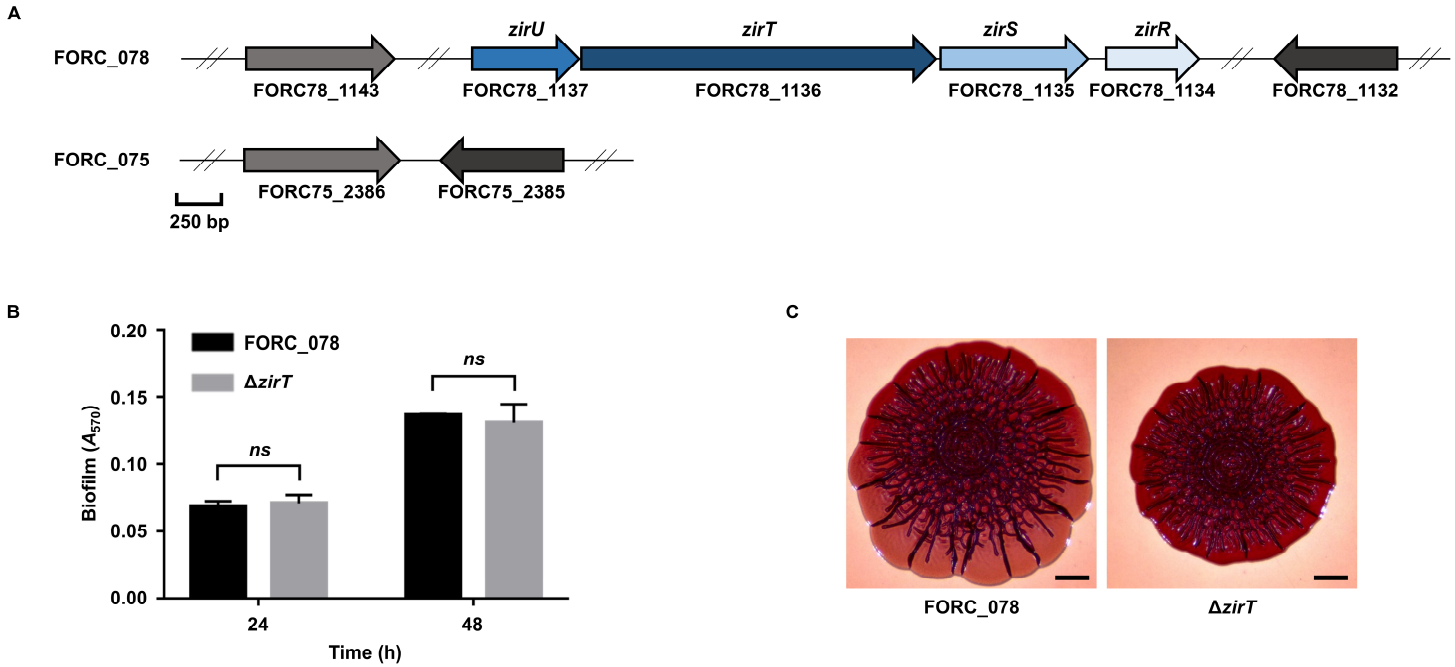

Figure II-5. Effects of the *zirT* mutation on biofilm formation and colony morphology. (A) The genomic region containing the *zir* operon was compared between FORC_078 and FORC_075. Genes are represented by the arrows with the direction of transcription. Identical genes are shown by the same color. Gene names and locus tags are indicated above and below each arrow, respectively. (B) Biofilms of the *S.* Enteritidis strains were grown on 96-well microtiter plates for 24 and 48 h and quantified using CV staining. Error bars represent the SD from three independent

experiments. Statistical significance was determined by Student's *t* test. *ns*, not significant. (C) The *S.* Enteritidis strains were spotted onto CR agar plates and incubated for 96 h. The colony morphology was visualized using a stereomicroscope (Stemi 305, Zeiss) at 4 × magnification. Scale bars, 2 mm. FORC_078, parent strain; Δ*zirT*, *zirT* mutant.

Table II-5. Non-synonymous SNPs unique to the FORC_075 strain

Position in FORC_078 (nucleotide)[a]	Position in FORC_075 (nucleotide)[b]	Amino acid change	Gene	Function	PROVEAN score (prediction)	SNAP2 score (prediction)	SIFT score (prediction)[c]
467447 (G)	1806812 (A)	E113K	*phsA*	Thiosulfate reductase	1.142 (neutral)	-61 (neutral)	1.00 (tolerated)
943379 (C)	2282762 (T)	G186S	-	Peptidase	-5.526 (deleterious)	60 (effect)	N/A
949118 (C)	2288501 (T)	P176L	*bioD*	ATP-dependent dethiobiotin synthetase	-9.206 (deleterious)	59 (effect)	0.00 (affect protein function)
1754770 (A)	3084775 (C)	E142A	*dps*	Non-specific DNA-binding protein Dps	-0.073 (neutral)	-12 (neutral)	0.27 (tolerated)
2115383 (C)	3445390 (T)	A139T	*ybaO*	HTH-type transcriptional regulator YbaO	-3.746 (deleterious)	59 (effect)	0.14 (tolerated)
2331756 (G)	3661765 (A)	P161S	-	Chitinase	-3.649 (deleterious)	33 (effect)	0.01 (affect protein function)
2704053 (A)	4034070 (G)	H109R	*hypT*	HOCl-specific transcription factor HypT	-7.449 (deleterious)	72 (effect)	0.59 (tolerated)
2769014 (G)	4099014 (A)	S510N	*nrdD*	Ribonucleotide reductase of class III (anaerobic), large subunit	1.705 (neutral)	-97 (neutral)	0.59 (tolerated)
3757731 (C)	380056 (T)	P248L	*envZ*	Osmolarity sensory histidine kinase EnvZ	-9.653 (deleterious)	73 (effect)	0.00 (affect protein function)

[a]The nucleotide position in the chromosome of FORC_078 (RefSeq assembly accession number GCF_004135835.1).

[b]The nucleotide position in the chromosome of FORC_075 (RefSeq assembly accession number GCF_003429365.1).

[c]N/A, not analyzed by the server.

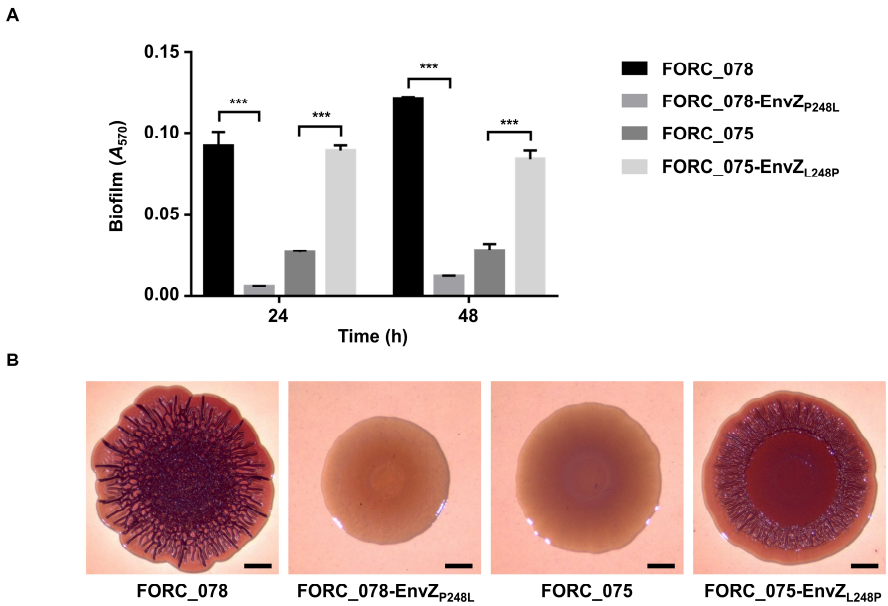

Figure II-6. SNP in *envZ* responsible for the distinct biofilm phenotypes. (A) Biofilms of the *S.* Enteritidis strains were grown on 96-well microtiter plate for 24 and 48 h and quantified using CV staining. Error bars represent the SD from three independent experiments. Statistical significance was determined by Student's *t* test. ***, $p<0.001$. (B) The *S.* Enteritidis strains were spotted onto CR agar plates and incubated for 96 h. The colony morphology was visualized using a stereomicroscope (Stemi 305, Zeiss) at 4 × magnification. Scale bars, 2 mm. FORC_078 and FORC_075, parent strains; FORC_078-EnvZ$_{P248L}$, FORC_078 expressing EnvZ$_{P248L}$; FORC_075-EnvZ$_{L248P}$, FORC_075 expressing EnvZ$_{L248P}$.

II-3-4. SNP in *envZ* increases OmpR-P level and alters OmpR regulon expression

To determine whether the SNP in *envZ* affects EnvZ function indeed, the phosphorylated status of OmpR in the *S.* Enteritidis strains was examined. The P248L substitution in the FORC_078 genetic background significantly increased the OmpR-P level (Fig. II-7A), while the L248P substitution in the FORC_075 genetic background decreased the OmpR-P level to a level not detectable by immunoblotting (Fig. II-7C). Because the amount of OmpR-P governs *ompF* and *ompC* transcriptions, the effects of the SNP in *envZ* on the expression levels of *ompF* and *ompC* were further investigated. As expected, the P248L substitution resulting in a greater amount of OmpR-P in FORC_078 decreased the *ompF* expression by 20-fold and increased the *ompC* expression by almost 4-fold (Fig. II-7B). Similarly, the L248P substitution resulting in a smaller amount of OmpR-P in FORC_075 increased the *ompF* expression and decreased the *ompC* expression (Fig. II-7D). These results demonstrate that the non-synonymous SNP in *envZ* modifies EnvZ function, increasing the OmpR-P level in *S.* Enteritidis and altering the expression levels of *ompF* and *ompC.*

To examine the effect of the SNP in *envZ* on the expression of other OmpR regulon, *csgD* and *fliC* expressions in the *S.* Enteritidis strains were also compared. The *csgD* expressions in the FORC_078-EnvZ$_{P248L}$ and FORC_075 strains showing increased OmpR-P levels were significantly lower than those in the FORC_078 and

FORC_075$_{L248P}$ strains showing decreased OmpR-P levels, respectively (Fig. II-7). The results were consistent with the previous reports that a high level of OmpR-P has a repressive effect on the *csgD* expression (Gerstel et al., 2006; Gerstel et al., 2003). Meanwhile, the *fliC* expression was also reduced in the FORC_078 strain by the P248L substitution (Fig. II-7B) and elevated in the FORC_075 strain by the L248P substitution (Fig. II-7D). To examine the effect of the altered expression of *fliC* on motility, the swimming areas of the *S.* Enteritidis strains on a semisolid plate surface were compared. The diameter of the swimming area of the FORC_078-EnvZ$_{P248L}$ strain was decreased to approximately 70% of that of the FORC_078 strain (Fig. II-8). Similar to the decreasing effect of the P248L substitution on motility, the FORC_075 strain was less motile than the FORC_075-EnvZ$_{L248P}$ strain (Fig. II-8). This results suggest that the SNP in *envZ* decreases the expression level of *fliC* and thus, results in a reduction in motility of *S.* Enteritidis. Collectively, these results indicate that functional modification of EnvZ induced by the SNP in *envZ* increases the phosphorylated status of OmpR and alters the expression of the OmpR regulon, leading to phenotypic changes in biofilm formation and motility of *S.* Enteritidis.

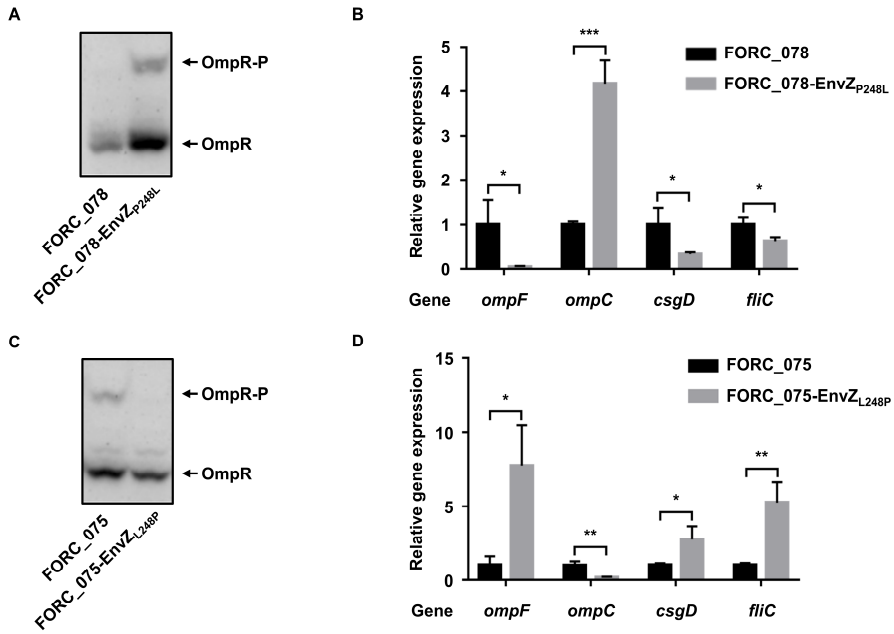

Figure II-7. Effects of the SNP in *envZ* on the OmpR-P level and OmpR regulon expression. Total proteins and RNAs were isolated from the *S.* Enteritidis strains grown to an A_{600} of 2.5. (A and C) The cellular levels of phosphorylated and unphosphorylated OmpR were determined by Western blot analysis using Phos-tag SDS-PAGE gels (Wako). (B and D) The *ompF*, *ompC*, *csgD*, and *fliC* transcript levels were determined by qRT-PCR. The transcript levels in each parent strain were set as 1. Error bars represent the SD from three independent experiments. Statistical significance was determined by Student's *t* test. *, $p<0.05$; **, $p<0.005$; ***, $p<0.001$. FORC_078 and FORC_075, parent strains; FORC_078-EnvZ$_{P248L}$, FORC_078 expressing EnvZ$_{P248L}$; FORC_075-EnvZ$_{L248P}$, FORC_075 expressing EnvZ$_{L248P}$.

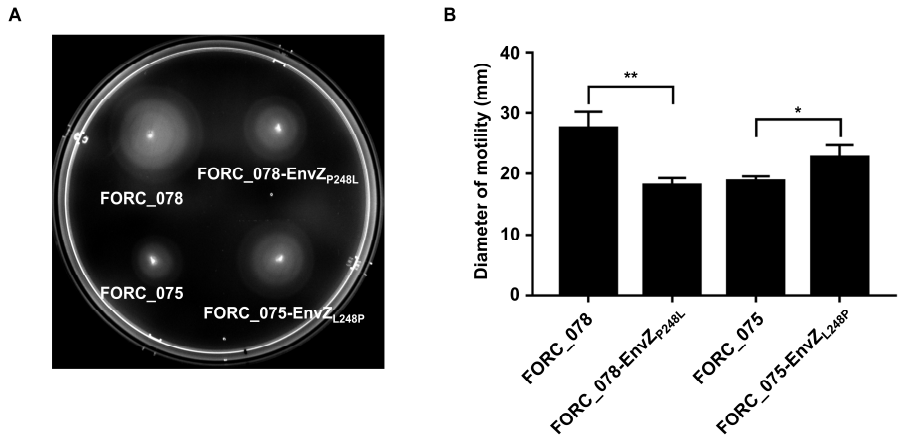

Figure II-8. Effect of SNP in *envZ* on motility. (A) The areas of motility of the *S.* Enteritidis strains grown on LB plates with 0.3% agar for 7 h were photographed. (B) The motility areas were expressed as the diameter (mm). Error bars represent the SD from three independent experiments. Statistical significance was determined by Student's *t* test. *, $p<0.05$; **, $p<0.005$. FORC_078 and FORC_075, parent strains; FORC_078-$EnvZ_{P248L}$, FORC_078 expressing $EnvZ_{P248L}$; FORC_075-$EnvZ_{L248P}$, FORC_075 expressing $EnvZ_{L248P}$.

II-3-5. SNP in *envZ* determines the virulence-related phenotypes of *S.* Enteritidis

To extend our understanding of the role of the SNP in *envZ* in *S.* Enteritidis pathogenesis, the effects of the exchange of the SNP allele on the virulence-related phenotypes were examined. When HeLa human epithelial cells and RAW 264.7 murine macrophage cells were infected with the *S.* Enteritidis strains, the adhesion of FORC_078 to the epithelial and macrophage cells was significantly increased by the P248L substitution to the level comparable to that of FORC_075 (Fig. II-9A and C). Consistent with this result, the adhesion of FORC_075 to both host cells was reduced by the L248P substitution (Fig. II-9A and C). In addition, although it was not possible to assess the invasion of FORC_075 because of its gentamicin resistance (Table II-1), the invasion of FORC_078 to HeLa and RAW 264.7 cells was greatly increased by the P248L substitution (Fig. II-9B and D). These combined results indicate that the SNP in *envZ* leading to $EnvZ_{L248}$ increases the infectivity of *S.* Enteritidis to host cells.

The effect of the SNP in *envZ* on survival of *S.* Enteritidis under acid stress was also assessed. The survival of acid-unadapted and –adapted FORC_078 at pH 3.0 was increased by more than 2-fold by the P248L substitution (Fig. II-10). Similarly, the survival of FORC_075 at pH 3.0 was reduced by the L248P substitution to the level comparable to that of FORC_078 in both acid-unadapted and –adapted cells (Fig. II-10). These results indicate that the SNP in *envZ* leading to $EnvZ_{L248}$ enhances the

acid resistance of *S.* Enteritidis, regardless of the prior acid adaptation. Altogether, the results suggest that the SNP in *envZ* improves *S.* Enteritidis pathogenesis by elevating its infectivity to host cells and survival under acid stress during the course of infection.

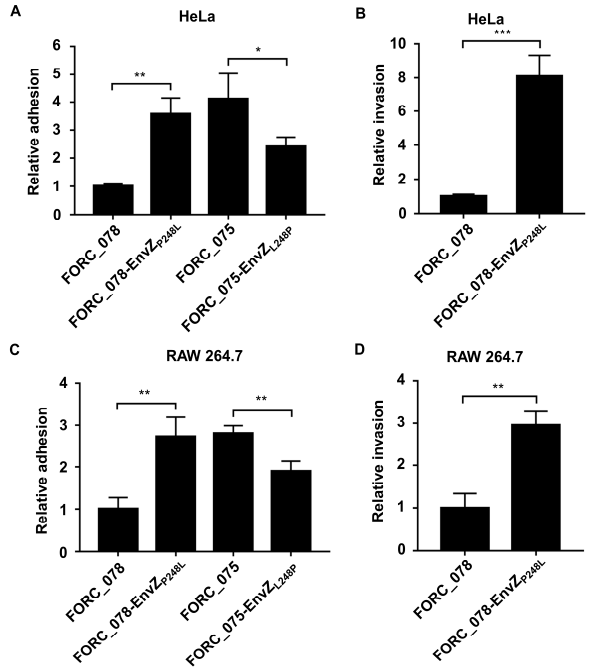

Figure II-9. Effect of SNP in *envZ* on infectivity to host cells. HeLa cells and RAW 264.7 cells were infected with the *S.* Enteritidis strains at an MOI of 10 for 30 min. (A and C) Adhesion to HeLa cells (A) and RAW 264.7 cells (C) was expressed as the ratio of the number of adhered cells to the total number of cells used for infection. Relative adhesion of FORC_078 was set as 1. (B and D) Invasion to HeLa cells (B) and RAW 264.7 cells (D) was expressed as the ratio of the number of intracellular cells to the total number of cells used for infection. Relative invasion of FORC_078 was set as 1. Error bars represent the SD from three independent experiments. Statistical significance was determined by Student's *t* test. *, $p<0.05$, **, $p<0.005$, ***, $p<0.001$. FORC_078 and FORC_075, parent strains; FORC_078-$EnvZ_{P248L}$, FORC_078 expressing $EnvZ_{P248L}$; FORC_075-$EnvZ_{L248P}$, FORC_075 expressing $EnvZ_{L248P}$.

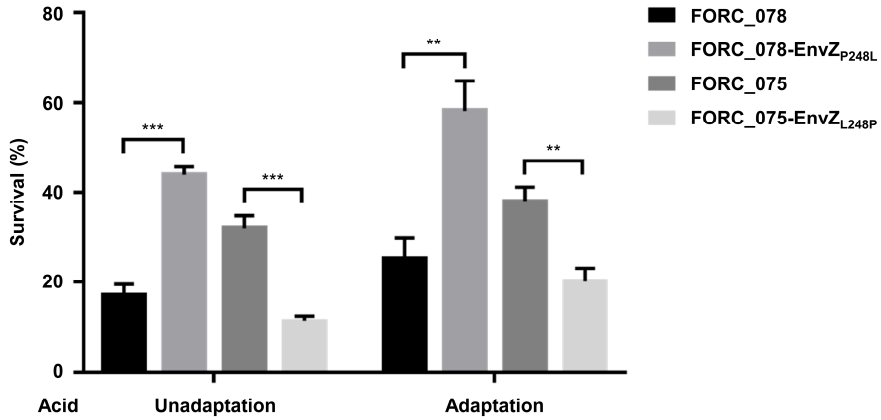

Figure II-10. Effect of SNP in *envZ* on survival under acid stress. The acid-unadapted and -adapted *S.* Enteritidis strains were compared for their abilities to survive under acid stress (pH 3.0). Survival was expressed as the ratio of the number of surviving cells to the number of initially inoculated cells. Error bars represent the SD from three independent experiments. Statistical significance was determined by Student's *t* test. **, $p<0.005$; ***, $p<0.001$. FORC_078 and FORC_075, parent strains; FORC_078-$EnvZ_{P248L}$, FORC_078 expressing $EnvZ_{P248L}$; FORC_075-$EnvZ_{L248P}$, FORC_075 expressing $EnvZ_{L248P}$.

II-3-6. The effects of the SNP in *envZ* are not dependent on a particular *S.* Enteritidis genetic background

To investigate whether the effects of the SNP in *envZ* are specific to the FORC strains, a ATCC 13076-EnvZ$_{P248L}$ mutant was constructed using a standard strain of *S.* Enteritidis, ATCC 13076. The P248L substitution in the ATCC 13076 genetic background increased OmpR-P level and altered the expression of the OmpR regulon (Fig. II-11A and B). Moreover, the P248L substitution decreased biofilm formation of ATCC 13076, while increasing its infectivity to host cells as well as survival under acid stress (Fig. II-11C-G). All these results observed in ATCC 13076 were identical to those in the FORC_078, suggesting that the effects of the SNP in *envZ* are not dependent on a specific genetic background.

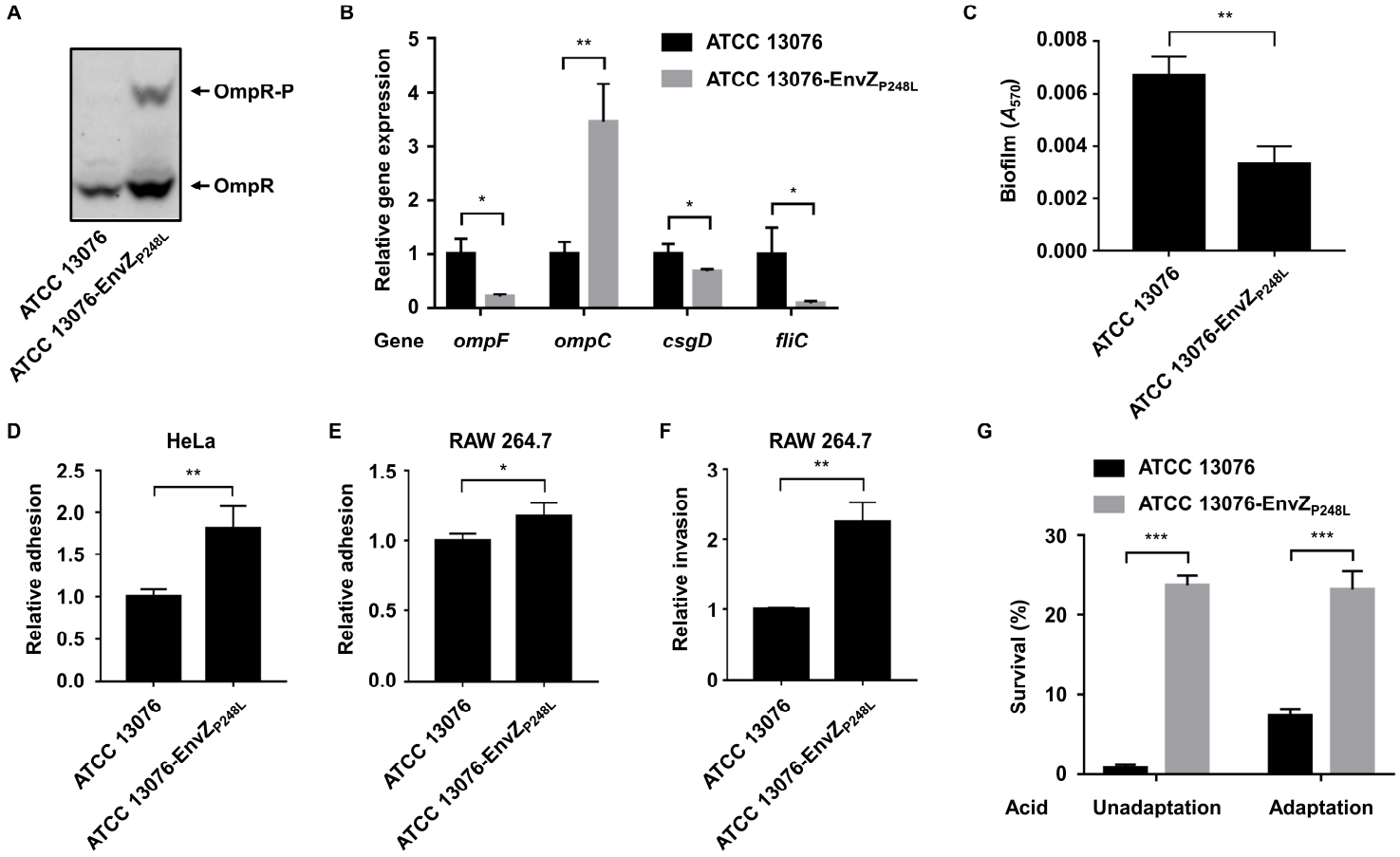
A
OmpR-P
OmpR
ATCC 13076
ATCC 13076-EnvZP248L
B
Relative gene expression
ATCC 13076
ATCC 13076-EnvZP248L
Gene
ompF
ompC
csgD
fliC
C
Biofilm (A570)
ATCC 13076
ATCC 13076-EnvZP248L
D
HeLa
Relative adhesion
ATCC 13076
ATCC 13076-EnvZP248L
E
RAW 264.7
Relative adhesion
ATCC 13076
ATCC 13076-EnvZP248L
F
RAW 264.7
Relative invasion
ATCC 13076
ATCC 13076-EnvZP248L
G
ATCC 13076
ATCC 13076-EnvZP248L
Survival (%)
Acid
Unadaptation
Adaptation

Figure II-11. Effects of the SNP in *envZ* on various phenotypes of ATCC 13076. (A and B) Total proteins and RNAs were isolated from the *S.* Enteritidis strains grown to an A_{600} of 2.5. (A) The cellular levels of phosphorylated and unphosphorylated OmpR were determined by Western blot analysis using Phos-tag SDS-PAGE gels (Wako). (B) The *ompF*, *ompC*, *csgD*, and *fliC* transcript levels were determined by qRT-PCR. The transcript levels in the parent strain were set as 1. (C) Biofilms of the *S.* Enteritidis strains were grown on 96-well microtiter plates for 48 h and quantified using CV staining. (D to F) HeLa cells and RAW 264.7 cells were infected with the *S.* Enteritidis strains at an MOI of 10 for 30 min. (D and E) Adhesion to HeLa cells (D) and RAW 264.7 cells (E) was expressed as the ratio of the number of adhered cells to the total number of cells used for infection. Relative adhesion of the parent strain was set as 1. (F) Invasion to RAW 264.7 cells was expressed as the ratio of the number of intracellular cells to the total number of cells used for infection. Relative invasion of the parent strain was set as 1. (G) The acid-unadapted and -adapted *S.* Enteritidis strains were compared for their abilities to survive under acid stress (pH 3.0). Survival was expressed as the ratio of the number of surviving cells to the number of initially inoculated cells. Error bars represent the SD from three independent experiments. Statistical significance was determined by Student's *t* test. *, $p<0.05$; **, $p<0.005$; ***, $p<0.0001$. ATCC 13076, parent strain; ATCC 13076-$EnvZ_{P248L}$, ATCC 13076 expressing $EnvZ_{P248L}$.

II-3-7. The SNP in *envZ* can naturally occur in other *Salmonella* strains

To determine whether the SNP in *envZ* is also found in other *Salmonella* strains, the presence of the strain expressing $EnvZ_{L248}$, instead of $EnvZ_{P248}$, was examined in the NCBI database. A total of 10 isolates of *Salmonella* including FORC_075 were identified to carry the same SNP in *envZ* (Table II-6). The isolation source of BCW_2682 and SLM287 was chicken meat, and that of CFSAN083304 was cattle intestine (Table II-6), indicating that the strain expressing $EnvZ_{L248}$ can survive in various environments. These results imply that the spontaneous SNP in *envZ* is not a dead-end mutation.

Table II-6. *Salmonella* strains carrying the SNP allele of FORC_075 *envZ*

Strain	Assembly accession number	BioSample accession number	Collected institution[a]	Source of isolation	Year of isolation
S. Enteritidis					
BCW_2682	GCF_002065725.1	SAMN02368561	Technical University of Denmark	Chicken meat	2006
BCW_2860	GCF_002063265.1	SAMN02368726	Technical University of Denmark	Missing	Missing
BCW_2877	GCF_002062265.1	SAMN02368742	Technical University of Denmark	Missing	Missing
BCW_2906	GCF_002062045.1	SAMN03358713	Missing	Missing	Missing
CFSAN083304	GCA_006079855.1	SAMN11897920	University of Ilorin	Cattle intestine	2014
R17.5427	GCA_010254135.1	SAMN09899636	Taiwan CDC	Missing	2017
SLM287	GCA_016916275.1	SAMN16708151	Missing	Chicken	2017
QLUZ102	GCA_021119285.1	SAMN15007349	Missing	Missing	Missing
S. Bareilly					
PNUSAS039121	GCA_007662705.1	SAMN08981904	CDC	Missing	Missing

[a]CDC, Centers for Disease Control and Prevention.

II-4. Discussion

Together with the accumulation of bacterial genomic data, comparative genomic analysis has allowed us to understand dynamic genetic changes leading to phenotypic differences (Stabler et al., 2009; Thomson et al., 2008). Acquisition or loss of accessory genes and small genetic changes in core genes may have a significant impact on phenotypes, which increases the virulence and survival of bacterial pathogens under a variety of environmental stresses. In the present study, we evaluated the phenotypes of 8 strains of *S.* Enteritidis whose genetic similarity is very high (Fig. II-1). Among the 8 strains, however, FORC_075 exhibited distinct phenotypes of biofilm formation and colony morphology (Fig. II-3). We demonstrated that an SNP in *envZ* is responsible for the impaired biofilm formation and SAW colony morphology of FORC_075 (Table II-5 and Fig. II-6).

The SNP in *envZ* of FORC_075 resulted in $EnvZ_{L248}$, different from $EnvZ_{P248}$ in other strains including FORC_078 (Table II-5). The Pro248 is positioned in an H box that is well conserved in sensor kinases including EnvZ and important for its autophosphorylation and phosphotransfer to OmpR (Tomomori et al., 1999). Thus, mutation in the Pro248 is mostly possible to affect the phosphorylated status of OmpR and thereby its activity to regulate downstream genes. In this study, we detected higher OmpR-P levels in the *S.* Enteritidis strains expressing $EnvZ_{L248}$ instead of $EnvZ_{P248}$ (Fig. II-7A, 7C, and 11A) and also confirmed that the expression of the OmpR regulon was significantly altered depending on the amount of OmpR-

P (Fig. II-7B, 7D, and 11B). Our combined results imply that this SNP has naturally occurred at a critical site in *envZ* that leads to changes in the phosphorylated status of OmpR and in its regulatory activity.

FORC_075 is a clinical strain isolated from human stool (Table II-2) and carries the SNP in *envZ* leading to $EnvZ_{L248}$. There are several lines of evidence that genetic changes frequently occur in sensor kinase of signal transduction system during host-bacteria interaction, possibly affecting the bacterial pathogenic features. For example, *S.* Typhimurium strains, isolated from gallbladder of mouse, had a truncated mutation in *envZ* and showed hyper-biofilm formation (Neiger et al., 2019). For group A *Streptococcus* (GAS), signal transduction systems such as LiaFSR three-component system and CovSR two-component system play an important role in virulence of the pathogen (Horstmann et al., 2014; Ichikawa et al., 2011). GAS isolates, recovered from a patient, carried an SNP in the H box of sensor kinase LiaS, and this mutation decreased virulence of GAS but increased its colonization to host cells (Flores et al., 2015). In addition, GAS strains, isolated after mouse infection, contained an amino acid change from Pro285 of sensor kinase CovS (corresponding to Pro248 of EnvZ) to Ser, which affects its phosphatase activity altering the expression of virulence genes (Horstmann et al., 2018). Along with these previous reports, it is possible to suggest that the SNP in *envZ* of the FORC_075 genome also occurred spontaneously during the course of host infection.

During host infection, modulation of the virulence-related phenotypes is important

for *S.* Enteritidis to obtain optimal fitness and successful pathogenesis. In this study, we identified that the SNP in *envZ* of FORC_075 decreases biofilm formation and motility but elevates infectivity to host cells and acid resistance (Fig. II-6 and 8-10). It has been shown that loss of biofilm components could alleviate host immune responses and lead to efficient invasion of *Salmonella* to host cells and its hypervirulence *in vivo* (Ahmad et al., 2011; Pontes et al., 2015; Tukel et al., 2010; White et al., 2008). Similarly, flagella are required for motility but stimulate host immune system, and thus, their overexpression results in attenuation of *Salmonella* in mouse model (Miao et al., 2010; Winter et al., 2010). Accordingly, the decreased expression of biofilm components and flagella resulting from the SNP in *envZ* is expected to be beneficial for survival of *S.* Enteritidis in host environments by reducing the chances to be detected by the immune system. Furthermore, adhesion and invasion to host cells are essential for *Salmonella* to cause infection, and induction of acid resistance enables the bacteria to survive in acidic conditions such as stomach (Alvarez-Ordonez et al., 2012; Fabrega & Vila, 2013; Yuk & Schneider, 2006). Thus, the enhanced infectivity to host cells and acid resistance resulting from the SNP in *envZ* could contribute to *Salmonella* pathogenesis. Altogether, these phenotypic changes introduced by the SNP in *envZ* may confer selective advantage to the *S.* Enteritidis strains expressing $EnvZ_{L248}$. Especially, if the SNP in *envZ* is conserved in the *Salmonella* strains, it could lead to food-borne outbreaks in South Korea in the future, considering the location where the pathogen was isolated (Table

II-4).

In recent years, single nucleotide mutations underlying the clonal expansion of *Salmonella* have been reported, suggesting their evolutionary impact. An SNP in the promoter region of virulence gene *pgtE*, causing hyperinvasion of *Salmonella*, was proposed as a genetic signature of isolates in *S.* Typhimurium ST313 lineage 2 (Hammarlof et al., 2018). In addition, conserved SNPs in multiple loci, leading to impaired biofilm formation of *Salmonella*, were presented as strong evidences of the parallel evolution in invasive *Salmonella* lineages (MacKenzie et al., 2019). According to these recent works, we expect that the SNP in *envZ* serves as a pathoadaptive mutation that could potentially play a role in bacterial evolution. The emergence of several *Salmonella* strains carrying the same SNP allele in *envZ* also supports our expectation (Table II-6).

In summary, we revealed that 8 FORC strains of *S.* Enteritidis had almost identical genome sequences. However, FORC_075 showed impaired biofilm- and RDAR colony-forming abilities, which was distinct from other FORC strains including FORC_078. Among non-synonymous SNPs unique to FORC_075, an SNP in *envZ* leading to an amino acid change from Pro248 to Leu248 was identified to result in the impaired biofilm formation and SAW colony morphology of *S.* Enteritidis. The effects of the SNP in *envZ* on phenotypic changes of *S.* Enteritidis are summarized in Fig. II-12. The SNP in *envZ* induced functional modification of EnvZ, which increased the cellular level of OmpR-P in *S.* Enteritidis and altered the expression of

the OmpR regulon. The SNP in *envZ* led to the decrease in motility but the increase in adhesion and invasion to host cells and even in acid resistance of *S.* Enteritidis. Taken together, these results suggest that the SNP in *envZ* plays a key role in differentiating the virulence-related phenotypes. Considering that the EnvZ/OmpR system is highly conserved in *Enterobacteriaceae*, it could be suggested as a good target for development of broad-spectrum antivirulence agents against many pathogens. This study would provide insights into the natural occurrence of SNP that potentially contributes to phenotypic diversity of *S.* Enteritidis for optimal fitness and successful pathogenesis.

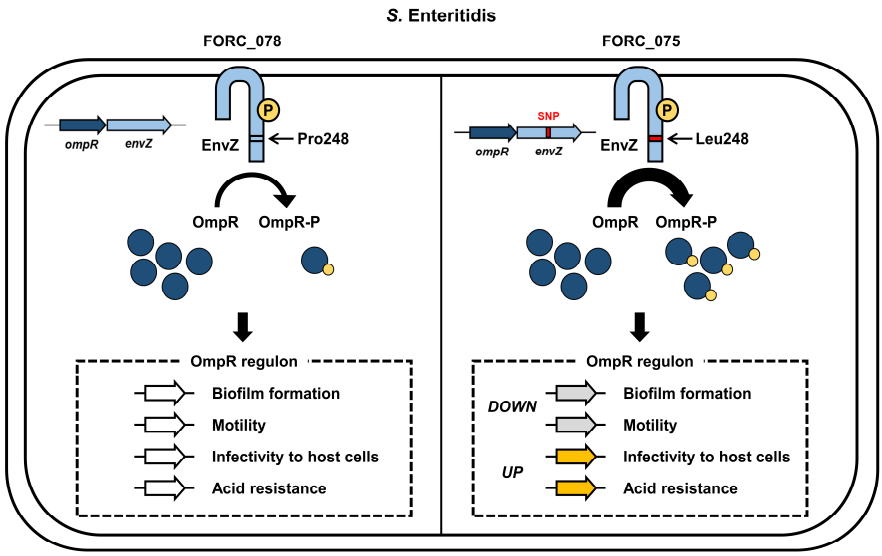

Figure II-12. Proposed model for the effects of the SNP in *envZ*. A non-synonymous SNP in *envZ* of FORC_075 results in amino acid change of EnvZ from Pro248 in FORC_078 to Leu248 in FORC_075. This amino acid change modifies EnvZ function and leads to an increase in the cellular level of OmpR-P. As a result, the expression of OmpR regulon would be altered, which results in the decreases in biofilm formation and motility and the increases in infectivity to host cells and acid resistance. Taken together, this phenotypic changes induced by the SNP in *envZ* could improve fitness and pathogenesis of *S.* Enteritidis during infection, increasing the selective pressure on FORC_075.

Chapter III.

Mechanism of antibiotic resistance mediated by EnvZ/OmpR two-component system in *Salmonella enterica* serovar Enteritidis

III-1. Introduction

Outer membrane porins (OMPs) are unique architecture of Gram-negative bacteria, which form water-filled open channels and allow the diffusion of small hydrophilic antibiotics into the cells (Pages et al., 2008; Vergalli et al., 2020). Because most antibiotics should access intracellular targets to inhibit essential cellular processes, the antibiotic activity toward bacteria is greatly affected by OMPs. In *Escherichia coli* and *Salmonella enterica*, the loss of OmpC or OmpF, two abundant OMPs, enhances the resistance to β-lactams and fluoroquinolones (Gu et al., 2021; Hirai et al., 1986; Jaffe et al., 1982; Medeiros et al., 1987). In *S. enterica* serovar Typhimurium, a reduced expression of the OmpD porin, often accompanied by an increased expression of OMPs encoded by STM1530 and STM3031, enhances the resistance to β-lactams (Hu et al., 2011; Lin et al., 2019). Furthermore, a reduced expression of the OmpW porin is also associated with the resistance in *S.* Typhimurium to β-lactams (Hu et al., 2005). Accordingly, compositional modulation of OMPs is one of the key strategies for bacteria to improve their antibiotic resistance (Blair et al., 2015; Pages et al., 2008).

EnvZ/OmpR two-component system consists of a sensor kinase EnvZ and its cognate response regulator OmpR. When specific environmental signals are sensed by EnvZ, a phosphoryl group is transferred from His243 of EnvZ to Asp55 of OmpR (Delgado et al., 1993; Forst et al., 1989; Mizuno, 1998), resulting in an active state

of EnvZ/OmpR. Canonically, the phosphorylated OmpR (OmpR-P) controls the expression of *ompC* and *ompF*. A recent study showed that EnvZ/OmpR affects the antibiotic resistance in *E. coli*, independently of *ompC* and *ompF* (Adler et al., 2016). However, the exact mechanism of EnvZ/OmpR that contributes to antibiotic resistance has not yet been established.

A human pathogen *S. enterica* serovar Enteritidis is a leading cause of food-borne diseases, and infection by *S.* Enteritidis often results in severe invasive disease, which should be treated with antibiotics (Chen et al., 2013; European Food Safety et al., 2018; Gordon, 2008; Rule et al., 2019). In this study, we found that the *S.* Enteritidis strain with the active state of EnvZ/OmpR is highly resistant to β-lactams. Transcriptome analysis newly discovered that the active state of EnvZ/OmpR leads to a differential expression of multiple OMP genes besides *ompC* and *ompF*, including SEN1522, SEN2875 (homologous to STM1530 and STM3031 in *S.* Typhimurium, respectively), *ompD*, and *ompW*. Biochemical analyses demonstrated that OmpR directly activates SEN1522 and SEN2875 but represses *ompD* and *ompW*, altering the OMP composition. Interestingly, the cellular level of OmpR increased by the active state of EnvZ/OmpR determines the expression of the four OMP genes. Moreover, phosphorylation of OmpR is not required for the repression of *ompD* and *ompW*. Phenotypic analysis revealed that among the EnvZ/OmpR regulon encoding OMPs, a decreased expression of *ompD*, in addition to *ompF*, is responsible for the EnvZ/OmpR-mediated resistance to β-lactams. Notably, EnvZ/OmpR increases its

own expression and represses *ompD* and *ompF* in response to the external β-lactams, providing benefits for survival of *S*. Enteritidis in the presence of the antibiotics. Taken together, this study suggests that EnvZ/OmpR mediates the enhancement of antibiotic resistance in *S*. Enteritidis by remodeling the OMP composition in response to β-lactams.

III-2. Materials and Methods

III-2-1. Strains, plasmids, and culture conditions

The strains and plasmids used in this study are listed in Table II-1. Unless otherwise stated, all strains were grown in Luria-Bertani (LB) medium at 37°C. When required, antibiotics were added to the medium at the following concentrations: ampicillin, 100 μg ml^{-1}; chloramphenicol, 20 μg ml^{-1}; tetracycline, 5 μg ml^{-1}; kanamycin, 100 μg ml^{-1}. Growth of the *S.* Enteritidis strains was monitored spectrophotometrically at 600 nm (A_{600}). When indicated, 2×10^8 CFU ml^{-1} of the *S.* Enteritidis strains grown to an A_{600} of 1.0 were further incubated for 2 h in M9 minimal medium containing 10 mM glucose (M9G) with or without various antibiotics. Comparative genomic analysis.

III-2-2. Mutant construction

The ATCC 13076-$EnvZ_{P248L}$ strain was previously constructed (Ko & Choi, 2021) and used in this study (Table II-1). For construction of the ATCC 13076-$EnvZ_{H243A}$ strain, the *envZ* gene was first replaced with the chloramphenicol resistance cassette as described previously (Datsenko & Wanner, 2000; Ko & Choi, 2021). Then, mutated *envZ* region was amplified using the PCR-mediated linker-scanning method as described previously (Hwang et al., 2021). Pairs of primers, ENVZPM-F1 and –R1 and ENVZPM-F2 and –R2, were used for the amplification of the 5’ amplicon

and 3' amplicon, respectively, and the *envZ*$_{H243A}$ gene was amplified by PCR using a mixture of both amplicons as the templates and ENVZPM-F1 and –R2 as the primers (Table II-3). The resulting fragment was ligated into SacI-SphI-digested pCVD442 to generate pDH1907 (Table II-1). *E. coli* S17-1 λ*pir* containing pDH1907 was used as a conjugal donor to the *envZ*::*cat* strain to generate ATCC 13076-EnvZ$_{H243A}$ (Table II-1). The conjugation and isolation of the transconjugants were conducted as described previously (Ko & Choi, 2021). Similar experimental procedures were adopted for construction of the ATCC 13076-OmpR$_{D55A}$ strain (Table II-1) using the appropriate pairs of primers (Table II-3).

To generate the deletion mutants, target genes were inactivated *in vitro* by deletion of each open reading frame using the PCR-mediated linker-scanning mutation method as described above. The deleted target genes were amplified by PCR with the appropriate pairs of primers (Table II-3), and each deleted gene was ligated into SacI-SphI-digested pCVD442. *E. coli* S17-1 λ*pir* containing pCVD442 with the deleted genes was used as a conjugal donor to an appropriate *S.* Enteritidis strain to generate the deletion mutants (Table II-1). The conjugation and isolation of the transconjugants were conducted as described above.

III-2-3. Western blot analysis

The *S.* Enteritidis cells were lysed using B-PER Bacterial Protein Extraction Reagent with Enzymes (Thermo Fisher Scientific, Waltham, MA). The protein levels of

OmpR and DnaK were detected using mouse anti-*S.* Enteritidis OmpR antibody and mouse anti-*E. coli* DnaK antibody (Enzo Life Science, Farmingdale, NY) as described previously (Ko & Choi, 2021).

III-2-4. Antimicrobial susceptibility test

The MICs for antibiotics in the *S.* Enteritidis strains were determined by broth microdilution method according to CLSI guidelines (Franklin et al., 2012) with minor modification. Briefly, the antibiotics were serially diluted 2-fold in LB medium, and the MIC was determined after static incubation for 22 h. For further analysis of antimicrobial susceptibility, survival of the *S.* Enteritidis strains in the presence of antibiotics was analyzed by monitoring their growth in LB medium with or without antibiotics. The overnight cultures of the *S.* Enteritidis strains diluted to an A_{600} of 0.05 were used to inoculate the medium and aerobically incubated for 6 h.

III-2-5. Transcriptome analysis and quantitative reverse transcription-PCR (qRT-PCR)

Total RNAs were isolated from the wild-type, *envZ*$_{P248L}$, and *envZ*$_{H243A}$ strains using a RNeasy mini kit (Qiagen, Valencia, CA). Strand-specific cDNA libraries constructed from two biological replicates of each sample were sequenced using Hiseq 2500 (Illumina, San Diego, CA) by ChunLab (Seoul, South Korea) as described previously (Hwang et al., 2021). The raw sequencing reads were mapped

to the reference genome of *S.* Enteritidis P125109 (GenBank accession number: GCA_000009505.1). The expression level of each gene was calculated, normalized, and analyzed statistically as described previously (Hwang et al., 2021) to identify the genes differentially expressed (log_2[fold change] > 1.5 with adjusted *p* value < 0.05). Gene ontology (GO) enrichment analysis was performed using the *goseq* R package version 1.42.0 (Young et al., 2010) to identify significantly enriched GO terms (*p* value < 0.0005). *k-means* clustering (MacQueen, 1967) was performed using R version 4.0.3 with a *k* value of 4 to cluster the genes by their expression pattern.

For qRT-PCR, total RNAs from the *S.* Enteritidis strains were quantified using a NanoDrop One Microvolume UV-visible Spectrophotometer (Thermo Fisher Scientific), and cDNA was synthesized from 1 μg of the total RNA using an iScript cDNA synthesis kit (Bio-Rad, Hercules, CA). Real-time PCR amplification of the cDNA was performed using a CFX96 real-time PCR detection system (Bio-Rad) with pairs of specific primers (Table II-3) as described previously (Choi et al., 2020). Relative expression of each gene was calculated using the 16S rRNA expression as an internal reference for normalization.

III-2-6. Outer membrane protein purification and identification

For outer membrane protein purification, the overnight culture of the *S.* Enteritidis strains were harvested by centrifugation at 5, 000 g for 10 min at 4°C. The cells were

resuspended in TM buffer [10 mM Tris-Cl (pH 7.5) and 10 mM $MgCl_2$] and lysed by sonication. After removing the cell debris by centrifugation, the clear cell lysate was centrifuged at 16,000 g for 1 h at 4°C to collect the membrane fraction. The inner membrane proteins were solubilized in 2% Triton X-100 and removed by centrifugation at 16,000 g for 1 h at 4°C. The residual insoluble fraction containing outer membrane proteins was resuspended in 100 mM Tris-Cl (pH 7.5). The concentration of the total outer membrane proteins was determined using Bradford method (Bradford, 1976), and the same amount of each sample was resolved by SDS-PAGE. For protein identification, the SDS gel containing the appropriate protein band was cut with a clean scalpel. The excised gels were digested with trypsin and analyzed using liquid chromatography-tandem mass spectrometry (LC-MS/MS) by National Instrumentation Center for Environmental Management (Seoul, South Korea).

III-2-7. Purification of OmpR, electrophoretic mobility shift assay (EMSA), and DNase I protection assay.

To overexpress OmpR, pDH2003 carrying the *ompR* gene on pET-28a(+) (Novagen, Madison, WI) was previously generated (Ko & Choi, 2021) and used in this study (Table II-1). The His_6-tagged OmpR was expressed in *E. coli* BL21(DE3) and purified by affinity chromatography (Qiagen).

For EMSA, the SEN1522 upstream region was amplified by PCR using unlabeled

PSEN1522-F and 6-carboxyfluorescein (6-FAM)-labeled PSEN1522-R as primers (Table II-3). Similarly, the SEN2875, *ompD*, and *ompW* upstream regions were amplified by PCR using the appropriate unlabeled forward primer and 6-FAM-labeled reverse primer (Table II-3). The 6-FAM-labeled DNA probes (10 nM) were incubated with different amounts of the purified OmpR for 30 min at 30°C in a 20-μl reaction mixture containing 1× OmpR binding buffer [10 mM Tris-Cl (pH 8.0), 50 mM KCl, 5 mM $MgCl_2$, 1 mM dithiothreitol, 0.1 μg μl^{-1} bovine serum albumin, and 5% glycerol] and 0.05 μg of poly(dI-dC) (Sigma-Aldrich, St. Louis, MO). For competition analysis, the same but unlabeled DNA was used as a self-competitor. Electrophoretic analysis of the OmpR-DNA complexes was performed as described previously (Choi et al., 2021).

For DNase I protection assay, the same labeled DNA probes for SEN1522, SEN2875, *ompD*, and *ompW* upstream regions were used. Each labeled DNA probe (40 nM) was incubated with the purified OmpR for 30 min at 30°C in a 20-μl reaction mixture containing 1× OmpR binding buffer and 0.05 μg of poly(dI-dC) (Sigma-Aldrich). The OmpR-DNA complexes were digested with DNase I as described previously (Choi et al., 2021). The digested DNA products were precipitated with ethanol, eluted in sterilized water, and analyzed using an ABI 3730xl DNA analyzer (Applied Biosystems, Foster City, CA) with Peak Scanner software version 1.0 (Applied Biosystems).

III-2-8. Manipulation of the cellular level of OmpR

To manipulate the cellular levels of wild-type OmpR and $OmpR_{D55A}$ in the *S.* Enteritidis strains, the wild-type *ompR* and *ompR*$_{D55A}$ regions were amplified from the wild-type and *ompR*$_{D55A}$ strains, respectively, using a pair of primers OMPRP-F and –R (Table II-3). The resulting fragments were subcloned into pJK1113 (Lim et al., 2014) under the arabinose-inducible promoter P_{BAD} to generate pDH2104 and pDH2108, respectively (Table II-1). The plasmids were transferred into an appropriate *S.* Enteritidis strain by electroporation, as described previously (Datsenko & Wanner, 2000). The cellular levels of OmpR were manipulated by adding different concentrations of arabinose in the growth medium.

III-2-9. Construction of *ompR-lacZ* transcriptional fusion reporter and β-galactosidase activity assay.

The P_{ompR} regulatory region (positions -271 to +18 relative to the first base of the *ompR* start codon) was amplified using a pair of primers PompR-F and –R (Table II-3) and then fused to the promoterless *lacZ* of pRKΩlacZ (Park et al., 2006) to generate pDH2105 (Table II-1). *E. coli* S17-1 λ*pir* containing pDH2105 was used as a conjugal donor to an appropriate *S.* Enteritidis strain as described previously (Lee et al., 2020). To determine the P_{ompR} activity, the β-galactosidase activities of the *S.* Enteritidis strains carrying pDH2105 were measured as described previously by Miller (Miller, 1972).

III-2-10. Data analysis

Average and standard deviation (SD) were calculated from at least three independent experiments. Statistical analyses were performed as indicated in the figure legends using GraphPad Prism 7.0 (GraphPad Software). The significance of differences between experimental groups was accepted at a p value < 0.05.

III-2-11. Accession number

All raw transcriptome data have been deposited in the NCBI BioProject database (https://www.ncbi.nlm.nih.gov/bioproject) under accession number PRJNA795528.

III-3. Results

III-3-1. The antibiotic resistance in *S.* Enteritidis is enhanced by the active state of EnvZ/OmpR

Previously, we proposed that the substitution of Pro248 of EnvZ with Leu (an *envZ*$_{P248L}$ mutation) increases the cellular level of OmpR-P in *S.* Enteritidis (Ko & Choi, 2021), mimicking the active state of EnvZ/OmpR. In this study, we substituted His243 of EnvZ with Ala (an *envZ*$_{H243A}$ mutation) to abolish the kinase activity of EnvZ and mimic the inactive state of EnvZ/OmpR. Indeed, the OmpR-P level was significantly higher in the *envZ*$_{P248L}$ strain than that in the wild type, while it was not detectable in the *envZ*$_{H243A}$ strain (Fig. III-1). To examine whether EnvZ/OmpR has an impact on antibiotic resistance in *S.* Enteritidis, MICs for various antibiotics in the wild type were compared with those in the *envZ*$_{P248L}$ and *envZ*$_{H243A}$ strains. The MICs in the *envZ*$_{P248L}$ strain were increased by 4-fold for β-lactams including ceftriaxone, cefotaxime, and ampicillin and by 2-fold for tetracycline, ciprofloxacin, and chloramphenicol, while the MICs in the *envZ*$_{H243A}$ strain were identical to those in the wild type (Table III-1). The MIC for polymyxin B did not differ in the wild-type, *envZ*$_{P248L}$ and *envZ*$_{H243A}$ strains (Table III-1). To further examine whether the effects of the *envZ*$_{P248L}$ mutation on the increased antibiotic resistance is dependent on OmpR, the MICs for the antibiotics in the Δ*ompR* and Δ*ompR envZ*$_{P248L}$ strains were determined. The MICs for the antibiotics in the Δ*ompR* strain were not

increased by the additional *envZ*$_{P248L}$ mutation (Table III-1), indicating that OmpR is required for the increased antibiotic resistance observed in the *envZ*$_{P248L}$ strain. These results indicated that the resistance to antibiotics, especially β-lactams, is enhanced by the active state of EnvZ/OmpR in *S.* Enteritidis.

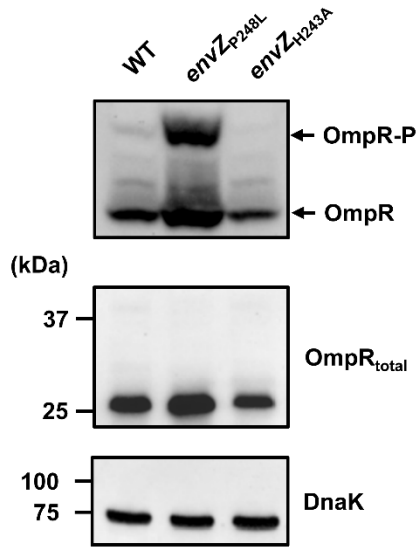

Figure III-1. The phosphorylation level of OmpR in *S.* Enteritidis with different genetic backgrounds. Total proteins were isolated from the *S.* Enteritidis strains grown to an A_{600} of 1.0. The phosphorylated status of OmpR was determined by Western blot analysis using Phos-tag SDS-PAGE gel (Wako, Osaka, Japan). The cellular levels of $OmpR_{total}$ and DnaK (as an internal control) were determined by Western blot analysis using standard SDS-PAGE gel. Molecular size markers (Bio-Rad) are shown in kilodaltons. WT, wild type; *envZ*$_{P248L}$, a strain expressing EnvZ$_{P248L}$; *envZ*$_{H243A}$, a strain expressing EnvZ$_{H243A}$.

Table III-1. Antibiotic resistance in *S.* Enteritidis with different genetic backgrounds

Strain name	MIC (mg l^{-1}) for antibiotics[a, b]						
	CRO	CTX	AMP	TET	CIP	CHL	PMB
ATCC 13076	0.0625	0.0625	1	1	0.016	4	0.25
ATCC 13076-$EnvZ_{P248L}$	0.25	0.25	4	2	0.032	8	0.25
ATCC 13076-$EnvZ_{H243A}$	0.0625	0.0625	1	1	0.016	4	0.25
Δ*ompR*	0.0625	0.0625	1	1	0.016	4	ND
Δ*ompR envZ*$_{P248L}$	0.0625	0.0625	1	1	0.016	4	ND

[a]CRO, ceftriaxone; CTX, cefotaxime; AMP, ampicillin; TET, tetracycline; CIP, ciprofloxacin; CHL, chloramphenicol; PMB, polymyxin B.

[b]ND, not determined.

III-3-2. The active state of EnvZ/OmpR induces differential expression of antibiotic resistance-related OMP genes

Because the *envZ*$_{P248L}$ mutation represses the *ompF* expression (Ko & Choi, 2021), the decreased expression of *ompF* might account for the increased antibiotic resistance in the *envZ*$_{P248L}$ strain. Thus, the effect of the *ompF* deletion on the MICs for β-lactams was examined in *S.* Enteritidis. The *ompF* deletion increased the MICs for β-lactams in the wild type by 2-fold but did not affect those in the *envZ*$_{P248L}$ strain (Table III-2), suggesting that down-regulation of *ompF* only partially contributes to the enhancement of antibiotic resistance in *S.* Enteritidis. To further identify genetic basis for the increased antibiotic resistance, transcriptomes of the wild-type, *envZ*$_{P248L}$, and *envZ*$_{H243A}$ strains were analyzed using RNA-seq. Transcriptome analysis revealed that 451 and 201 genes were differentially expressed by the *envZ*$_{P248L}$ and *envZ*$_{H243A}$ mutations, respectively (Table III-3). Then, the differentially expressed genes (DEGs) were grouped into four clusters with similar expression patterns using *k-means* clustering (MacQueen, 1967). As shown in Fig. III-2A, the genes in cluster A were activated by the *envZ*$_{P248L}$ mutation, showing two different patterns depending on whether their expression was altered by the *envZ*$_{H243A}$ mutation (cluster A-I) or not (cluster A-II). The genes in cluster B and C were down- and up-regulated by the *envZ*$_{H243A}$ mutation, respectively, whereas the expression of the genes in cluster D was down-regulated by the *envZ*$_{P248L}$ mutation but not affected by the *envZ*$_{H243A}$ mutation (Fig. III-2A). Because the resistance to multiple antibiotics

was elevated only by the *envZ*$_{P248L}$ mutation (Table III-1), the genes in clusters A-II and D, differentially expressed by the *envZ*$_{P248L}$ mutation but not by the *envZ*$_{H243A}$ mutation, were expected to contribute to antibiotic resistance.

To analyze the physiological roles of the genes in clusters A-II and D, GO enrichment analysis was performed. The GO terms linked to flagella-mediated motility and OMP activity were significantly enriched (Fig. III-2B). Within the enriched GO terms, antibiotic resistance-related OMP genes including SEN1522, SEN2875, *ompD*, and *ompW* (Hu et al., 2011; Hu et al., 2009; Lin et al., 2019) were particularly detected (Table III-4). Because the four OMP genes were newly recognized as an EnvZ/OmpR regulon, their expression was reevaluated by qRT-PCR. The expression of SEN1522 and SEN2875 was increased, and that of *ompD* and *ompW* was decreased by the *envZ*$_{P248L}$ mutation, while the expression of the four OMP genes was not affected by the *envZ*$_{H243A}$ mutation (Fig. III-2C), validating the RNA-seq results. Accordingly, the differential expression of the four OMP genes was considered as the most likely candidate responsible for the EnvZ/OmpR-mediated antibiotic resistance in *S.* Enteritidis.

Table III-2. Effects of the OMP genes on antibiotic resistance in *S.* Enteritidis

Strain name	MIC (mg l^{-1}) for antibiotics[a]		
	CRO	**CTX**	**AMP**
ATCC 13076	0.0625	0.0625	1
ATCC 13076-EnvZ$_{P248L}$	0.25	0.25	4
Δ*ompF*	0.125	0.125	2
Δ*ompF envZ*$_{P248L}$	0.25	0.25	4
ΔSEN1522	0.0625	0.0625	1
ΔSEN2875	0.0625	0.0625	1
Δ*ompW*	0.0625	0.0625	1
Δ*ompD*	0.125	0.25	2
Δ*ompD envZ*$_{P248L}$	0.25	0.5	4
Δ*ompD* Δ*ompF*	0.25	0.25-0.5	2-4

[a]CRO, ceftriaxone; CTX, cefotaxime; AMP, ampicillin.

Table III-3. List of DEGs by the *envZ*$_{P248L}$ and *envZ*$_{H243A}$ mutations

Locus tag[a]	Fold change (log_2)[b, c]		Gene product
	envZ$_{P248L}$/ WT	*envZ*$_{H243A}$/ WT	
IRO93_RS00050	2.43	0.36	Conserved hypothetical protein
IRO93_RS00055	2.8	-0.14*	Possible exported protein
IRO93_RS00060	0.03	-1.53	DnaK protein
IRO93_RS00065	-0.1	-1.57	DnaJ protein
IRO93_RS00275	-2.31	-0.36	Sensor kinase
IRO93_RS00295	-2.8*	0.68	Citrate-sodium symporter
IRO93_RS00320	-2.26*	-0.34	CitX protein
IRO93_RS00360	3.55	-0.68	Carnitine racemase
IRO93_RS00365	2.66	-0.35	Probable crotonobetaine/carnitine-CoA ligase
IRO93_RS00370	3.79	-0.24	L-carnitine dehydratase
IRO93_RS00375	4.49	-0.12	Probable carnitine operon oxidoreductase CaiA
IRO93_RS00420	5.29	-0.8	Probable secreted protein
IRO93_RS00425	9.67	-0.34	Putative sulfatase
IRO93_RS00525	1.68	-0.84	Arabinose operon regulatory protein
IRO93_RS00530	1.69	-0.11	DedA family integral membrane protein
IRO93_RS00590	1.58	-0.68*	Probable activator protein in leuABCD operon
IRO93_RS00800	8.95	0.06*	Probable secreted protein
IRO93_RS00805	3.92	0.15	Probable secreted protein
IRO93_RS01025	-1.07*	-1.93*	Minor fimbrial subunit StfF
IRO93_RS01075	2.78	-0.81	DegP protein
IRO93_RS01485	4.8	-0.5	Probable secreted protein
IRO93_RS01495	0.46	-1.97	Possible acyl-CoA dehydrogenase
IRO93_RS01735	5.39	-1.16	Putative metabolite transport protein
IRO93_RS01785	-2.5*	-0.49	Probable secreted protein
IRO93_RS01795	-2	3.05	Putative carboxyvinyl-carboxyphosphonate phosphorylmutase
IRO93_RS01800	-2.13	2.6	Methylcitrate synthase
IRO93_RS01805	-1.46	2.76	PrpD protein
IRO93_RS01810	-0.21	2.43	PrpE protein
IRO93_RS01830	1.56	0.09	Penicillin-binding protein AmpH
IRO93_RS01870	-2.02	-0.5	Conserved hypothetical protein

IRO93_RS02020	-2.65	-0.57	Nucleoside-specific channel-forming protein tsx precursor
IRO93_RS02135	2.98	0.38	Hpothetical major facilitator family transport protein
IRO93_RS02390	-0.21	-2.02	Heat shock protein HtpG
IRO93_RS02415	-2.61	0.42	Putative transport protein
IRO93_RS02420	1.89	0.39	Fosmidomycin resistance protein
IRO93_RS02425	-2.44	-0.27	UDP-sugar hydrolase
IRO93_RS02505	-2.83	0.06	Lipoprotein
IRO93_RS02510	-2.27	0.08	ABC transporter ATP-binding protein
IRO93_RS02665	-2.88*	-0.03	Type-1 fimbrial protein, a chain precursor
IRO93_RS02710	-1.68*	-0.96	Fimbrial protein
IRO93_RS02725	-0.14	2.13	Putative membrane protein
IRO93_RS02730	-0.59*	2.02	Bactoprenol glucosyl transferase
IRO93_RS02735	0.75*	2.96*	Bactoprenol-linked glucose translocase
IRO93_RS02905	-1.96	-0.91	Carbon starvation protein A
IRO93_RS02955	4.76*	0.1*	Conserved hypothetical protein
IRO93_RS02960	3.02	0.09	Molybdopterin-containing oxidoreductase catalytic subunit
IRO93_RS02965	3.83	0.16	Molybdopterin-containing oxidoreductase iron-sulfur subunit
IRO93_RS02995	0.21	1.71	Citrate carrier
IRO93_RS03010	-1.97	0.97	Citrate lyase alpha chain
IRO93_RS03015	-1.71	0.56	Citrate lyase beta chain
IRO93_RS03020	-2.19	0.41	Citrate lyase acyl carrier protein
IRO93_RS03025	-2.07	-0.47	[citrate (pro-3S)-lyase] ligase
IRO93_RS03040	-2.57	1.24	C4-dicarboxylate anaerobic carrier
IRO93_RS03160	-1.73	0.2	Probable permease
IRO93_RS03200	-1.52	-0.09	Chaperone heat shock protein
IRO93_RS03220	0.4	-1.98	Glutamate/aspartate transport ATP-binding protein GltL
IRO93_RS03225	0.19	-1.67	Glutamate/aspartate transport system permease protein GltK
IRO93_RS03235	-0.18	-2.42	ABC transporter periplasmic binding protein
IRO93_RS03310	-1.6	1.86	Asparagine synthetase B
IRO93_RS03345	-3.64	-0.96	Putative outer membrane protein
IRO93_RS03355	2.2	-0.67	Citrate-proton symporter
IRO93_RS03360	1.8	-0.75	Citrate utilization protein B

IRO93_RS03365	3.09	-0.27	Conserved hypothetical protein
IRO93_RS03410	0.22	3.41	Possible 5-nitroimidazole antibiotic resistance
IRO93_RS03415	-0.49	3.41	Putrescine-ornithine antiporter
IRO93_RS03420	-0.46	1.95	Ornithine decarboxylase
IRO93_RS03470	2.28	0.52	PTR2-family transport protein
IRO93_RS03505	-0.63	-1.53	Citrate synthase
IRO93_RS03510	-0.48	-1.53	Putative exported protein
IRO93_RS03530	0.71	-1.55	Succinate dehydrogenase iron-sulfur protein
IRO93_RS03545	-0.09	-1.64	Succinyl-CoA synthetase beta chain
IRO93_RS03550	-0.15	-1.74	Succinyl-CoA synthetase alpha chain
IRO93_RS03715	2.7	-0.98*	ABC transporter permease
IRO93_RS03720	2.47	-0.19	ABC transporter ATP-binding protein
IRO93_RS03725	-0.43	-1.87	Phosphoglycerate mutase 1
IRO93_RS03820	1.54	-1.57	Histidine ammonia-lyase
IRO93_RS03825	4.43	-1.2	Conserved hypothetical protein
IRO93_RS03850	1.66	0.41	Dethiobiotin synthetase
IRO93_RS04010	-2.21	-0.41	Glutamine-binding periplasmic protein precursor
IRO93_RS04015	1.63	-0.41	DNA protection during starvation protein
IRO93_RS04135	1.86*	-0.06*	Conserved hypothetical protein
IRO93_RS04140	1.85	0.19	Putative electron transfer flavoprotein (beta subunit)
IRO93_RS04145	2.43*	1.14*	Putative electron transfer flavoprotein (alpha subunit)
IRO93_RS04160	2.41	0.17	Putative flavoprotein
IRO93_RS04180	2.85	-0.65	PQQ-dependent sugar dehydrogenase
IRO93_RS04185	2.9	-0.71	Glutathione s-transferase family protein
IRO93_RS04415	2.49*	0.3*	Conserved hypothetical protein
IRO93_RS04535	-1.61	-0.96	Putative sopD2 type III secretion system effector protein
IRO93_RS04650	1.77	-0.23	Putative exported protein
IRO93_RS04670	-9.89	-2.38	Outer membrane protein F precursor
IRO93_RS04750	2.34	-0.57	Hypothetical phage protein
IRO93_RS04990	0.94	-1.58	4-hydroxyphenylacetate degradation bifunctional isomerase/decarboxylase

IRO93_RS05100	0.68	-2.43	Proline dehydrogenase
IRO93_RS05105	0.37	-2.38	Sodium/proline symporter
IRO93_RS05125	-1.74	0	Conserved hypothetical protein
IRO93_RS05135	-1.18*	2.71*	Putative secreted protein
IRO93_RS05320	-1.77*	0.19	Flagellar biosynthetic protein FliR
IRO93_RS05330	-2.22	0.05	Flagellar biosynthetic protein flip precursor
IRO93_RS05335	-3.85	-0.31	Flagellar protein FliO
IRO93_RS05340	-3.65	-0.43	Flagellar motor switch protein FliN
IRO93_RS05345	-4.06	-0.55	Flagellar motor switch protein FliM
IRO93_RS05350	-4.58	-0.39	FliL protein
IRO93_RS05355	-4.19	-0.59	Flagellar hook-length control protein
IRO93_RS05360	-4.46	-0.64	Flagellar FliJ protein
IRO93_RS05365	-4.15	-0.35	Flagellum-specific ATP synthase
IRO93_RS05370	-4.41	-0.71	Flagellar assembly protein FliH
IRO93_RS05375	-4.31	-0.44	Flagellar motor switch protein FliG
IRO93_RS05380	-4.27	-0.46	Flagellar basal-body M-ring protein
IRO93_RS05385	-4.8*	-0.53	Flagellar hook-basal body complex protein FliE
IRO93_RS05390	-2.21*	-0.43	Putative exported protein
IRO93_RS05395	0.1	-1.93	Conserved hypothetical protein
IRO93_RS05415	-5.77	-1.73	Flagellar protein FliT
IRO93_RS05420	-6.39	-1.93	Flagellar protein FliS
IRO93_RS05425	-7.48	-2.46	Flagellar hook associated protein FliD
IRO93_RS05430	-7.61*	-1.18	Hypothetical protein
IRO93_RS05435	-7.56	-1.05	Flagellin
IRO93_RS05440	-5.97	-0.85	Lysine-N-methylase
IRO93_RS05445	-5.25	-1.92	RNA polymerase sigma transcription factor for flagellar operon
IRO93_RS05450	-4.53	-1.75	Regulatory protein FliZ
IRO93_RS05475	-2.78	-1.84	Cell-division regulatory protein
IRO93_RS05525	-2	-0.3	Putative exported protein
IRO93_RS05530	-2.53	0.24	Conserved hypothetical protein
IRO93_RS05555	-3.57*	-0.63	Putative lipoprotein
IRO93_RS05600	-2.13	0.47	Flagellar transcriptional activator FlhD
IRO93_RS05605	-2.18	0.65	Flagellar transcriptional activator
IRO93_RS05610	-6.46	-2.27	Motility protein A

IRO93_RS05615	-5.3	-2.12	Motility protein B
IRO93_RS05620	-4.53	-1.96	Chemotaxis protein CheA
IRO93_RS05625	-4.92	-2.59	Purine binding chemotaxis protein
IRO93_RS05630	-6.89	-2.28	Methyl-accepting chemotaxis protein II
IRO93_RS05635	-5.6	-2.06	Chemotaxis protein methyltransferase
IRO93_RS05640	-4.65	-1.98	Chemotaxis response regulator protein-glutamate methylesterase
IRO93_RS05645	-4.45	-1.57	Chemotaxis protein CheY
IRO93_RS05650	-4.15	-1.37	Chemotaxis protein CheZ
IRO93_RS05655	-3.15	-0.11	Flagellar biosynthetic protein FlhB
IRO93_RS05660	-2.54	-0.09	Flagellar biosynthesis protein FlhA
IRO93_RS05665	-2.65	-0.1	Flagellar protein FlhE precursor
IRO93_RS05675	3.22	0.16	Penicillin-binding protein
IRO93_RS05710	4.04	0.09	Conserved hypothetical protein
IRO93_RS05715	4.38	-0.81	Putative hydrolase
IRO93_RS05765	-1.5	0.28	High-affinity zinc uptake system ATP-binding protein
IRO93_RS05840	1.53	0.02	Conserved hypothetical protein
IRO93_RS05880	1.93	0.32	Putative phage protein
IRO93_RS05885	1.95*	1.83*	Hypothetical phage protein
IRO93_RS05905	-1.73	-0.63	Hypothetical phage protein
IRO93_RS05910	-4.38	-0.36	Putative phage lipoprotein
IRO93_RS06005	-1.21	-3.47*	Putative phage membrane protein
IRO93_RS06095	-1.69	-0.53	Hypothetical protein
IRO93_RS06100	3.41*	-3.56*	Conserved hypothetical protein
IRO93_RS06165	2.6	0.8	Putative membrane transport protein
IRO93_RS06200	3.81	0.67	Penicillin-binding protein
IRO93_RS06205	1.55	0.48	RRNA guanine-N1-methyltransferase
IRO93_RS06235	-1.54	0.11	Putative membrane protein
IRO93_RS06330	-0.36	-1.54	Conserved hypothetical protein
IRO93_RS06385	-4.29	-1.57	Conserved hypothetical protein
IRO93_RS06450	1.22*	1.6*	Putative membrane protein
IRO93_RS06545	-0.76	-2.61	Nitrate/nitrite response regulator protein NarL
IRO93_RS06550	-0.35	-2.97	Nitrate/nitrite sensor protein NarX
IRO93_RS06555	-0.78	-7.6	Nitrite extrusion protein
IRO93_RS06560	-1.04	-7.31	Respiratory nitrate reductase 1 alpha chain

IRO93_RS06565	-2.46	-5.37	Respiratory nitrate reductase 1 beta chain
IRO93_RS06570	-2.35	-4.9	Respiratory nitrate reductase 1 delta chain
IRO93_RS06575	-1.62	-3.83	Respiratory nitrate reductase 1 gamma chain
IRO93_RS06740	-1.57	0.39	Putative outer membrane protein
IRO93_RS06890	-1.53	0.04	Putative regulatory protein
IRO93_RS06910	1.96	-0.17	Conserved hypothetical protein
IRO93_RS06925	-0.8*	-1.72*	Hypothetical protein
IRO93_RS07130	-3.88	-0.25	Putative chemo-receptor protein
IRO93_RS07210	2.33*	0.96*	Predicted phage protein
IRO93_RS07265	-1.04	-1.54	Conserved hypothetical protein
IRO93_RS07270	3.01	-0.8	Probable pyruvate-flavodoxin oxidoreductase
IRO93_RS07275	3.83*	1.27*	Conserved hypothetical protein
IRO93_RS07335	-2.33	-0.47	Conserved hypothetical protein
IRO93_RS07380	1.55*	0.02*	Conserved hypothetical protein
IRO93_RS07395	-5.29	-2	Methyl-accepting chemotaxis protein III
IRO93_RS07430	1.63	-1.64	Putative hexonate dehydrogenase
IRO93_RS07435	2.64	-1.62*	Putative hexonate sugar transport protein
IRO93_RS07440	2.41	-0.98	Putative hexonate dehydrogenase
IRO93_RS07445	1.59	-0.94	Putative dehydratase
IRO93_RS07540	-2.88*	-1.2*	Putative membrane protein
IRO93_RS07575	-2.02	-0.2	Putative virulence effector protein
IRO93_RS07580	-3.35	-0.41	Putative virulence effector protein
IRO93_RS07585	-3.12	-0.34	Putative virulence effector protein
IRO93_RS07625	6.54*	-0.63*	Putative lipoprotein
IRO93_RS07685	-2.72	0.42	Conserved hypothetical protein
IRO93_RS07690	-8.08	-0.23	Outer membrane porin protein
IRO93_RS07700	-1.62	-0.39	Formate dehydrogenase, nitrate-inducible, major subunit
IRO93_RS07705	-1.57	-0.4	Formate dehydrogenase, nitrate-inducible, iron-sulfur subunit
IRO93_RS07710	-1.51	-0.33	Formate dehydrogenase, nitrate-inducible, cytochrome subunit
IRO93_RS07715	2.7	-1.95	Alcohol dehydrogenase
IRO93_RS07740	-2.53	-0.7	Putative secreted protein
IRO93_RS07780	1.81*	0.12*	Hypothetical protein
IRO93_RS07840	6.74	-1.9	Putative secreted hydrolase

IRO93_RS07845	4.4	-3.59	Uptake hydrogenase small subunit
IRO93_RS07850	4.36	-2.66	Uptake hydrogenase-1 large subunit
IRO93_RS07855	3.65	-1.79	Ni/Fe-hydrogenase 1 b-type cytochrome subunit
IRO93_RS07860	3.35	-1.59	Hydrogenase 1 maturation protease
IRO93_RS07865	3.03	-1.28	Hydrogenase isoenzymes formation protein
IRO93_RS07870	2.93	-1.21	Hydrogenase-1 operon protein
IRO93_RS07875	3.17	-0.92	Hydrogenase-1 operon protein
IRO93_RS07880	3.01	-0.85	Putative ATP/GTP-binding protein
IRO93_RS07885	3.18	-1.49*	Hydrogenase nickel incorporation protein (HypA)
IRO93_RS07890	11.49	-2.11*	Outer membrane protein
IRO93_RS07895	6.2	-1.42	Putative exported protein
IRO93_RS07940	1.58	0.48	Multiple antibiotic resistance protein MarA
IRO93_RS08045	0.26	2.07	Putative dimethyl sulphoxide reductase subunit A
IRO93_RS08050	0.35	2.18	Putative dimethyl sulphoxide reductase subunit
IRO93_RS08055	0.64	1.97	Putative anaerobic dimethyl sulfoxide reductase
IRO93_RS08095	-2.18	-0.08	Dethiobiotin synthetase
IRO93_RS08115	2.92	0.6	Acid shock protein
IRO93_RS08130	-0.75	1.93	Putative drug resistance protein
IRO93_RS08170	5.5	-1.55	Outer membrane protein
IRO93_RS08320	-2.16	-0.24	Transcriptional regulator
IRO93_RS08455	-1.63	-0.49	Putative type III secretion protein
IRO93_RS08485	-1.74*	-0.86	Putative secretion system protein
IRO93_RS08495	-2.61*	-1.21*	Putative pathogenicity island protein
IRO93_RS08500	-1.65*	-1.91*	Putative pathogenicity island lipoprotein
IRO93_RS08510	-1.57*	-3.18*	Putative pathogenicity island protein
IRO93_RS08585	1.6	-2.08*	Putative two-component sensor kinase
IRO93_RS08620	3.13*	0.96*	Tetrathionate reductase subunit B
IRO93_RS08635	-2.91*	-0.19	Putative ribokinase/regulatory protein
IRO93_RS08645	-1.75	0.35	Putative hydrolase
IRO93_RS08690	-0.99	-1.63	Putative ABC transport ATP-binding subunit
IRO93_RS08695	-0.84	-1.81	Conserved hypothetical protein
IRO93_RS08700	-1.59	-2.49*	Conserved hypothetical protein

IRO93_RS08900	-1.57	-0.61	Putative DNA/RNA non-specific endonuclease
IRO93_RS08910	-2.87*	-0.76	Putative outer membrane protein
IRO93_RS08945	1.55	-0.03	Conserved hypothetical protein
IRO93_RS08950	2.53	-0.76	Putative sodium:dicarboxylate symporter
IRO93_RS08970	-1.53	0.83	Phospho-beta-glucosidase B
IRO93_RS08985	-2.24	0.04	PTS system, cellobiose-specific IIC component
IRO93_RS08990	-1.57	-0.35	PTS system, cellobiose-specific IIB component
IRO93_RS09045	-2.94	-1.76	Putative MutT-family protein
IRO93_RS09050	-3.61	-2.41	Putative exported protein
IRO93_RS09075	2.07	0.45	Protease IV
IRO93_RS09080	2.29	0.17	L-Asparaginase I
IRO93_RS09085	2.41	0.23	Pyrazinamidase/nicotinamidase
IRO93_RS09150	2.98	0.03	Putative oxidoreductase
IRO93_RS09155	6.66	-0.12	Putative regulatory protein
IRO93_RS09160	-4.82	-0.47	Putative outer membrane protein
IRO93_RS09235	3.26	0.08	Putative membrane protein
IRO93_RS09240	0.32	-1.72*	Conserved hypothetical protein
IRO93_RS09245	0.31	-2.47*	Conserved hypothetical protein
IRO93_RS09280	-3.17*	-0.93	Conserved hypothetical protein
IRO93_RS09325	-0.08	-2.69	Putative lipoprotein
IRO93_RS09330	-1.81	-0.81	Putative cytochrome
IRO93_RS09345	-3.54*	-0.06	Hypothetical protein
IRO93_RS09350	-2.54	0.08	Putative secreted protein
IRO93_RS09360	-3.08	-0.77	Outer membrane invasion protein
IRO93_RS09375	-3.66*	0.4	Putative lipoprotein
IRO93_RS09665	-4.83	-1.8	Flagellar hook-associated protein 3
IRO93_RS09670	-5.96	-1.85	Flagellar hook-associated protein 1
IRO93_RS09675	-3.86	-0.01	Flagellar protein FlgJ
IRO93_RS09680	-4.45	0.03	Flagellar P-ring protein precursor
IRO93_RS09685	-5.07	-0.27	Flagellar L-ring protein precursor
IRO93_RS09690	-4.55	-0.54	Flagellar basal-body rod protein FlgG (distal rod protein)
IRO93_RS09695	-4.98	-0.52	Putative flagellar basal-body rod protein FlgF (proximal rod protein)
IRO93_RS09700	-5.06	-0.65	Flagellar hook protein FlgE
IRO93_RS09705	-4.83	0.01	Flagellar hook formation protein FlgD

IRO93_RS09710	-4.77	0.33	Putative flagellar basal-body rod protein FlgC (proximal rod protein)
IRO93_RS09715	-4.53	0.18	Putative flagellar basal-body rod protein FlgB (proximal rod protein)
IRO93_RS09720	-4.2	-0.77	Flagellar basal body P-ring protein FlgA precursor
IRO93_RS09725	-5.48	-2.15	Negative regulator of flagellin synthesis (anti-sigma factor)
IRO93_RS09730	-4.59	-2.05	Flagella synthesis protein FlgN
IRO93_RS09735	2.09	0.4	Virulence factor MviN
IRO93_RS09800	-1.77	-1.82	Putative exported protein
IRO93_RS09855	-2.62	-1.02	Conserved hypothetical protein
IRO93_RS09865	-2.39*	0.35*	Major curlin subunit precursor
IRO93_RS09875	-3.28*	-3.09*	Csg operon transcriptional regulator protein
IRO93_RS09880	-5.27*	-1.86*	Assembly/transport component in curli production
IRO93_RS10280	-2.25*	-0.46	Putative type IV prepilin
IRO93_RS10455	1.8	0	Putative membrane transport protein
IRO93_RS10465	-0.04	1.5	Putative exported protein
IRO93_RS10470	0.52	2.75	Nicotinate-nucleotide--dimethylbenzimidazole phosphoribosyltransferase
IRO93_RS10475	0.89	3.43	Cobalamin (5'-phosphate) synthase
IRO93_RS10480	0.79	3.41	Cobinamide kinase and guanylyltransferase
IRO93_RS10485	0.71	3.22	Putative cobyric acid synthase
IRO93_RS10490	1.02	3.17	Putative cobalt transport ATP-binding protein
IRO93_RS10495	1.64	3.72	Putative cobalt transport protein
IRO93_RS10500	1.83	3.43	Putative cobalt transport protein CbiN
IRO93_RS10505	1.93	3.49	Cobalamin biosynthesis protein
IRO93_RS10510	1.81	3.09	Precorrin-2 C20-methyltransferase
IRO93_RS10515	2.15	3.07	Sirohydrochlorin cobaltochelatase
IRO93_RS10520	2.14	2.31	Cobalt-precorrin-6a reductase
IRO93_RS10525	2.11	2.13	Precorrin-3 C17-methyltransferase
IRO93_RS10530	2.33	1.64	Cobalamin biosynthesis protein
IRO93_RS10535	2.16	1.19	Precorrin-4 C11-methyltransferase
IRO93_RS10540	2.22	-0.37	Precorrin-8W decarboxylase
IRO93_RS10545	2.29	-0.49	Precorrin-6Y C5,15-methyltransferase [decarboxylating]
IRO93_RS10550	1.6	-0.07	Cobalt-precorrin-6A synthase

			[deacetylating]
IRO93_RS10590	0.62	1.62	Glycerol dehydratase large subunit
IRO93_RS10595	0.96*	1.64*	Diol dehydratase medium subunit
IRO93_RS10600	1.18*	3.49*	Diol dehydratase small subunit
IRO93_RS10670	0.88*	2.04*	Putative propanediol utilization protein PduV
IRO93_RS10675	0.39	2.09	Acetokinase.
IRO93_RS10690	1.88	-0.2	Putative membrane protein
IRO93_RS10695	2.41	-0.77	Putative DNA gyrase inhibitory protein
IRO93_RS10700	4.46	0.25	Penicillin-binding protein
IRO93_RS10705	-2.49	0.24	Thiosulfate reductase cytochrome b subunit
IRO93_RS10710	-3.57	0.23	Thiosulfate reductase electron transport protein PhsB
IRO93_RS10715	-4.39	-0.15	Thiosulfate reductase precursor
IRO93_RS11000	2.42*	0.48*	Putative polysaccharide export protein
IRO93_RS11150	2.21	-0.46	Conserved hypothetical protein
IRO93_RS11155	1.68	-0.04	Putative exported protein
IRO93_RS11170	-3.04*	-1.46*	Putative fimbrial subunit protein
IRO93_RS11190	-1.62*	-0.13	Putative lipoprotein
IRO93_RS11255	1.53	0.67	Penicillin-binding protein
IRO93_RS11270	1.72	-0.06	Putative oxidoreductase
IRO93_RS11275	3.11	-0.23	Putative lipoprotein
IRO93_RS11330	1.86	0.07	Cytidine deaminase
IRO93_RS11390	2.46	-0.31	Putative DNA-binding protein
IRO93_RS11395	5.47	-0.32	Putative L-serine dehydratase
IRO93_RS11400	2.71*	0.79*	Putative hydrolase
IRO93_RS11435	-1.58	-3.54	PTS system, fructose-specific IIBC component
IRO93_RS11440	-1.2	-4.23	1-phosphofructokinase
IRO93_RS11445	-1.21	-4.75	Pts system, fructose-specific IIA/FPR component
IRO93_RS11605	-3.36	0.66	Cytochrome c-type biogenesis protein H1
IRO93_RS11610	-3.23	0.44	Thiol:disulfide interchange protein
IRO93_RS11615	-3.3	0.39	Cytochrome C-type biogenesis protein
IRO93_RS11620	-3.81	-0.34	Cytochrome C-type biogenesis protein
IRO93_RS11625	-3.97*	-0.54	Heme exporter protein D

IRO93_RS11630	-3.61	-0.79	Heme exporter protein C
IRO93_RS11635	-3.35	-0.64	Heme exporter protein B1
IRO93_RS11640	-4.79	-1.49	Cytochrome C biogenesis ATP-binding export protein
IRO93_RS11645	-4.95	-1.85	Cytochrome c-type protein NapC
IRO93_RS11650	-5.91	-1.92	Cytochrome c-type protein NapB precursor
IRO93_RS11655	-5.08	-1.44	Ferredoxin-type protein NapH
IRO93_RS11660	-6.62	-1.53	Ferredoxin-type protein NapG
IRO93_RS11665	-6.01	-1.77	Probable nitrate reductase
IRO93_RS11670	-6.53*	-2.08	Putative napAB assembly protein
IRO93_RS11675	-5.99	-2.11	Ferredoxin-type protein NapF
IRO93_RS11700	1.04	-1.97	Thiamine biosynthesis protein
IRO93_RS11705	0.98	-6.67	Outer membrane protein C
IRO93_RS11770	-1.75	0.37	Putative transcriptional regulator
IRO93_RS11775	-2.58	-0.05	Glycerophosphoryl diester phosphodiesterase periplasmic precursor
IRO93_RS11780	-3.04	0.01	Glycerol-3-phosphate transporter
IRO93_RS11795	-1.54	0.36	Anaerobic glycerol-3-phosphate dehydrogenase subunit C
IRO93_RS11835	2.75	-1.48	Conserved hypothetical protein
IRO93_RS11935	-5.39	-2.7	Putative receptor/regulator protein
IRO93_RS11940	-1.83	-1.32	Lipoprotein
IRO93_RS12070	-0.21	1.9	Putative transketolase C-terminal section
IRO93_RS12075	-0.33	1.75	Putative transketolase N-terminal section
IRO93_RS12175	-1.11	-2.96	Putative transcriptional regulator
IRO93_RS12325	-2.75	0.14	Long-chain fatty acid transport protein precursor
IRO93_RS12400	4.57	4.33	Phosphoglycerate transporter protein
IRO93_RS12410	1.22	1.55	Putative acyltransferase
IRO93_RS12565	2.6	-1.21	Cysteine synthase A
IRO93_RS12620	3.76	-2.22	Sulphate transport ATP-binding protein CysA
IRO93_RS12625	4.59	-0.88	Sulphate transport system permease protein CysW
IRO93_RS12630	4.71	-1.05	Sulphate transport system permease protein CysT
IRO93_RS12635	4.73	-1.23	Thiosulphate-binding protein precursor
IRO93_RS12665	2.6	-0.41	Probable N-acetylmuramoyl-L-

			alanine amidase
IRO93_RS12670	2.6	0.04	Coproporphyrinogen III oxidase, aerobic
IRO93_RS12675	2.44*	1.04*	Putative membrane protein
IRO93_RS12820	-5.6	-1.22	Protein YpfM
IRO93_RS12975	-0.17	1.56	Inosine-5'-monophosphate dehydrogenase
IRO93_RS13075	-1.73	0.24	Dimethyl sulfoxide reductase
IRO93_RS13085	-1.82	0	Putative lipoprotein
IRO93_RS13160	-0.17	1.67	Extragenic suppressor protein SuhB
IRO93_RS13170	-1.8	-1.13	Anaerobic sulfite reductase subunit A
IRO93_RS13225	-0.75	2.1	Lysine decarboxylase
IRO93_RS13395	1.74	1.46	Putative membrane protein
IRO93_RS13515	2.01	0.62	Phospho-2-dehydro-3-deoxyheptonate aldolase, tyr-sensitive
IRO93_RS13520	-1.63	0.5	Putative exported protein
IRO93_RS13695	-2.57	0.85	Putative transcriptional regulator
IRO93_RS13700	5.71	-0.13	Putative cation transporter
IRO93_RS13715	-0.79	-3.94	Putative exported protein
IRO93_RS13720	-0.73	-3.83	Putative membrane protein
IRO93_RS13725	-0.16	-2.23	Putative membrane protein
IRO93_RS13760	-1.74*	-1.46	Conserved hypothetical protein
IRO93_RS13815	-0.03*	-2.75*	Putative glutaredoxin
IRO93_RS13820	-0.55*	-2.6*	Conserved hypothetical protein.
IRO93_RS13845	-1.06	-1.6	Glycine betaine-binding periplasmic protein precursor
IRO93_RS14000	0.73*	1.53*	Electron transport protein
IRO93_RS14045	1.83*	3.18*	Formate hydrogenlyase subunit 2
IRO93_RS14050	3.08*	5.06*	Formate hydrogenlyase regulatory protein
IRO93_RS14115	2.06*	1.39*	Possible AraC-family transcriptional regulator
IRO93_RS14150	-2*	-0.61	Pathogenicity 1 island effector protein
IRO93_RS14155	-1.5	-0.09	Pathogenicity 1 island effector protein
IRO93_RS14160	-1.79	-0.27	AraC-family transcriptional regulator
IRO93_RS14200	-1.7*	-0.64	Pathogenicity island 1 effector protein
IRO93_RS14205	-1.64	-0.56	Pathogenicity island 1 effector

			protein
IRO93_RS14260	-2.19*	-0.95*	Secretory protein (associated with virulence)
IRO93_RS14285	2.08*	1.08*	Cell adherance/invasion protein
IRO93_RS14360	0.25	1.52	Conserved hypothetical protein
IRO93_RS14370	1.5*	1.44*	Possible sugar aldolase
IRO93_RS14375	1.4	2.06	Conserved hypothetical protein
IRO93_RS14450	5.02	-1.21*	Conserved hypothetical protein
IRO93_RS14455	3.82	-0.65	Adenylylsulfate kinase
IRO93_RS14460	3.92	-0.89	Sulfate adenylyltransferase subunit 1
IRO93_RS14465	5.48	-0.55	Sulfate adenylyltransferase subunit 2
IRO93_RS14515	2.35	-0.42*	Possible secreted protein
IRO93_RS14520	4.36	-1.11	Phosphoadenosine phosphosulfate reductase
IRO93_RS14525	4.22	-0.64	Sulfite reductase (NADPH) hemoprotein alpha subunit
IRO93_RS14530	3.88	-0.03	Sulfite reductase (NADPH) flavoprotein beta subunit
IRO93_RS14565	3.53*	0.67*	Major fimbrial subunit
IRO93_RS14625	-0.32	2.25	Glucarate dehydratase-related protein
IRO93_RS14630	-0.46	3.44	Glucarate transporter
IRO93_RS14775	2.11	0.11	N-acetylmuramoyl-L-alanine amidase
IRO93_RS14885	-0.3	1.62	Diaminopimelate decarboxylase
IRO93_RS14970	2.45	-1.33*	Probable fimbrial protein
IRO93_RS14975	6.47	0.04	Conserved hypothetical protein
IRO93_RS14980	7.43	-0.38	Outer membrane protein
IRO93_RS15265	1.53	0.91	Conserved hypothetical protein
IRO93_RS15285	2.51	-0.54	Galactose-proton symport
IRO93_RS15415	-1.59*	-0.17	Conserved hypothetical protein
IRO93_RS15435	-0.64	-1.54	Putative LysR-family transcriptional regulator
IRO93_RS15445	1.83	0.18	Arylsulfatase regulator
IRO93_RS15455	-1.96*	-0.02	Hypothetical protein
IRO93_RS15500	-0.09	-2.06	Hexuronate transporter
IRO93_RS15505	0.16	-1.57	D-mannonate hydrolase
IRO93_RS15520	-4.76	-1.05	Hypothetical protein
IRO93_RS15585	-3.39*	-1.64*	Conserved hypothetical protein
IRO93_RS15590	-3.26	-0.97	Methyl-accepting chemotaxis protein

IRO93_RS15600	-3.28	-0.71	Exported protein
IRO93_RS15605	-4.3*	-0.25	Hypothetical protein
IRO93_RS15610	-2.99*	-0.21	Hypothetical protein
IRO93_RS15675	2.08	-0.19	Putative membrane transport protein (periplasmic component)
IRO93_RS15925	-3.51	-2.94	Methyl-accepting chemotaxis protein II
IRO93_RS15930	-3.12	-2.39	Aerotaxis receptor protein
IRO93_RS15970	-4.27	-0.58	Probable membrane transport protein
IRO93_RS15975	-3.15	0.3	Putative membrane protein
IRO93_RS15980	-2.63	0.55	Putative exported protein
IRO93_RS16020	1.68	0.24	Possible LysR-family transcriptional regulator
IRO93_RS16040	-2.11	-0.23	Putative membrane transport protein
IRO93_RS16045	-0.21	3.71	L-serine dehydratase
IRO93_RS16050	-0.15	5.92	Formate acetyltransferase
IRO93_RS16055	-0.23	3.83	Propionate kinase
IRO93_RS16060	-1.03	2.3	Threonine/serine transporter
IRO93_RS16065	-2.68	1.46	Catabolic threonine dehydratase
IRO93_RS16070	-3.11	0.15	TDC operon transcriptional activator
IRO93_RS16080	0.35	2.4	Glycerate kinase
IRO93_RS16085	0.4	2.75	Tartronate semialdehyde reductase
IRO93_RS16090	-0.01	3.15	5-keto-4-deoxy-D-glucarate aldolase
IRO93_RS16095	0.52	2.06	D-galactarate dehydratase
IRO93_RS16220	0.73	2.07	ATP-dependent RNA helicase (dead-box protein)
IRO93_RS16445	1.63	-0.14	Phosphocarrier protein
IRO93_RS16515	-1.95	-1.24	Putative sialic acid transporter
IRO93_RS16520	-2.97	0.07	N-acetylneuraminate lyase
IRO93_RS16620	0.18	-1.87	Malate dehydrogenase
IRO93_RS16630	3.23	0.22	Conserved hypothetical protein
IRO93_RS16635	2.72	0.46	Conserved hypothetical protein
IRO93_RS16785	3.7	-0.69	Possible lipoprotein
IRO93_RS17190	1.86	0.6	Peptidyl-prolyl cis-trans isomerase
IRO93_RS17195	2.27	0.66	Putative membrane protein
IRO93_RS17200	-0.73	-5.29	Nitrite reductase large subunit
IRO93_RS17205	-1.53	-4.5	Nitrite reductase (NAD(P)H) small subunit
IRO93_RS17210	-2.35	-3.62	Putative nitrite transporter

IRO93_RS17295	1.92	0.03	Putative NUDIX hydrolase
IRO93_RS17330	2.27	0.07	Two-component sensor kinase EnvZ
IRO93_RS17335	2.05	-0.53	Two-component response regulator OmpR
IRO93_RS17350	1.78	-1.93	Putative ferrous iron transport protein
IRO93_RS17355	1.67	-1.98	Ferrous iron transport protein B
IRO93_RS17360	1.23	-1.8	Conserved hypothetical protein
IRO93_RS17385	0.56	-1.83	High-affinity gluconate transporter
IRO93_RS17390	-1.85	-0.12	4-alpha-glucanotransferase
IRO93_RS17395	-1.51	0.26	Maltodextrin phosphorylase
IRO93_RS17400	-3.43	-0.51	MalT regulatory protein
IRO93_RS17405	-1.77	-0.24	Conserved hypothetical protein
IRO93_RS17485	-1.51	-0.77	Putative IclR-family transcriptional regulator
IRO93_RS17625	-1.74	-1.01	High-affinity branched-chain amino acid transport ATP-binding protein
IRO93_RS17640	-1.53	-0.53	Leucine-specific binding protein
IRO93_RS17705	-3.98	-1.96	Methyl-accepting chemotaxis citrate transducer
IRO93_RS17810	1.67	0.09	L-asparginase
IRO93_RS17815	3.16	0.38	Anaerobic C4 dicarboxylate membrane transport protein
IRO93_RS17820	3.68	1.14	Putative carbohydrate kinase
IRO93_RS17825	3.62	0.33	Putative phosphosugar-binding protein
IRO93_RS17840	-4.38	-0.98	Putative membrane protein
IRO93_RS17845	1.77*	-0.77*	Phage-like lysozyme
IRO93_RS17850	3.2	-1.56*	Hypothetical luxR-family transcriptional regulator
IRO93_RS17865	-1.56	-0.51	Hypothetical metabolite transport protein
IRO93_RS17875	-6.58	-2.34	Conserved hypothetical protein
IRO93_RS17890	-2.34	-0.79	C4-dicarboxylate transport protein
IRO93_RS17960	-3.87	-1.59	Dipeptide transport ATP-binding protein DppF
IRO93_RS17965	-3.95	-1.47	Dipeptide transport ATP-binding protein DppD
IRO93_RS17970	-4.1	-1.16	Dipeptide transport system permease protein DppC
IRO93_RS17975	-5.01	-1.3	Dipeptide transport system permease protein DppB
IRO93_RS17980	-5.42	-1.18	Periplasmic dipeptide transport protein precursor

IRO93_RS18040	1.87*	0.56*	Long polar fimbria protein A (LpfA)
IRO93_RS18065	4.06	-0.71	Putative outer membrane protein
IRO93_RS18105	-2.35*	-0.29	Putative acetyltransferase
IRO93_RS18130	1.7	0.16	Putative membrane protein
IRO93_RS18160	-1.65	0.75	Alpha-amylase
IRO93_RS18305	2.96	0.4	Putative L-lactate dehydrogenase operon regulator
IRO93_RS18310	3.17	0.36	Putative L-lactate dehydrogenase
IRO93_RS18575	1.8	-0.92	Putative exported protein
IRO93_RS18580	1.72	-0.99	Putative glycosyl hydrolase
IRO93_RS18585	1.83	-0.68	Sodium:galactoside family symporter
IRO93_RS18650	4.68	-1*	Putative hydrolase
IRO93_RS18670	2.13*	1.1*	Mg(2+) transport ATPase protein C
IRO93_RS18675	2.62	-0.33	Putative membrane protein
IRO93_RS18710	1.63*	2.45*	Putative PTS system protein
IRO93_RS18810	2.16	0.19	Type I toxin-antitoxin system toxin TisB
IRO93_RS18825	2.41	-0.36	Hypothetical protein
IRO93_RS18885	-2.88	0.63	Cytochrome C-type biogenesis protein
IRO93_RS18920	-4.13	-0.97	Heme exporter protein A2
IRO93_RS18925	-1.83	0.79	Probable cytochrome c peroxidase
IRO93_RS18930	-1.54*	0.26	TorD protein
IRO93_RS18940	-1.51	0.41	Cytochrome c-type protein
IRO93_RS18990	-1.53*	-0.47	Putative membrane transport protein
IRO93_RS19200	-0.89	3.15	Asparagine synthetase A
IRO93_RS19205	0.07	1.56	Conserved hypothetical protein
IRO93_RS19580	1.98*	1.2*	Conserved hypothetical protein
IRO93_RS19585	-3.78	0.25	Detergent-resistant phospholipase A
IRO93_RS19640	1.7	-0.59	Uridine phosphorylase
IRO93_RS19705	0.8	-3.18	Small (beta) subunit of the fatty acid-oxidizing multienzyme complex
IRO93_RS19710	0.95	-2.87	Large (alpha) subunit of the fatty acid-oxidizing multienzyme complex
IRO93_RS19910	-0.29	-1.61	Putative sugar kinase
IRO93_RS20070	-1	-2.61	Manganese superoxide dismutase
IRO93_RS20115	3.92	-0.99	Periplasmic sulphate binding protein
IRO93_RS20130	-0.56	-1.68	Putative carbohydrate kinase

IRO93_RS20135	-0.81	-1.51	Hypothetical protein
IRO93_RS20230	0.9	-1.66	Glycerol kinase
IRO93_RS20325	1.75	-0.45	Conserved hypothetical protein
IRO93_RS20460	-1.6	0.74	Vitamin B12 receptor protein
IRO93_RS20585	2.15*	0.78*	Conserved hypothetical protein
IRO93_RS20590	2.12	0.03	Conserved hypothetical protein
IRO93_RS20595	2.27*	0.77*	Conserved hypothetical protein
IRO93_RS20610	-0.18	-1.9*	Thiamine biosynthesis protein
IRO93_RS20725	-0.29	-1.64	Isocitrate lyase
IRO93_RS20750	2.43	-0.55	Putative membrane protein
IRO93_RS20850	-1.67	-0.42	Maltose transport inner membrane protein
IRO93_RS20855	-1.61	0.01	Maltose transport inner membrane protein
IRO93_RS20860	-2.18	-0.63	Periplasmic maltose-binding protein
IRO93_RS20865	-2.49	0.13	Maltose/maltodextrin transport ATP-binding protein
IRO93_RS20870	-3.18	-0.14	Maltoporin precursor
IRO93_RS21080	-1.79	-2.59	Putative membrane protein
IRO93_RS21085	0.78	-2.49	Acetyl-coenzyme A synthetase
IRO93_RS21090	-4.29	-2.47	Cytochrome c552 precursor
IRO93_RS21095	-3.27	-1.64	Cytochrome c-type protein NrfB precursor
IRO93_RS21100	-2.18	-0.7	Cytochrome c-type biogenesis protein
IRO93_RS21105	-2.5*	-0.2	Cytochrome c-type biogenesis protein
IRO93_RS21190	-2.39	-0.05	Putative AraC family regulatory protein
IRO93_RS21200	-1.05	-1.74	Melibiose operon regulatory protein
IRO93_RS21215	-1.35	1.73	Fumarate hydratase class I
IRO93_RS21220	-3.18	1.3	Anaerobic C4-dicarboxylate transporter
IRO93_RS21225	-2.8	-0.13	Hypothetical protein
IRO93_RS21305	1.71	0.48	Nonspecific acid phosphatase precursor
IRO93_RS21355	-0.3	-2.32	GroES protein
IRO93_RS21360	-0.28	-2.22	GroEL protein
IRO93_RS21435	3.48	0.49	Putative amino acid permease
IRO93_RS21580	-2.21*	0.17*	Putative membrane protein
IRO93_RS21620	3.09	-0.43	Conserved hypothetical protein
IRO93_RS21625	2.69	-0.66	Putative transport protein SgaT

IRO93_RS21630	2.57	-0.6	Putative PTS system IIB protein
IRO93_RS21635	2.91	-0.3	Probable sugar phosphotransferase
IRO93_RS21640	2.87	0.14	Putative hexulose-6-phosphate synthase
IRO93_RS21645	2.97	0.09	Conserved hypothetical protein
IRO93_RS21650	2.53	-0.3	Probable class II aldolase
IRO93_RS21705	-2.04	-0.31	Putative lipoprotein
IRO93_RS21755	-2.04	-0.68	Peptide methionine sulfoxide reductase
IRO93_RS21760	-2.35	-0.02	Putative exported protein
IRO93_RS21780	1.7	-0.12	Hypothetical protein
IRO93_RS21940	-0.27	3.5	Putative membrane protein
IRO93_RS21945	-1.93	4.77	Ornithine carbamoyltransferase
IRO93_RS21950	-2.43	3.15	Carbamate kinase
IRO93_RS21955	-2.34	2.68	Arginine deiminase
IRO93_RS21985	3.53	0.24	Putative acetyltransferase
IRO93_RS22030	-1.66	0.5	Gluconate 5-dehydrogenase
IRO93_RS22085	-2.52	-0.29	Fimbrial protein precursor
IRO93_RS22090	-2.78*	0.78	Fimbrial chaperone protein
IRO93_RS22095	-2.72	0.2	Outer membrane fimbrial usher protein
IRO93_RS22100	-2.71*	0.38	Fimbrial adhesin subunit
IRO93_RS22105	-2.18*	-0.29	Fimbrial operon positive regulatory protein
IRO93_RS22190	-1.82	0.15	Conserved hypothetical protein
IRO93_RS22315	1.17	5.31	Probable carbon starvation protein
IRO93_RS22320	-5.59	-1.61	Methyl-accepting chemotaxis protein
IRO93_RS22355	-2.1	0.1	Putative sugar isomerase
IRO93_RS22565	1.76	-0.24	Right origin-binding protein
IRO93_RS22620	2.66	0	Putative exported protein

[a]Locus tags are based on the *S.* Enteritidis P125109 genome (RefSeq accession number: GCF_000009505.1).

[b]*, uncertain fold change due to the low read count.

[c]WT, wild type; *envZ*$_{P248L}$, a strain expressing EnvZ$_{P248L}$; *envZ*$_{H243A}$, a strain expressing EnvZ$_{H243A}$.

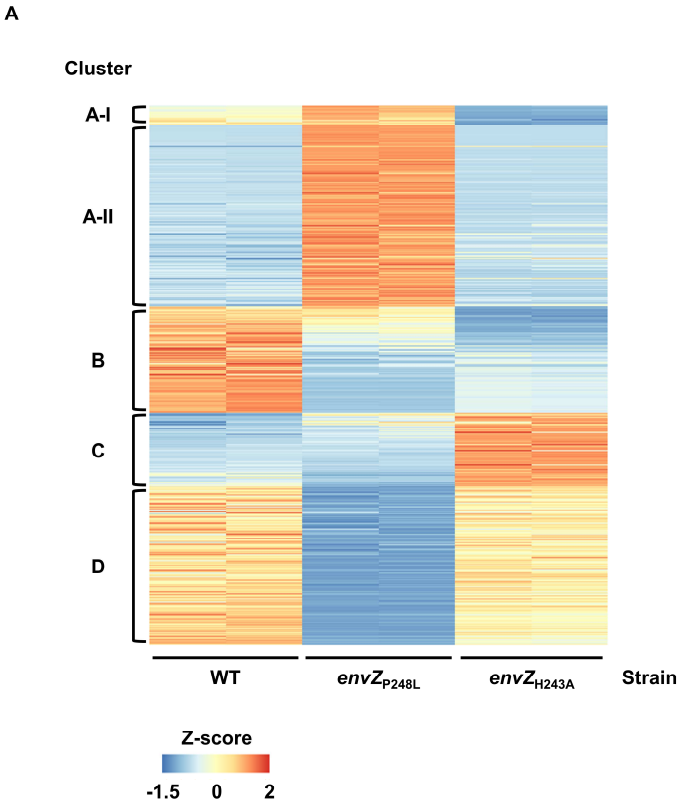
A
Cluster
A-I
A-II
B
C
D
WT
envZP248L
envZH243A
Strain
Z-score
-1.5
0
2

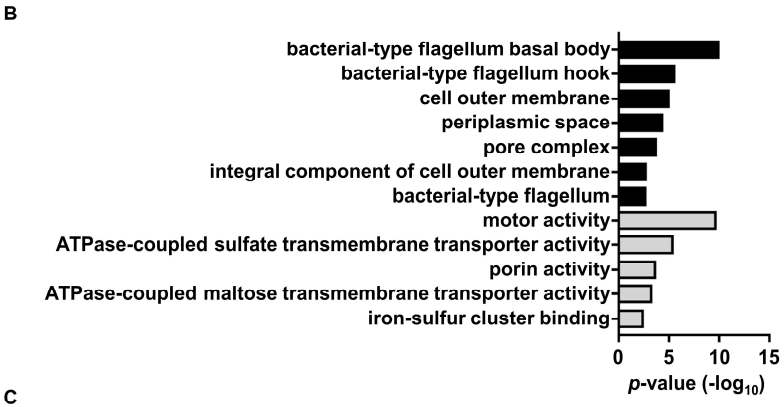
B
bacterial-type flagellum basal body
bacterial-type flagellum hook
cell outer membrane
periplasmic space
pore complex
integral component of cell outer membrane
bacterial-type flagellum
motor activity
ATPase-coupled sulfate transmembrane transporter activity
porin activity
ATPase-coupled maltose transmembrane transporter activity
iron-sulfur cluster binding
0
5
10
15
p-value (-log10)

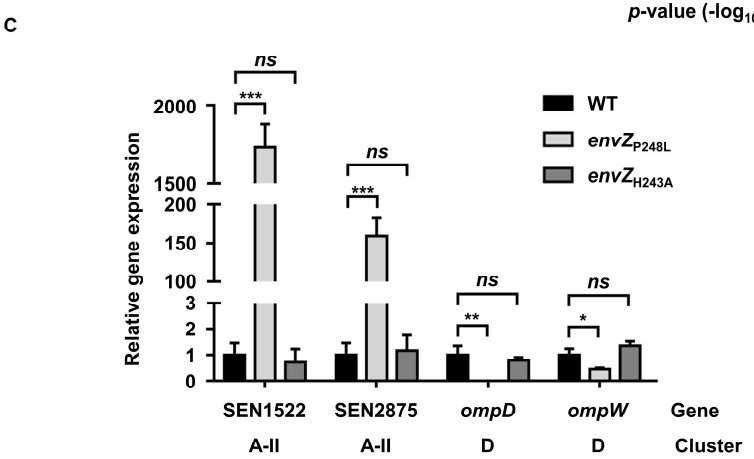
C
Relative gene expression
2000
1500
200
150
100
3
2
1
0
ns
***
ns
***
ns
**
ns
*
WT
envZP248L
envZH243A
SEN1522
SEN2875
ompD
ompW
Gene
A-II
A-II
D
D
Cluster

Figure III-2. Transcriptome analyses for DEGs by the *envZ*$_{P248L}$ and *envZ*$_{H243A}$ mutations. (A) The DEGs by the *envZ*$_{P248L}$ and *envZ*$_{H243A}$ mutations with similar expression pattern were grouped by *k-means* clustering algorithm, and the relative expression level of each DEG was visualized in the heat map. Scale bar, normalized read count transformed to Z-score. (B) The enriched GO terms in clusters A-II and D are shown by different colors based on the GO categories: black, cellular component; gray, molecular function. The GO terms belonging to biological process category are not shown. (C) Total RNAs were isolated from the *S.* Enteritidis strains grown to an A_{600} of 1.0. The transcript levels of SEN1522, SEN2875, *ompD*, and *ompW* were determined by qRT-PCR, and the transcript level of each gene in the wild type was set at 1. The cluster to which each gene belongs is shown below the gene name. Error bars represent the SD from three independent experiments. Statistical significance was determined by the Student's *t* test. *, $p<0.05$; **, $p<0.005$; ***, $p<0.001$; *ns*, not significant. WT, wild type; *envZ*$_{P248L}$, a strain expressing EnvZ$_{P248L}$; *envZ*$_{H243A}$, a strain expressing EnvZ$_{H243A}$.

Table III-4. List of DEGs belonging to the enriched GO terms in Figure III-1B

Locus tag[a]	Gene name	Cluster	GO term
IRO93_RS01075	*degP*	A-II	GO:0042597 (periplasmic space)
IRO93_RS01485	SEN0290	A-II	GO:0042597 (periplasmic space)
IRO93_RS02020	SEN0395	D	GO:0009279 (cell outer membrane); GO:0046930 (pore complex); GO:0015288 (porin activity)
IRO93_RS02960	SEN0580	A-II	GO:0042597 (periplasmic space)
IRO93_RS03345	*chiP*	D	GO:0009279 (cell outer membrane); GO:0046930 (pore complex); GO:0015288 (porin activity)
IRO93_RS05320	*fliR*	D	GO:0009425 (bacterial-type flagellum basal body)
IRO93_RS05330	*fliP*	D	GO:0009425 (bacterial-type flagellum basal body)
IRO93_RS05335	*fliO*	D	GO:0009425 (bacterial-type flagellum basal body)
IRO93_RS05340	*fliN*	D	GO:0009425 (bacterial-type flagellum basal body); GO:0003774 (motor activity)
IRO93_RS05345	*fliM*	D	GO:0009425 (bacterial-type flagellum basal body); GO:0003774 (motor activity)
IRO93_RS05350	*fliL*	D	GO:0009425 (bacterial-type flagellum basal body)
IRO93_RS05355	*fliK*	D	GO:0009424 (bacterial-type flagellum hook)
IRO93_RS05360	*fliJ*	D	GO:0003774 (motor activity)
IRO93_RS05370	*fliH*	D	GO:0003774 (motor activity)
IRO93_RS05375	*fliG*	D	GO:0009425 (bacterial-type flagellum basal body); GO:0003774 (motor activity)
IRO93_RS05380	*fliF*	D	GO:0003774 (motor activity)
IRO93_RS05385	*fliE*	D	GO:0009425 (bacterial-type flagellum basal body); GO:0003774 (motor activity)
IRO93_RS06740	*ompW*	D	GO:0009279 (cell outer membrane)
IRO93_RS07690	*ompD*	D	GO:0009279 (cell outer membrane); GO:0046930 (pore complex); GO:0015288 (porin activity)
IRO93_RS07700	*fdnG*	D	GO:0042597 (periplasmic space)
IRO93_RS07740	*hdeB*	D	GO:0042597 (periplasmic space)
IRO93_RS07845	SEN1513	A-II	GO:0042597 (periplasmic space)

IRO93_RS07890	SEN1522	A-II	GO:0009279 (cell outer membrane); GO:0046930 (pore complex); GO:0015288 (porin activity)
IRO93_RS08115	*asr*	A-II	GO:0042597 (periplasmic space)
IRO93_RS08170	*ompS2*	A-II	GO:0009279 (cell outer membrane); GO:0015288 (porin activity)
IRO93_RS08455	*ssaQ*	D	GO:0009425 (bacterial-type flagellum basal body); GO:0003774 (motor activity)
IRO93_RS08620	*ttrB*	A-II	GO:0042597 (periplasmic space)
IRO93_RS09160	SEN1766	D	GO:0009279 (cell outer membrane)
IRO93_RS09360	*pagC*	D	GO:0009279 (cell outer membrane)
IRO93_RS09675	*flgJ*	D	GO:0042597 (periplasmic space)
IRO93_RS09685	*flgH*	D	GO:0003774 (motor activity); GO:0009279 (cell outer membrane)
IRO93_RS09690	*flgG*	D	GO:0009424 (bacterial-type flagellum hook)
IRO93_RS09695	SEN1870	D	GO:0009425 (bacterial-type flagellum basal body); GO:0009424 (bacterial-type flagellum hook)
IRO93_RS09700	*flgE*	D	GO:0009425 (bacterial-type flagellum basal body); GO:0009424 (bacterial-type flagellum hook)
IRO93_RS09705	*flgD*	D	GO:0009424 (bacterial-type flagellum hook)
IRO93_RS09710	*flgC*	D	GO:0009424 (bacterial-type flagellum hook)
IRO93_RS09715	*flgB*	D	GO:0009424 (bacterial-type flagellum hook)
IRO93_RS09720	*flgA*	D	GO:0042597 (periplasmic space)
IRO93_RS10715	*phsA*	D	GO:0042597 (periplasmic space)
IRO93_RS11000	SEN2114	A-II	GO:0009279 (cell outer membrane); GO:0046930 (pore complex); GO:0015288 (porin activity)
IRO93_RS11275	*mdtQ*	A-II	GO:0009279 (cell outer membrane)
IRO93_RS11775	*glpQ*	D	GO:0042597 (periplasmic space)
IRO93_RS12325	*fadL*	D	GO:0009279 (cell outer membrane)
IRO93_RS12620	*cysA*	A-II	GO:0015419 (ATPase-coupled sulfate transmembrane transporter activity)
IRO93_RS12625	*cysW*	A-II	GO:0015419 (ATPase-coupled sulfate transmembrane transporter activity)
IRO93_RS12630	*cysT*	A-II	GO:0015419 (ATPase-coupled sulfate transmembrane transporter activity)

IRO93_RS12635	*cysP*	A-II	GO:0015419 (ATPase-coupled sulfate transmembrane transporter activity); GO:0042597 (periplasmic space)
IRO93_RS14285	*invH*	A-II	GO:0009279 (cell outer membrane)
IRO93_RS14980	SEN2875	A-II	GO:0009279 (cell outer membrane)
IRO93_RS17190	*ppiA*	A-II	GO:0042597 (periplasmic space)
IRO93_RS17640	*livK*	D	GO:0042597 (periplasmic space)
IRO93_RS17810	SEN3421	A-II	GO:0042597 (periplasmic space)
IRO93_RS17980	SEN3454	D	GO:0042597 (periplasmic space)
IRO93_RS18065	SEN3468	A-II	GO:0009279 (cell outer membrane)
IRO93_RS19585	*pldA*	D	GO:0009279 (cell outer membrane)
IRO93_RS20115	SEN3853	A-II	GO:0015419 (ATPase-coupled sulfate transmembrane transporter activity); GO:0042597 (periplasmic space)
IRO93_RS20860	*malE*	D	GO:0042597 (periplasmic space)
IRO93_RS20870	SEN4000	D	GO:0009279 (cell outer membrane); GO:0046930 (pore complex); GO:0015288 (porin activity)
IRO93_RS21760	*tamA*	D	GO:0009279 (cell outer membrane)
IRO93_RS22095	*sefC*	D	GO:0009279 (cell outer membrane)

[a]Locus tags are based on the *S.* Enteritidis P125109 genome (RefSeq accession number: GCF_000009505.1).

III-3-3. OmpR directly regulates the SEN1522, SEN2875, *ompD*, and *ompW* genes and alters the OMP composition

We investigated whether the regulatory effect of the $envZ_{P248L}$ mutation on the four OMP genes requires OmpR. The $envZ_{P248L}$ mutation in the Δ*ompR* strain background was unable to increase the SEN1522 and SEN2875 transcript levels and decrease the *ompD* and *ompW* transcript levels (Fig. III-3), indicating the OmpR-mediated regulation of the four OMP genes. To further determine whether OmpR directly regulates the four OMP genes by binding to their upstream regions, EMSAs were performed. The addition of OmpR to a labeled DNA probe resulted in a single retarded band of OmpR-DNA complex in an OmpR concentration-dependent manner (Fig. III-4). The same but unlabeled DNA fragment, which was used as a self-competitor, showed the competition for OmpR binding in a dose-dependent manner (Fig. III-4), indicating that OmpR binds specifically to each upstream region of the four OMP genes. Then, DNase I protection assays were performed using the same labeled DNA probes to identify the OmpR binding sites. When OmpR was added to the DNA probes for SEN1522, SEN2875, and *ompW*, OmpR protected a single region of 47-bp, 49-bp, and 101-bp from DNase I digestion, respectively (Fig. III-5A, 5B, and 5D). The addition of OmpR to the DNA probe for *ompD* resulted in the protection of two distant regions of 38-bp and 44-bp, respectively (Fig. III-5C). Combined with the EMSA results, these results suggested that OmpR regulates the expression of the four OMP genes by directly and specifically binding to their upstream regions.

Additionally, outer membrane proteins from the *S.* Enteritidis strains were analyzed by SDS-PAGE and identified by LC-MS/MS. A protein band containing OmpW was not detectable in the condition we used, which might be due to its low cellular level

(Gil et al., 2007). However, the intensity of the bands corresponding to the OMPs encoded by SEN1522, SEN2875, and *ompD*, in addition to *ompC* and *ompF*, was apparently changed by the *envZ*$_{P248L}$ mutation in an OmpR-dependent manner (Fig. III-6). The combined results indicated that OmpR directly regulates the four OMP genes, leading to the altered OMP composition in *S.* Enteritidis.

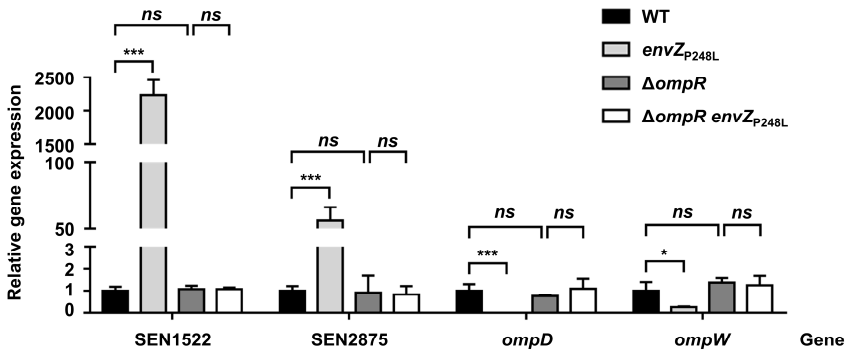

Figure III-3. Effects of the *ompR* deletion on the expression of OMP genes. Total RNAs were isolated from the *S.* Enteritidis strains grown to an A_{600} of 1.0. The transcript levels of SEN1522, SEN2875, *ompD*, and *ompW* were determined by qRT-PCR, and the transcript level of each gene in the wild type was set at 1. Error bars represent the SD from three independent experiments. Statistical significance was determined by the Student's *t* test. *, $p<0.05$; ***, $p<0.001$; *ns*, not significant. WT, wild type; *envZ*$_{P248L}$, a strain expressing EnvZ$_{P248L}$; Δ*ompR*, *ompR* mutant; Δ*ompR envZ*$_{P248L}$, *ompR* mutant expressing EnvZ$_{P248L}$.

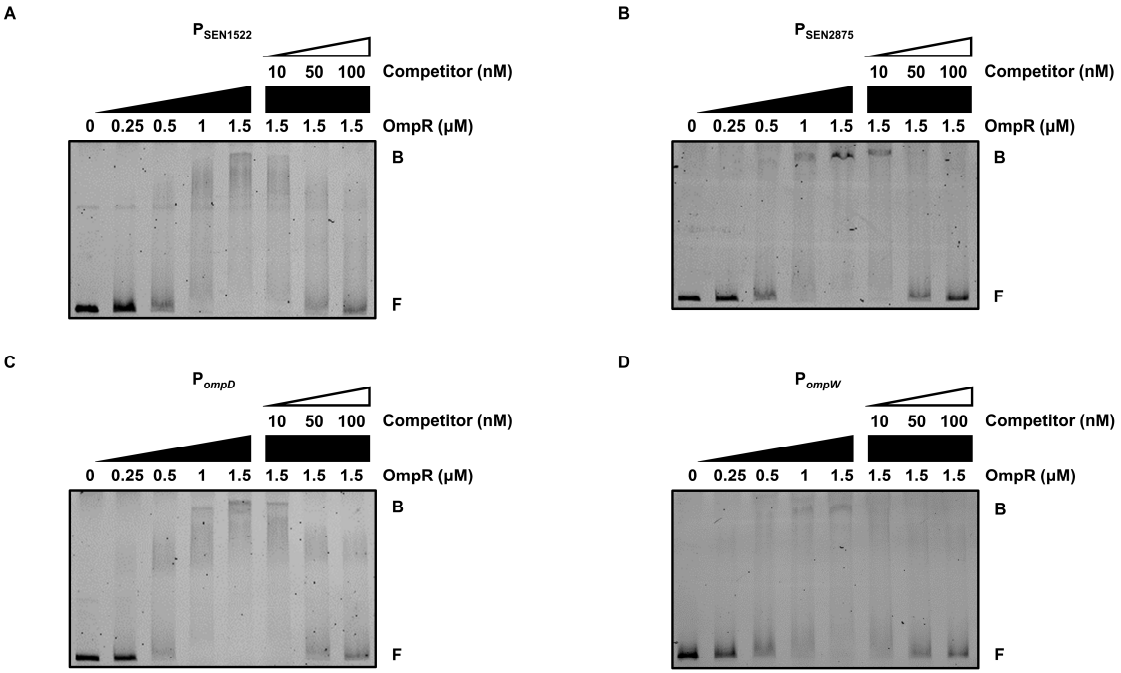

Figure III-4. Direct binding of OmpR to the upstream regions of the EnvZ/OmpR regulon. The 6-FAM-labeled DNA probes (10 nM) for the upstream regions of SEN1522 (A), SEN2875 (B), *ompD* (C), and *ompW* (D) were incubated with increasing amounts of OmpR as indicated. For competition analysis, the same but unlabeled DNA fragments were used as self-competitors, and various amounts of self-competitors were added to the reaction buffer before the addition of OmpR (1.5 μM). B, bound DNA; F, Free DNA

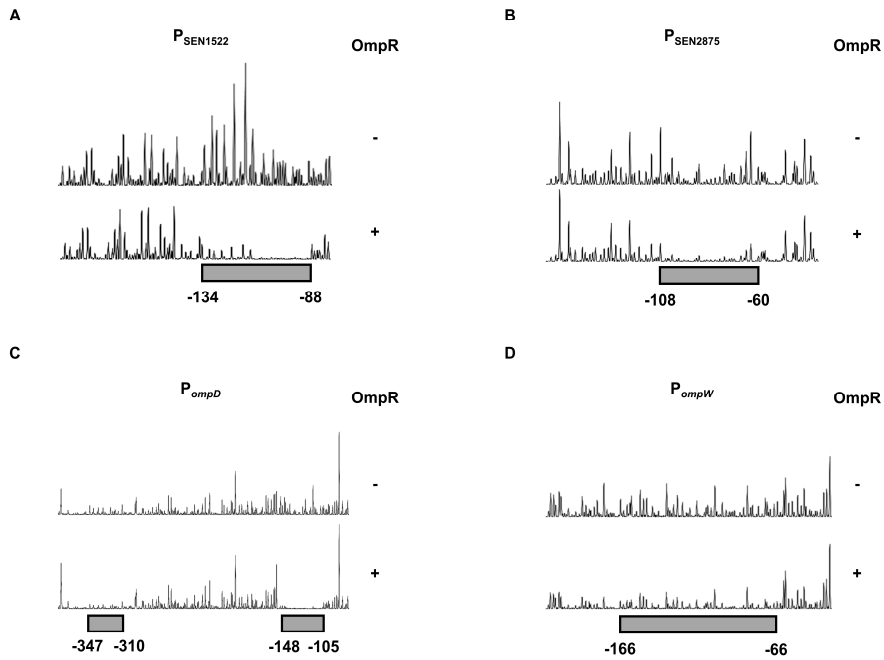

Figure III-5. Specific binding of OmpR to the upstream regions of the EnvZ/OmpR regulon. The 6-FAM-labeled DNA probes (40 nM) for the upstream regions of SEN1522 (A), SEN2875 (B), *ompD* (C), and *ompW* (D) were incubated with or without OmpR (2 μM) and digested with DNase I. The regions protected by OmpR are indicated by gray boxes. Nucleotides are numbered relative to the first base of each start codon.

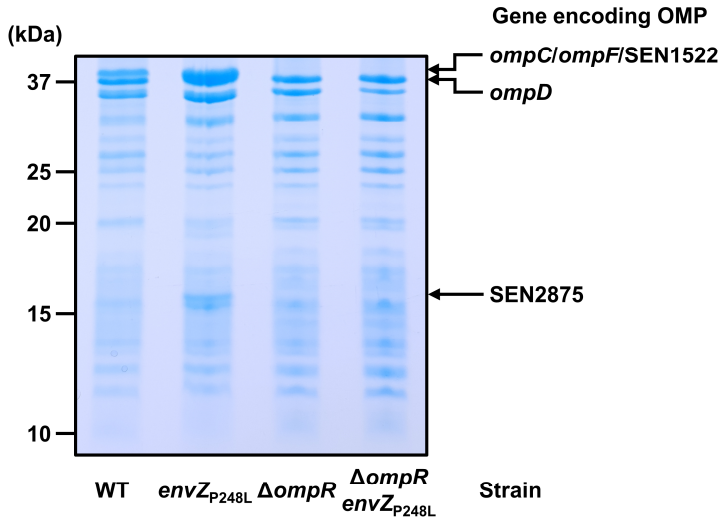

Figure III-6. The OMP composition of *S.* Enteritidis with different genetic backgrounds. Total outer membrane proteins were isolated from the *S.* Enteritidis strains and resolved by SDS-PAGE. The SDS gel was stained with Coomassie brilliant blue. The protein bands indicated by arrows were identified by LC-MS/MS. Molecular size markers (Bio-Rad) are shown in kilodaltons. WT, wild type; *envZ*$_{P248L}$, a strain expressing EnvZ$_{P248L}$; Δ*ompR*, *ompR* mutant; Δ*ompR envZ*$_{P248L}$, *ompR* mutant expressing EnvZ$_{P248L}$.

III-3-4. High cellular level of OmpR is required for the regulation of the four OMP genes

It is unclear why the expression of the four OMP genes in the wild type is not altered by the *envZ*$_{H243A}$ mutation or *ompR* deletion (Fig. III-2C & 3). We hypothesized that the OmpR-mediated regulation of the four OMP genes would be possible only when the cellular level of OmpR is increased above a certain level, as observed in the *envZ*$_{P248L}$ strain (Fig. III-1). To test our hypothesis, the cellular level of OmpR was increased using a plasmid pDH2104 which carries the *ompR* gene under the control of an arabinose-inducible promoter P_{BAD}, and the expression of the four OMP genes was examined. As the concentrations of arabinose increase, the cellular levels of OmpR-P as well as total OmpR ($OmpR_{total}$) were gradually elevated (Fig. III-7A). The expression of SEN1522 and SEN2875 was sharply increased by the addition of more than 0.5 mM arabinose, and that of *ompD* and *ompW* was decreased in an arabinose concentration-dependent manner (Fig. III-7B). These results supported our hypothesis that an increased cellular level of OmpR is required to regulate the four OMP genes.

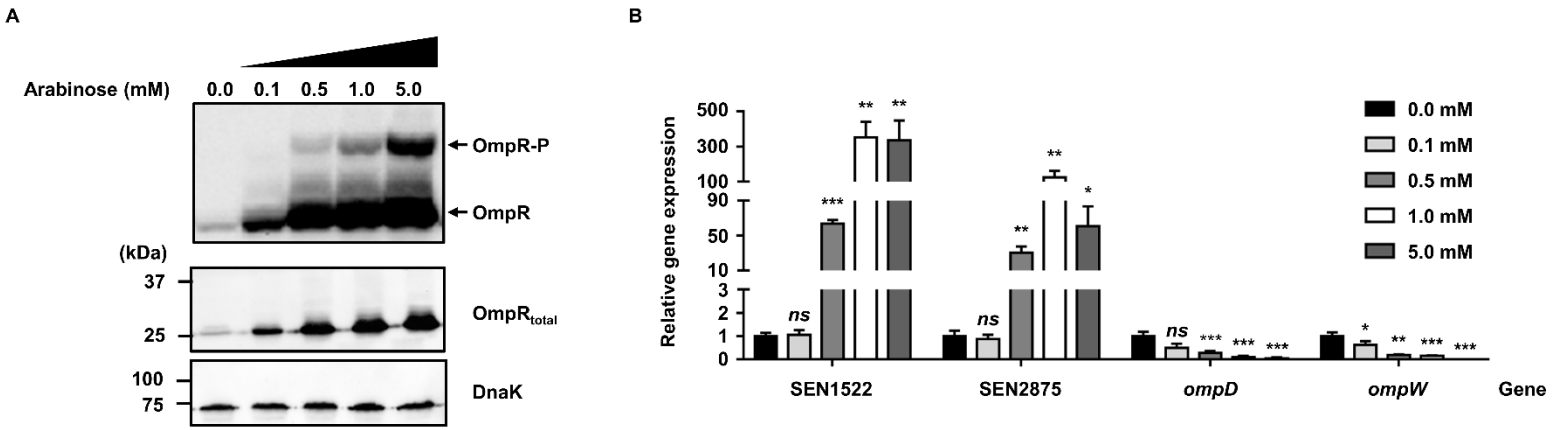

Figure III-7. Effects of the cellular level of OmpR on the expression of the EnvZ/OmpR regulon. Total proteins and RNAs were isolated from the Δ*ompR* strain harboring pDH2104 grown to an A_{600} of 1.0 with different concentrations of arabinose as indicated. (A) The phosphorylated status of OmpR was determined by Western blot analysis using Phos-tag SDS-PAGE gel (Wako, Osaka, Japan). The cellular levels of $OmpR_{total}$ and DnaK (as an internal control) were determined by Western blot analysis using standard SDS-PAGE gel. Molecular size markers (Bio-Rad) are shown in kilodaltons. (B) The transcript levels of SEN1522, SEN2875, *ompD*, and *ompW* were determined by qRT-PCR, and the transcript level of each gene in the strain grown without arabinose was set at 1. Error bars represent the SD from three independent experiments. Statistical significance was determined by the Student's *t* test. *, $p<0.05$; **, $p<0.005$; ***, $p<0.001$; *ns*, not significant relative to the strain grown without arabinose.

III-3-5. Phosphorylation of OmpR is not necessary for the repression of the *ompD* and *ompW* genes

We further examined whether the unphosphorylated OmpR could regulate the four OMP genes. Thus, a plasmid pDH2108, the same as pDH2104 but carrying the *ompR*$_{D55A}$ gene, was used to induce OmpR$_{D55A}$ that mimics the unphosphorylated OmpR. As shown in Fig. III-8A, the Δ*ompR* strain harboring pDH2108 produced only the unphosphorylated form of OmpR. The expression of the four OMP genes in the wild-type and Δ*ompR* strains harboring empty vector (pJK1113) was similar (Fig. III-8B), supporting our hypothesis again that the function of OmpR in its low cellular level is insignificant for the regulation of the four OMP genes. When the *ompR* expression is induced, the expression of SEN1522 and SEN2875 was increased by the wild-type OmpR but not by OmpR$_{D55A}$ (Fig. III-8B), indicating that OmpR-P is required for the activation of SEN1522 and SEN2875. In contrast, the expression of *ompD* and *ompW* was significantly decreased by both the wild-type OmpR and OmpR$_{D55A}$ (Fig. III-8B), indicating that not only OmpR-P but also unphosphorylated OmpR functions as a negative regulator of *ompD* and *ompW*. These results suggested that phosphorylation of OmpR is not necessary for the repression of *ompD* and *ompW*, which is non-canonical as a response regulator.

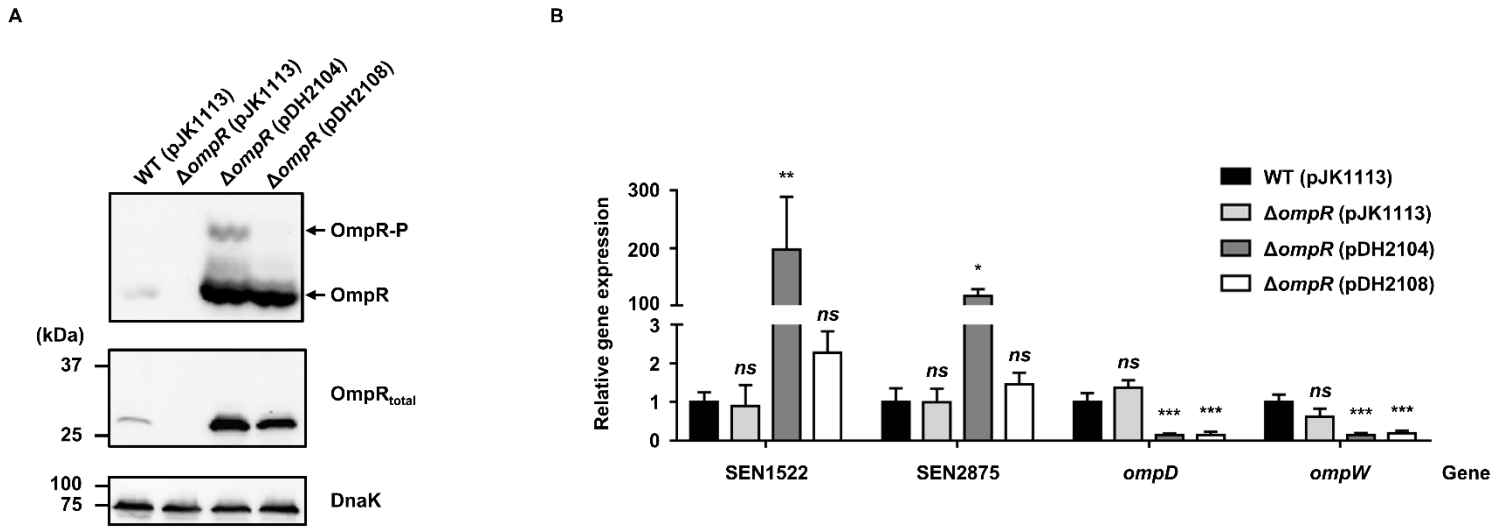

Figure III-8. Effects of unphosphorylated OmpR on the expression of the EnvZ/OmpR regulon. Total proteins and RNAs were isolated from the *S.* Enteritidis strains grown to an A_{600} of 1.0 with arabinose (1 mM). (A) The phosphorylated status of OmpR was determined by Western blot analysis using Phos-tag SDS-PAGE gel (Wako). The cellular levels of $OmpR_{total}$ and DnaK (as an internal control) were determined by Western blot analysis using standard SDS-PAGE gel. Molecular size markers (Bio-Rad) are shown in kilodaltons. (B) The transcript levels of SEN1522, SEN2875, *ompD,* and *ompW* were determined by qRT-PCR, and the transcript level of each gene in the wild type was set at 1. Error bars represent the SD from three independent experiments. Statistical significance was determined by the multiple comparisons after one-way analysis of

variance (ANOVA). *, $p<0.05$; **, $p<0.005$; ***, $p<0.001$; *ns*, not significant relative to wild type. WT (pJK1113), wild type; Δ*ompR* (pJK1113), *ompR* mutant; Δ*ompR* (pDH2104), *ompR* mutant expressing wild-type OmpR; *ompR* (pDH2108), *ompR* mutant expressing $OmpR_{D55A}$.

III-3-6. The *ompD* and *ompF* genes play a major role in the EnvZ/OmpR-mediated antibiotic resistance

To examine which OMP gene contributes to the EnvZ/OmpR-mediated resistance to β-lactams, isogenic mutants lacking each of the four OMP genes were generated, and their MICs for β-lactams were determined. The MICs for β-lactams in the ΔSEN1522, ΔSEN2875, and Δ*ompW* strains were identical to those in the wild type (Table III-2), indicating that the three OMP genes may not individually contribute to antibiotic resistance in *S.* Enteritidis. In contrast, the MICs for β-lactams in the Δ*ompD* strain were significantly higher than those in the wild type (Table III-2). Furthermore, the Δ*ompD* $envZ_{P248L}$ strain showed only 2-fold higher MICs than the Δ*ompD* strain, which is lower than the 4-fold increase observed between the $envZ_{P248L}$ and wild-type strains (Table III-2), suggesting that *ompD*, similar to *ompF*, is involved in the EnvZ/OmpR-mediated antibiotic resistance in *S*. Enteritidis. In addition, the MICs for β-lactams in the Δ*ompD* Δ*ompF* strain increased to the level similar to those in the $envZ_{P248L}$ strain (Table III-2). Collectively, these results suggested that the decreased expression of *ompD* and *ompF* is responsible for the EnvZ/OmpR-mediated resistance to β-lactams in *S.* Enteritidis.

III-3-7. EnvZ/OmpR specifically responds to β-lactams and enhances antibiotic resistance

Because a fundamental role of EnvZ/OmpR is to sense and appropriately respond to specific environmental signals, we questioned whether β-lactams could be an environmental signal for EnvZ/OmpR to increase the *ompR* expression. To investigate whether the *ompR* expression is increased by β-lactams, the P_{ompR} activity in the *S.* Enteritidis cells grown with or without ceftriaxone was determined using the *ompR-lacZ* transcriptional fusion reporter. The P_{ompR} activity was significantly elevated by ceftriaxone in the wild type but not in the Δ*ompR, ompR*$_{D55A}$, and *envZ*$_{H243A}$ strains (Fig. III-9A). The results suggested that ceftriaxone induces positive autoregulation of *ompR* mediated by OmpR-P. The autoinduction of *ompR* was also facilitated by the addition of cefotaxime or ampicillin, but not by polymyxin B (Fig. III-10), suggesting that EnvZ/OmpR specifically responds to β-lactams. Next, we further assessed whether the increased expression of *ompR* leads to the reduction in the expression of *ompD* and *ompF*. The addition of ceftriaxone reduced the *ompD* and *ompF* transcript levels in the wild-type cells but did not affect those in the Δ*ompR* cells (Fig. III-9B).These results confirmed that EnvZ/OmpR increases its own expression in response to β-lactams and thereby represses *ompD* and *ompF*.

To determine whether the response of EnvZ/OmpR to β-lactams could provide a direct benefit for survival of *S.* Enteritidis, bacterial growth was monitored in the absence or presence of the antibiotics. The wild-type, Δ*ompR*, Δ*ompD* Δ*ompF*, and Δ*ompR* Δ*ompD* Δ*ompF* strains showed similar growth in the absence of ceftriaxone (Fig. III-11A). In the presence of ceftriaxone, the *ompR* deletion reduced the growth rate of wild type but did not affect that of the Δ*ompD* Δ*ompF* strain (Fig. III-11B). These results indicated that OmpR provides benefits for survival of *S.* Enteritidis

upon exposure to β-lactams through *ompD* and *ompF*. Altogether, the combined results suggested that EnvZ/OmpR specifically responds to the external β-lactams, leading to the autoinduction of *ompR*, repression of *ompD* and *ompF*, and thereby enhancement of antibiotic resistance in *S.* Enteritidis.

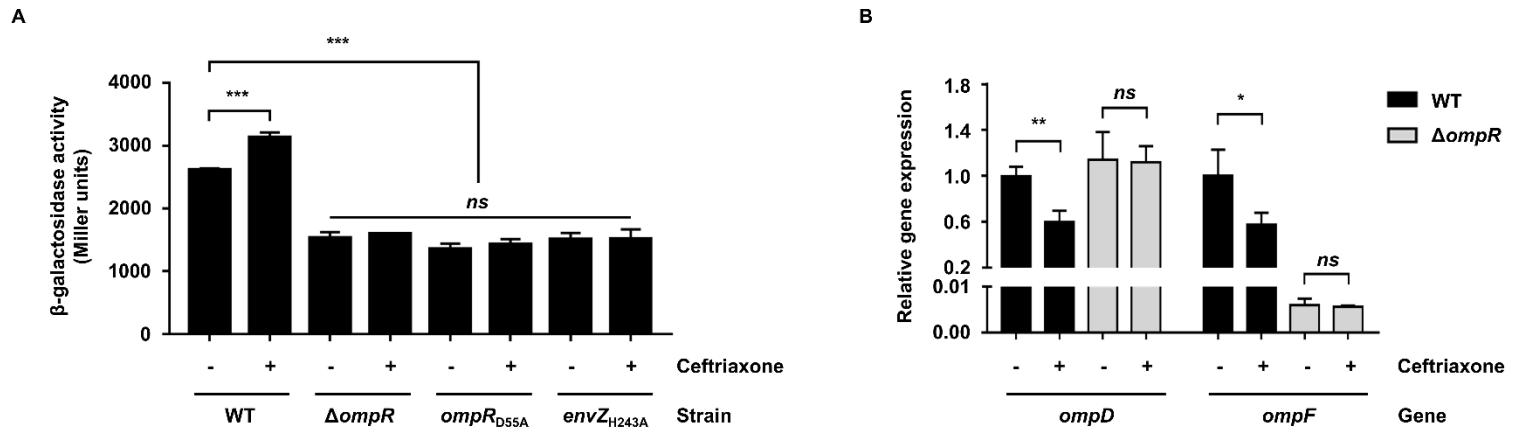

Figure III-9. Effects of ceftriaxone on the activity of P_{ompR} and expression of the EnvZ/OmpR regulon. (A) The *S.* Enteritidis strains harboring the reporter plasmid pDH2105 with P_{ompR} fused to promoterless *lacZ* were grown to an A_{600} of 1.0 and then exposed to M9G with or without ceftriaxone (0.1 μg ml^{-1}) as indicated. The *β*-galactosidase activity of the *S.* Enteritidis strains was measured and expressed in Miller units. Statistical significance was determined by the multiple comparisons after one-way ANOVA. WT, wild type harboring pDH2105; Δ*ompR*, *ompR* mutant harboring pDH2105; $ompR_{D55A}$, a strain expressing $OmpR_{D55A}$ and harboring pDH2105; $envZ_{H243A}$, a strain expressing $EnvZ_{H243A}$ and harboring pDH2105. (B) Total RNAs were isolated from the *S.* Enteritidis strains, grown to an A_{600} of 1.0 and then exposed to M9G with or without ceftriaxone (0.1 μg ml^{-1}) as indicated. The transcript levels of *ompD* and *ompF* were determined by qRT-PCR, and the transcript level of each gene

in the wild type not exposed to ceftriaxone was set at 1. Statistical significance was determined by the Student's *t* test. WT, wild type; Δ*ompR*, *ompR* mutant. Error bars represent the SD from three independent experiments. *, $p<0.05$; **, $p<0.005$; ***, $p<0.001$; *ns*, not significant.

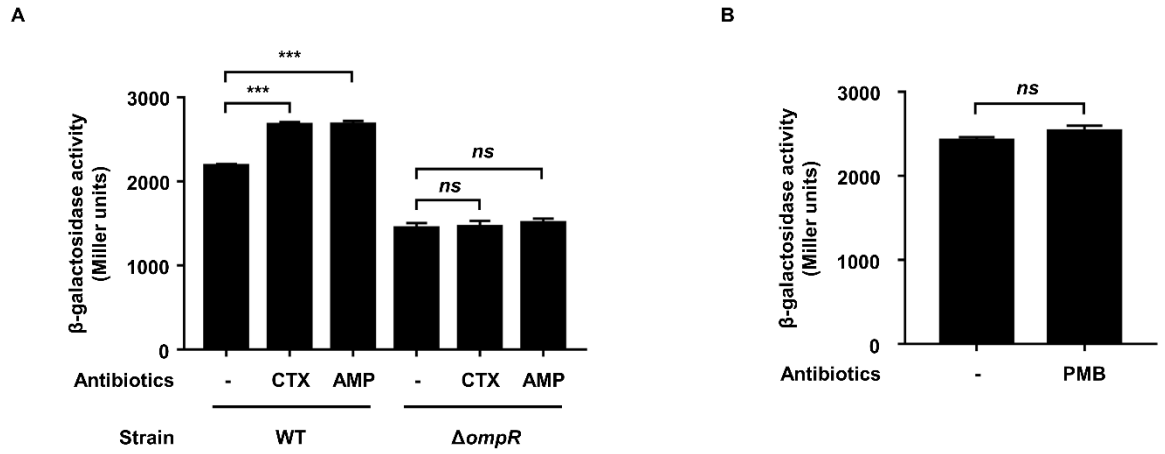

Figure III-10. Effects of various antibiotics on the activity of P_{ompR}. (A) The *S.* Enteritidis strains harboring the reporter plasmid pDH2105 with P_{ompR} fused to promoterless *lacZ* were grown to an A_{600} of 1.0 and then exposed to M9G with or without cefotaxime (0.1 μg ml^{-1}) or ampicillin (4 μg ml^{-1}) as indicated. CTX, cefotaxime; AMP, ampicillin; WT, wild type harboring pDH2105; Δ*ompR*, *ompR* mutant harboring pDH2105. (B) The wild type harboring pDH2105 was grown to an A_{600} of 1.0 and then exposed to M9G with or without polymyxin B (0.5 μg ml^{-1}) as indicated. PMB, polymyxin B. The β-galactosidase activity of the *S.* Enteritidis strains was measured and expressed in Miller units. Error bars represent the SD from three independent experiments. Statistical significance was determined by the Student's *t* test. ***, $p<0.001$; *ns*, not significant.

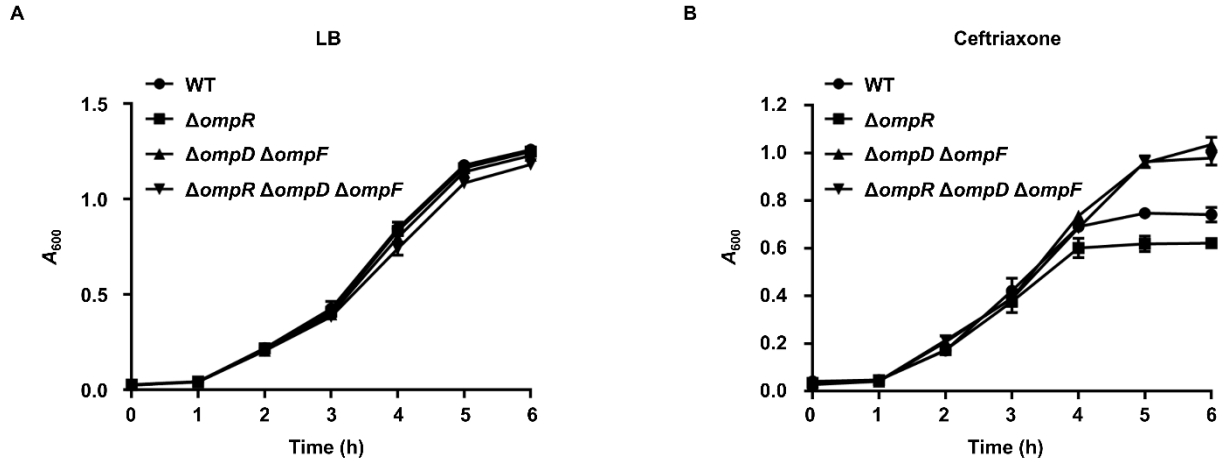

Figure III-11. Survival of *S.* Enteritidis upon exposure to β-lactams. The survival of the *S.* Enteritidis strains was monitored at 1 h intervals in the absence of antibiotics (A) and in the presence of ceftriaxone (0.1 μg ml^{-1}) (B). Error bars represent the SD from three independent experiments. WT, wild type; Δ*ompR*, *ompR* mutant; Δ*ompD* Δ*ompF*, *ompD ompF* double mutant; Δ*ompR* Δ*ompD* Δ*ompF*, *ompR ompD ompF* triple mutant.

III-4. Discussion

In this study, we found that the resistance in *S.* Enteritidis to various antibiotics is enhanced by the active state of EnvZ/OmpR (Table III-1). As EnvZ/OmpR has broader roles beyond modulating the ratio of OmpC and OmpF, a number of microarray and RNA-seq analyses have been performed to identify its regulon by comparing transcriptomes between the wild-type and Δ*ompR* strains (Perkins et al., 2013; Perkins et al., 2009). However, because EnvZ/OmpR in the wild-type strain of *S.* Enteritidis is minimally active, showing low cellular level of OmpR-P (Fig. III-1), certain genes may not be differentially expressed in the Δ*ompR* strain, possibly excluded from the EnvZ/OmpR regulon. Thus, comparison of transcriptome changes induced by the $envZ_{P248L}$ and $envZ_{H243A}$ mutations that mimic the active and inactive states of EnvZ/OmpR, respectively, enabled us to comprehensively analyze the EnvZ/OmpR regulon. As a result, the antibiotic resistance-related OMP genes, including SEN1522, SEN2875, *ompD*, and *ompW*, were newly identified as the EnvZ/OmpR regulon of *S*. Enteritidis (Fig. III-2).

OmpR activates the SEN1522 and SEN2875 genes but represses the *ompD* and *ompW* genes, by directly binding to the upstream region of each OMP gene (Fig. III-3 to 5). Interestingly, OmpR non-canonically regulates the four OMP genes only when its cellular level is above a certain level (Fig. III-7). Furthermore, a high cellular level of OmpR does not require phosphorylation to repress *ompD* and *ompW*

(Fig. III-8). The results suggested that the cellular level of OmpR is another important parameter besides the phosphorylation level of OmpR, determining the regulatory function of EnvZ/OmpR in *S.* Enteritidis. In this study, we observed that the *ompR* expression is positively autoregulated by OmpR-P (Fig. III-9A). Additionally, the regulation of *ompR* involves several transcription factors including a factor for inversion stimulation (FIS), an integration host factor (IHF), and a histone-like nucleoid-structuring protein (H-NS) (Bang et al., 2002; Cameron & Dorman, 2012; Tsui et al., 1991). The involvement of multiple regulators would integrate diverse signals to precisely control the cellular level of OmpR, allowing EnvZ/OmpR to regulate its non-canonical regulon such as the four OMP genes.

Two-component systems are often involved in antibiotic resistance in bacteria by sensing and responding to external antibiotics. In *Klebsiella aerogenes*, CpxA/CpxR contributes to antibiotic resistance by repressing the *ompF* gene and activating the *acrD* gene, which encodes the efflux pump, in the presence of β-lactams (Masi et al., 2020). In *Pseudomonas aeruginosa*, ParS/ParR and CprS/CprR also enhance antibiotic resistance by activating the *arnBCADTEF* operon, which participates in lipopolysaccharide modification, in response to antimicrobial peptides (Fernandez et al., 2010; Fernandez et al., 2012). In this study, we demonstrated that EnvZ/OmpR activates its own expression and thus represses *ompD* and *ompF* in response to external β-lactams, providing *S.* Enteritidis with direct benefits for survival in the presence of the antibiotics (Fig. III-9 & 11). These results proposed that EnvZ/OmpR

responds to the external β-lactams as an environmental signal and reduces the outer membrane permeability, improving resistance in *S.* Enteritidis to the antibiotics.

In summary, we revealed the mechanism by which the active state of EnvZ/OmpR enhances antibiotic resistance in *S.* Enteritidis (Fig. III-12). With environmental signals activating EnvZ/OmpR, EnvZ phosphorylates OmpR, and OmpR-P in turn positively autoregulates *ompR*. This study newly suggested β-lactams as an environmental signal to induce the positive autoregulation of *ompR*. Then, the active state of EnvZ/OmpR leads to compositional modulation of OMPs. First, OmpR-P activates *ompC* but represses *ompF* in a canonical way. In contrast, OmpR elevates the SEN1522 and SEN2875 expressions but reduces the *ompD* and *ompW* expressions non-canonically, only when its cellular level is high. Especially, OmpR-P is not required for the repression of *ompD* and *ompW*. Meanwhile, the OMPs may directly or indirectly affect the expression of other OMPs. For example, a decreased expression of *ompD* is often accompanied by an increased expression of SEN1522 and SEN2875 (Hu et al., 2011; Lin et al., 2019). As a result, the decreased expression of *ompD,* in addition to *ompF*, would reduce the outer membrane permeability and thus enhance antibiotic resistance in *S.* Enteritidis. This is the first report of the mechanism for *S.* Enteritidis to enhance antibiotic resistance through EnvZ/OmpR which remodels the OMP composition in response to β-lactams.

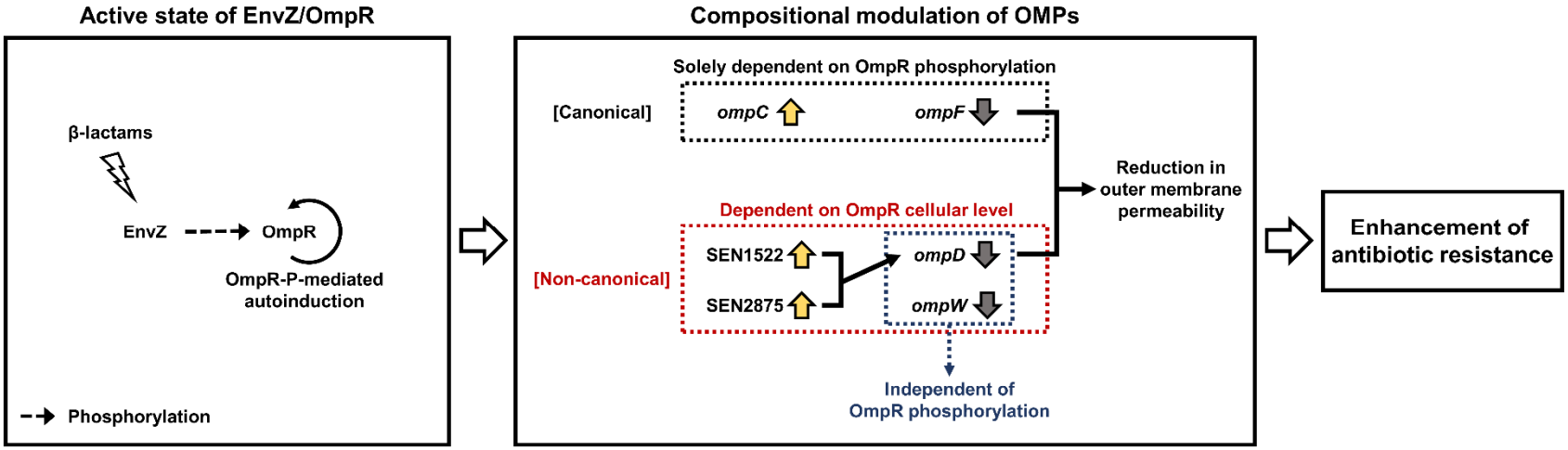

Figure III-12. Proposed mechanism of antibiotic resistance enhanced by EnvZ/OmpR in *S.* Enteritidis. When EnvZ/OmpR senses specific environmental signals, EnvZ phosphorylates OmpR, and then, OmpR-P positively autoregulates *ompR*. The external β-lactams could be an environmental signal for EnvZ/OmpR. Under this condition, the active state of EnvZ/OmpR modulates the composition of OMPs through at least three different ways. First, OmpR-P canonically activates *ompC* but represses *ompF* (indicated by black dotted line). In contrast, OmpR activates SEN1522 and SEN2875 but represses *ompD* and *ompW* non-canonically, only when its cellular level is high (indicated by red dotted line). In particular, OmpR-P is not necessary for the repression of *ompD* and *ompW* (indicated by blue dotted line). Additionally, increased expression of

SEN1522 and SEN2875 is associated with decrease in the expression of *ompD*. Collectively, the decreased expression of *ompD*, in addition to *ompF*, would lead to reduction in outer membrane permeability and thus enhancement of antibiotic resistance in *S.* Enteritidis.

Chapter IV.

Conclusion

Pathogenic bacteria possess multiple two-component systems to sense specific environmental changes and respond appropriately for survival and successful infection. The human food-borne pathogen *S.* Enteritidis senses and responds to changes in osmolarity and pH using EnvZ/OmpR two-component system. Because EnvZ/OmpR is a global regulatory system in *S.* Enteritidis, small genetic mutation occurring in this system could contribute to phenotypic diversity in nature. Spontaneous SNP in the *envZ* gene leading to amino acid change from Pro248 to Leu248 probably modifies the function of EnvZ and affects the signal transduction to OmpR. The SNP in *envZ* increases the cellular level of OmpR-P and alters the expression of OmpR regulon. As a result, the *S.* Enteritidis strain carrying the SNP in *envZ* shows impaired biofilm formation and motility but enhanced adhesion and invasion to host cells and acid resistance.

EnvZ/OmpR with the SNP in *envZ* is considered to be active because it leads to high cellular level of OmpR-P. *S.* Enteritidis carrying the active state of EnvZ/OmpR is more resistant to multiple antibiotics, especially to β-lactams. The active state of EnvZ/OmpR alters the expression of multiple OMP genes including SEN1522, SEN2875, *ompD*, and *ompW*, whose products are involved in antibiotic resistance. OmpR directly activates SEN1522 and SEN2875 but represses *ompD* and *ompW*. Interestingly, the cellular level of OmpR above a certain level is required for the regulation of the four OMP genes. Even phosphorylation of OmpR is not necessary for the repression of *ompD* and *ompW*. Among the OMP genes regulated by OmpR,

repression of *ompD* together with *ompF*, a classic OmpR regulon, plays a major role in enhancement of antibiotic resistance in *S.* Enteritidis. It is noteworthy that the expression of *ompR* is increased in response to external β-lactams, which results in down-regulation of *ompD* and *ompF*. This response of EnvZ/OmpR probably provides benefits for survival of *S.* Enteritidis under the presence of antibiotics.

In conclusion, EnvZ/OmpR, which is activated by genetic mutation or specific environmental signals, potentially leads to phenotypic diversity of *S.* Enteritidis and enhances its antibiotic resistance by remodeling the OMP composition (Fig. IV-1).

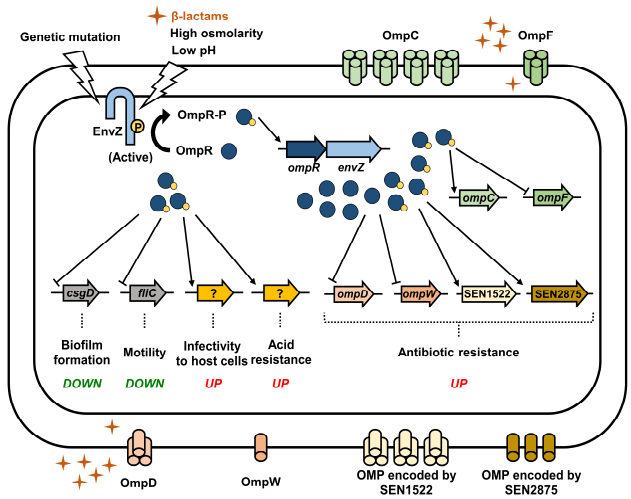

Figure IV-1. Phenotypic changes induced by the active state of EnvZ/OmpR in *S.* Enteritidis. The occurrence of genetic mutation or exposure to specific environmental signals often activates EnvZ/OmpR in *S.* Enteritidis, facilitating OmpR phosphorylation. Because *ompR* is positively autoregulated by OmpR-P, the cellular levels of OmpR as well as OmpR-P are increased by the activation of EnvZ/OmpR. Under the active state of EnvZ/OmpR, biofilm formation and motility of *S.* Enteritidis are decreased, but the infectivity to host cells and acid resistance are increased. Meanwhile, high cellular levels of OmpR and OmpR-P lead to compositional modulation of OMPs, resulting in the reduction in outer membrane permeability and thus enhancement of antibiotic resistance in *S.* Enteritidis.

References

Achtman, M., Wain, J., Weill, F. X., Nair, S., Zhou, Z. M., Sangal, V., Krauland, M. G., Hale, J. L., Harbottle, H., Uesbeck, A., Dougan, G., Harrison L. H., Brisse, S., & *S. enterica* MLST study group. 2012. Multilocus sequence typing as a replacement for serotyping in *Salmonella enterica*. *PLoS Pathog*, *8*(6).

Adler, M., Anjum, M., Andersson, D. I., & Sandegren, L. 2016. Combinations of mutations in *envZ*, *ftsI*, *mrdA*, *acrB* and *acrR* can cause high-level carbapenem resistance in *Escherichia coli*. *J Antimicrob Chemother*, *71*(5), 1188-1198.

Ahmad, I., Lamprokostopoulou, A., Le Guyon, S., Streck, E., Barthel, M., Peters, V., Hardt, WD., & Romling, U. 2011. Complex c-di-GMP signaling networks mediate transition between virulence properties and biofilm formation in *Salmonella enterica* serovar Typhimurium. *PLoS One*, *6*(12).

Aiba, H., & Mizuno, T. 1990. Phosphorylation of a bacterial activator protein, OmpR, by a protein kinase, EnvZ, stimulates the transcription of the *ompF* and *ompC* genes in *Escherichia coli*. *FEBS Lett*, *261*(1), 19-22.

Alvarez-Ordonez, A., Prieto, M., Bernardo, A., Hill, C., & Lopez, M. 2012. The acid tolerance response of *Salmonella* spp.: An adaptive strategy to survive in stressful environments prevailing in foods and the host. *Food Res Int*, *45*(2), 482-492.

Arber, W. 2000. Genetic variation: Molecular mechanisms and impact on microbial evolution. *FEMS Microbiol Rev*, *24*(1), 1-7.

Austin, J. W., Sanders, G., Kay, W. W., & Collinson, S. K. 1998. Thin aggregative fimbriae enhance *Salmonella enteritidis* biofilm formation. *FEMS Microbiol Lett*, *162*(2), 295-301.

Authority, E. F. S., Authority, E. F. S., & EFSA, C. D. P. C. 2018. The European Union summary report on trends and sources of zoonoses, zoonotic agents and food-borne outbreaks in 2017. *EFSA J*, *16*(12).

Bang, I. S., Audia, J. P., Park, Y. K., & Foster, J. W. 2002. Autoinduction of the *ompR* response regulator by acid shock and control of the *Salmonella enterica* acid tolerance response. *Mol Microbiol*, *44*(5), 1235-1250.

Bang, I. S., Kim, B. H., Foster, J. W., & Park, Y. K. 2000. OmpR regulates the stationary-phase acid tolerance response of *Salmonella enterica* serovar Typhimurium. *J Bacteriol*, *182*(8), 2245-2252.

Baumler, A. J., Tsolis, R. M., Ficht, T. A., & Adams, L. G. 1998. Evolution of host adaptation in *Salmonella enterica*. *Infect Immun*, *66*(10), 4579-4587.

Blair, J. M. A., Webber, M. A., Baylay, A. J., Ogbolu, D. O., & Piddock, L. J. V. 2015. Molecular mechanisms of antibiotic resistance. *Nat Rev Microbiol*, *13*(1), 42-51.

Blanc-Potard, A. B., & Groisman, E. A. 2021. How pathogens feel and overcome magnesium limitation when in host tissues. *Trends Microbiol*, *29*(2), 98-106.

Blondeau, J. M. 2004. Fluoroquinolones: Mechanism of action, classification, and development of resistance. *Surv Ophthalmol*, *49*, S73-S78.

Boyle, E. C., Brown, N. F., & Finlay, B. B. 2006. *Salmonella enterica* serovar Typhimurium effectors SopB, SopE, SopE2 and SipA disrupt tight junction structure and function. *Cell Microbiol*, *8*(12), 1946-1957.

Braden, C. R. 2006. *Salmonella enterica* serotype Enteritidis and eggs: A national epidemic in the United States. *Clin Infect Dis*, *43*(4), 512-517.

Bradford, M. M. 1976. A rapid and sensitive method for the quantitation of microgram quantities of protein utilizing the principle of protein-dye binding. *Anal Biochem*, *72*, 248-254.

Brenner, F. W., Villar, R. G., Angulo, F. J., Tauxe, R., & Swaminathan, B. 2000. *Salmonella* nomenclature. *J Clin Microbiol*, *38*(7), 2465-2467.

Cameron, A. D. S., & Dorman, C. J. 2012. A fundamental regulatory mechanism operating through OmpR and DNA topology controls expression of *Salmonella* pathogenicity islands SPI-1 and SPI-2. *PLoS Genet*, *8*(3).

Capra, E. J., & Laub, M. T. 2012. Evolution of two-component signal transduction systems. *Annu Rev Microbiol*, *66*, 325-347.

Carroll, R. K., Liao, X. B., Morgan, L. K., Cicirelli, E. M., Li, Y. H., Sheng, W. Y., Feng, X., & Kenney, L. J. 2009. Structural and functional analysis of the C-terminal DNA binding domain of the *Salmonella typhimurium* SPI-2 response regulator SsrB. *J Biol Chem*, *284*(18), 12008-12019.

Chakraborty, S., & Kenney, L. J. 2018. A new role of OmpR in acid and osmotic stress in *Salmonella* and *E. coli*. *Front Microbiol*, *9*.

Chakraborty, S., Mizusaki, H., & Kenney, L. J. 2015. A FRET-based DNA biosensor tracks OmpR-dependent acidification of *Salmonella* during macrophage infection. *PLoS Biol*, *13*(4).

Chakraborty, S., Winardhi, R. S., Morgan, L. K., Yan, J., & Kenney, L. J. 2017. Non-canonical activation of OmpR drives acid and osmotic stress responses in single bacterial cells. *Nat Commun*, *8*.

Chen, H. M., Wang, Y., Su, L. H., & Chiu, C. H. 2013. Nontyphoid *Salmonella* infection: Microbiology, clinical features, and antimicrobial therapy. *Pediatr Neonatol*, *54*(3), 147-152.

Choi, G., Jang, K. K., Lim, J. G., Lee, Z. W., Im, H., & Choi, S. H. 2020. The transcriptional regulator IscR integrates host-derived nitrosative stress and iron starvation in activation of the *vvhBA* operon in *Vibrio vulnificus*. *J Biol Chem*, *295*(16), 5350-5361.

Choi, G., Kim, D., Im, H., & Choi, S. H. 2021. A nitric oxide-responsive transcriptional regulator NsrR cooperates with Lrp and CRP to tightly control the *hmpA* gene in *Vibrio vulnificus*. *Front Microbiol*, *12*.

Choi, Y., & Chan, A. P. 2015. PROVEAN web server: a tool to predict the functional effect of amino acid substitutions and indels. *Bioinform*, *31*(16), 2745-2747.

CLSI. 2012. Methods for dilution antimicrobial susceptibility tests for bacteria that grow aerobically; approved standard ninth edition. *12*, 1-88.

Collery, M. M., Kuehne, S. A., McBride, S. M., Kelly, M. L., Monot, M., Cockayne, A., Dupuy, B., & Minton, N. P. 2017. What's a SNP between friends: The influence of single nucleotide polymorphisms on virulence and phenotypes of *Clostridium difficile* strain 630 and derivatives. *Virulence*, *8*(6), 767-781.

Croucher, N. J., Page, A. J., Connor, T. R., Delaney, A. J., Keane, J. A., Bentley, S. D., Parkhill, J., & Harris, S. R. 2015. Rapid phylogenetic analysis of large samples of recombinant bacterial whole genome sequences using Gubbins. *Nucleic Acids Res*, *43*(3), e15.

Datsenko, K. A., & Wanner, B. L. 2000. One-step inactivation of chromosomal genes in *Escherichia coli* K-12 using PCR products. *Proc Natl Acad Sci U S A*, *97*(12), 6640-6645.

De Vylder, J., Raspoet, R., Dewulf, J., Haesebrouck, F., Ducatelle, R., &

Van Immerseel, F. 2013. *Salmonella* Enteritidis is superior in egg white survival compared with other *Salmonella* serotypes. *Poult Sci*, *92*(3), 842-845.

Deiwick, J., Salcedo, S. P., Boucrot, E., Gilliland, S. M., Henry, T., Petermann, N., Waterman, S. R., Gorvel, JP., Holden, D. W., & Meresse, S. 2006. The translocated *Salmonella* effector proteins SseF and SseG interact and are required to establish an intracellular replication niche. *Infect Immun*, *74*(12), 6965-6972.

Delgado, J., Forst, S., Harlocker, S., & Inouye, M. 1993. Identification of a phosphorylation site and functional analysis of conserved aspartic acid residues of OmpR, a transcriptional activator for *ompF* and *ompC* in *Escherichia coli*. *Mol Microbiol*, *10*(5), 1037-1047.

Desai, S. K., & Kenney, L. J. 2017. To ~P or not to ~P? Non-canonical activation by two-component response regulators. *Mol Microbiol*, *103*(2), 203-213.

Desai, S. K., & Kenney, L. J. 2019. Switching lifestyles is an *in vivo* adaptive strategy of bacterial pathogens. *Front Cell Infect Microbiol*, *9*.

Desai, S. K., Winardhi, R. S., Periasamy, S., Dykas, M. M., Jie, Y., & Kenney, L. J. 2016. The horizontally-acquired response regulator SsrB drives a *Salmonella* lifestyle switch by relieving biofilm silencing. *Elife*, *5*.

Disney, M. D. 2012. Studying modification of aminoglycoside antibiotics by resistance-causing enzymes via microarray. *Carbohydrate Microarrays* (pp. 303-320). Humana Press.

Donnenberg, M. S., & Kaper, J. B. 1991. Construction of an *eae* deletion mutant of enteropathogenic *Escherichia coli* by using a positive-selection suicide vector. *Infect Immun*, *59*(12), 4310-4317.

Dorman, C. J., Chatfield, S., Higgins, C. F., Hayward, C., & Dougan, G. 1989. Characterization of porin and *ompR* mutants of a virulent strain of *Salmonella* Typhimurium: *ompR* mutants are attenuated *in vivo*. *Infect Immun*, *57*(7), 2136-2140.

Ellermeier, C. D., Ellermeier, J. R., & Slauch, J. M. 2005. HilD, HilC and RtsA constitute a feed forward loop that controls expression of the SPI1 type three secretion system regulator *hilA* in *Salmonella enterica* serovar Typhimurium. *Mol Microbiol*, *57*(3), 691-705.

European Food Safety Authority and European Centre for Disease

Prevention and Control (EFSA and ECDC) 2018. The European Union summary report on trends and sources of zoonoses, zoonotic agents and food-borne outbreaks in 2017. *EFSA J*, *16*(12), e05500.

Fabrega, A., & Vila, J. 2013. *Salmonella enterica* serovar Typhimurium skills to succeed in the host: Virulence and regulation. *Clin Microbiol Rev*, *26*(2), 308-341.

Feng, X. H., Oropeza, R., & Kenney, L. J. 2003. Dual regulation by phospho-OmpR of *ssrA/B* gene expression in *Salmonella* pathogenicity island 2. *Mol Microbiol*, *48*(4), 1131-1143.

Fernandes, M. M., Ivanova, K., Hoyo, J., Perez-Rafael, S., Francesko, A., & Tzanov, T. 2017. Nanotransformation of vancomycin overcomes the intrinsic resistance of Gram-negative bacteria. *ACS Appl Mater Interfaces*, *9*(17), 15022-15030.

Fernandez, L., Gooderham, W. J., Bains, M., McPhee, J. B., Wiegand, I., & Hancock, R. E. W. 2010. Adaptive resistance to the "last hope" antibiotics polymyxin B and colistin in *Pseudomonas aeruginosa* is mediated by the novel two-component regulatory system ParR-ParS. *Antimicrob Agents Chemother*, *54*(8), 3372-3382.

Fernandez, L., & Hancock, R. E. W. 2012. Adaptive and mutational resistance: Role of porins and efflux pumps in drug resistance. *Clin Microbiol Rev*, *25*(4), 661-681.

Fernandez, L., Jenssen, H., Bains, M., Wiegand, I., Gooderham, W. J., & Hancock, R. E. W. 2012. The two-component system CprRS senses cationic peptides and triggers adaptive resistance in *Pseudomonas aeruginosa* independently of ParRS. *Antimicrob Agents Chemother*, *56*(12), 6212-6222.

Flatman, P. W. 1991. Mechanisms of magnesium transport. *Annu Rev Physiol*, *53*, 259-271.

Flores, A. R., Jewell, B. E., Yelamanchili, D., Olsen, R. J., & Musser, J. M. 2015. A single amino acid replacement in the sensor kinase LiaS contributes to a carrier phenotype in group A *Streptococcus*. *Infect Immun*, *83*(11), 4237-4246.

Forst, S., Delgado, J., & Inouye, M. 1989. Phosphorylation of OmpR by the osmosensor EnvZ modulates expression of the *ompF* and *ompC* genes in *Escherichia coli*. *Proc Natl Acad Sci U S A*, *86*(16), 6052-6056.

French, G. L. 2010. The continuing crisis in antibiotic resistance. *Int J*

Antimicrob Agents, *36*, S3-S7.

Futoma-Koloch, B., Bugla-Ploskonska, G., Dudek, B., Dorotkiewicz-Jach, A., Drulis-Kawa, Z., & Gamian, A. 2019. Outer membrane proteins of *Salmonella* as potential markers of resistance to serum, antibiotics and biocides. *Curr Med Chem*, *26*(11), 1960-1978.

Gal-Mor, O., Boyle, E. C., & Grassl, G. A. 2014. Same species, different diseases: How and why typhoidal and non-typhoidal *Salmonella enterica* serovars differ. *Front Microbiol*, *5*, 391.

Gal-Mor, O., Gibson, D. L., Baluta, D., Vallance, B. A., & Finlay, B. B. 2008. A novel secretion pathway of *Salmonella enterica* acts as an antivirulence modulator during salmonellosis. *PLoS Pathog*, *4*(4).

Galan, J. E. 1996. Molecular genetic bases of *Salmonella* entry into host cells. *Mol Microbiol*, *20*(2), 263-271.

Gao, R., & Stock, A. M. 2009. Biological insights from structures of two-component proteins. *Ann Rev Microbiol*, *63*, 133-154.

Gerlach, R. G., & Hensel, M. 2007. *Salmonella* pathogenicity islands in host specificity, host pathogen-interactions, and antibiotics resistance of *Salmonella enterica*. *Berl Munch Tierarztl Wochenschr*, *120*(7-8), 317.

Gerstel, U., Kolb, A., & Romling, U. 2006. Regulatory components at the *csgD* promoter-additional roles for OmpR and integration host factor and role of the 5 ' untranslated region. *FEMS Microbiol Lett*, *261*(1), 109-117.

Gerstel, U., Park, C., & Romling, U. 2003. Complex regulation of *csgD* promoter activity by global regulatory proteins. *Mol Microbiol*, *49*(3), 639-654.

Gil, F., Ipinza, F., Fuentes, J., Pumeron, P., Villarreal, J. M., Aspee, A., Mora, G. C., Vasquez, C. C., Saavedra, C. 2007. The *ompW* (porin) gene mediates methyl viologen (paraquat) efflux in *Salmonella enterica* serovar Typhimurium. *Res Microbiol*, *158*(6), 529-536.

Gordon, M. A. 2008. *Salmonella* infections in immunocompromised adults. *J Infect*, *56*(6), 413-422.

Groisman, E. A. 2001. The pleiotropic two-component regulatory system PhoP-PhoQ. *J Bacteriol*, *183*(6), 1835-1842.

Groisman, E. A., Duprey, A., & Choi, J. 2021. How the PhoP/PhoQ system controls virulence and Mg^{2+} homeostasis: Lessons in signal transduction, pathogenesis, physiology, and evolution. *Microbiol Mol Biol Rev*, *85*(3),

e0017620.

Groisman, E. A., Hollands, K., Kriner, M. A., Lee, E. J., Park, S. Y., & Pontes, M. H. 2013. Bacterial Mg^{2+} homeostasis, transport, and virulence. *Annu Rev Genet, Vol 47*, *47*, 625-646.

Groisman, E. A., & Ochman, H. 1993. Cognate gene clusters govern invasion of host epithelial cells by *Salmonella typhimurium* and *Shigella flexneri*. *EMBO J*, *12*(10), 3779-3787.

Groisman, E. A., & Ochman, H. 1997. How *Salmonella* became a pathogen. *Trends Microbiol*, *5*(9), 343-349.

Gu, Y. F., Huang, L. L., Wu, C. R., Huang, J. H., Hao, H. H., Yuan, Z. H., & Cheng, G. Y. 2021. The evolution of fluoroquinolone resistance in *Salmonella* under exposure to sub-inhibitory concentration of enrofloxacin. *Int J Mol Sci*, *22*(22).

Hammar, M., Arnqvist, A., Bian, Z., Olsen, A., & Normark, S. 1995. Expression of two *csg* operons is required for production of fibronectin- and Congo red-binding curli polymers in *Escherichia coli* K-12. *Mol Microbiol*, *18*(4), 661-670.

Hammarlof, D. L., Kroger, C., Owen, S. V., Canals, R., Lacharme-Lora, L., Wenner, N., Schager, A. E., Wells, T. J., Henderson, I. R., Wigley, P., Hokamp, K., Feasey, N. A., Gordon, M. A., & Hinton, J. C. D. 2018. Role of a single noncoding nucleotide in the evolution of an epidemic African clade of *Salmonella*. *Proc Natl Acad Sci U S A*, *115*(11), E2614-E2623.

Head, C. G., Tardy, A., & Kenney, L. J. 1998. Relative binding affinities of OmpR and OmpR-phosphate at the *ompF* and *ompC* regulatory sites. *J Mol Biol*, *281*(5), 857-870.

Hecht, M., Bromberg, Y., & Rost, B. 2015. Better prediction of functional effects for sequence variants. *BMC Genomics*, *16*(8), 1-12.

Herrera, C. M., Crofts, A. A., Henderson, J. C., Pingali, S. C., Davies, B. W., & Trent, M. S. 2014. The *Vibrio cholerae* VprA-VprB two-component system controls virulence through endotoxin modification. *mBio*, *5*(6).

Hirai, K., Aoyama, H., Irikura, T., Iyobe, S., & Mitsuhashi, S. 1986. Differences in susceptibility to quinolones of outer membrane mutants of *Salmonella* Typhimurium and *Escherichia coli*. *Antimicrob Agents Chemother*, *29*(3), 535-538.

Horstmann, N., Saldana, M., Sahasrabhojane, P., Yao, H., Su, X. P., Thompson, E., Koller, A., & Shelburne, S. A. 2014. Dual-site phosphorylation of the control of virulence regulator impacts group A streptococcal global gene expression and pathogenesis. *PLoS Pathog, 10*(5).

Horstmann, N., Tran, C. N., Brumlow, C., DebRoy, S., Yao, H., Gonzalez, G. N., Makthal, N., Kumaraswami, M., & Shelburne, S. A. 2018. Phosphatase activity of the control of virulence sensor kinase CovS is critical for the pathogenesis of group A *streptococcus*. *PLoS Pathog, 14*(10).

Hu, W. S., Chen, H. W., Zhang, R. Y., Huang, C. Y., & Shen, C. F. 2011. The expression levels of outer membrane proteins STM1530 and OmpD, which are influenced by the CpxAR and BaeSR two-component systems, play important roles in the ceftriaxone resistance of *Salmonella enterica* serovar Typhimurium. *Antimicrob Agents Chemother, 55*(8), 3829-3837.

Hu, W. S., Li, PC., & Cheng, CY. 2005. Correlation between ceftriaxone resistance of *Salmonella enterica* serovar Typhimurium and expression of outer membrane proteins OmpW and Ail/OmpX-like protein, which are regulated by BaeR of a two-component system. *Antimicrob Agents Chemother, 49*(9), 3955-3958.

Hu, W. S., Lin, J. F., Lin, Y. H., & Chang, H. Y. 2009. Outer membrane protein STM3031 (Ail/OmpX-like protein) plays a key role in the ceftriaxone resistance of *Salmonella enterica* serovar Typhimurium. *Antimicrob Agents Chemother, 53*(8), 3248-3255.

Hwang, S. H., Im, H., & Choi, S. H. 2021. A master regulator BrpR coordinates the expression of multiple loci for robust biofilm and rugose colony development in *Vibrio vulnificus*. *Front Microbiol, 12*.

Ichikawa, M., Minami, M., Isaka, M., Tatsuno, I., & Hasegawa, T. 2011. Analysis of two-component sensor proteins involved in the response to acid stimuli in *Streptococcus pyogenes*. *Microbiol, 157*(11), 3187-3194.

Jaffe, A., Chabbert, Y. A., & Semonin, O. 1982. Role of porin proteins OmpF and OmpC in the permeation of beta-lactams. *Antimicrob Agents Chemother, 22*(6), 942-948.

Katz, L., & Baltz, R. H. 2016. Natural product discovery: Past, present, and future. *J Ind Microbiol Biotechnol, 43*(2-3), 155-176.

Kauffmann, F. 1966. The bacteriology of *Enterobacteriaceae*. Collected

studies of the author and his co-workers. *The bacteriology of Enterobacteriaceae. Collected studies of the author and his co-workers.*

Kelly, B. G., Vespermann, A., & Bolton, D. J. 2009. The role of horizontal gene transfer in the evolution of selected foodborne bacterial pathogens. *Food Chem Toxicol, 47*(5), 951-968.

Kim, S. M., Lee, D. H., & Choi, S. H. 2012. Evidence that the *Vibrio vulnificus* flagellar regulator FlhF is regulated by a quorum sensing master regulator SmcR. *Microbiol, 158*(8), 2017-2025.

Klumpp, J., & Fuchs, T. M. 2007. Identification of novel genes in genomic islands that contribute to *Salmonella typhimurium* replication in macrophages. *Microbiol, 153*(4), 1207-1220.

Ko, D., & Choi, S. H. 2021. Comparative genomics reveals an SNP potentially leading to phenotypic diversity of *Salmonella enterica* serovar Enteritidis. *Microb Genom, 7*(5).

Kumar, M., Dahiya, S., Sharma, P., Sharma, S., Singh, T. P., Kapil, A., & Kaur, P. 2015. Structure based *in silico* analysis of quinolone resistance in clinical isolates of *Salmonella* Typhi from India. *PLoS One, 10*(5).

Kurtz, S., Phillippy, A., Delcher, A. L., Smoot, M., Shumway, M., Antonescu, C., & Salzberg, S. L. 2004. Versatile and open software for comparing large genomes. *Genome Biol, 5*(2).

Lee, A. K., Detweiler, C. S., & Falkow, S. 2000. OmpR regulates the two-component system SsrA-SsrB in *Salmonella* pathogenicity island 2. *J Bacteriol, 182*(3), 771-781.

Lee, Z. W., Hwang, S. H., Choi, G., Jang, K. K., Lee, T. H., Chung, K. M., Kim, B. S., & Choi, S. H. 2020. A MARTX toxin *rtxA* gene is controlled by host environmental signals through a CRP-coordinated regulatory network in *Vibrio vulnificus*. *mBio, 11*(4).

Letunic, I., & Bork, P. 2016. Interactive tree of life (iTOL) v3: An online tool for the display and annotation of phylogenetic and other trees. *Nucleic Acids Res, 44*(W1), W242-W245.

Lieberman, T. D., Michel, J. B., Aingaran, M., Potter-Bynoe, G., Roux, D., Davis, M. R., Skurnik, D., Leiby, N., LiPuma, J. J., Goldberg, J. B., McAdam, A., J., Priebe, G. P., & Kishony, R. 2011. Parallel bacterial evolution within multiple patients identifies candidate pathogenicity genes. *Nat*

Genet, *43*(12), 1275-U1148.

Lim, J. G., Bang, Y. J., & Choi, S. H. 2014. Characterization of the *Vibrio vulnificus* 1-Cys peroxiredoxin Prx3 and regulation of its expression by the Fe-S cluster regulator IscR in response to oxidative stress and iron starvation. *J Biol Chem*, *289*(52), 36263-36274.

Lin, Y. H., Yang, T. C., & Hu, W. S. 2019. Characterization of *stm3030* and *stm3031* genes of *Salmonella enterica* serovar Typhimurium in relation to cephalosporin resistance. *J Microbiol Immun Infect*, *52*(2), 282-288.

Lushniak, B. D. 2014. Antibiotic resistance: A public health crisis. *Public Health Rep*, *129*(4), 314-316.

MacKenzie, K. D., Palmer, M. B., Koster, W. L., & White, A. P. 2017. Examining the link between biofilm formation and the ability of pathogenic *Salmonella* strains to colonize multiple host species. *Front Vet Sci*, *4*.

MacKenzie, K. D., Wang, Y., Musicha, P., Hansen, E. G., Palmer, M. B., Herman, D. J., Feasey, N. A., & White, A. P. 2019. Parallel evolution leading to impaired biofilm formation in invasive *Salmonella* strains. *PLoS Genet*, *15*(6), e1008233.

MacQueen, J. 1967. Some methods for classification and analysis of multivariate observations. In *Proceedings of the fifth Berkeley symposium on mathematical statistics and probability* (Vol. 1, No. 14, pp. 281-297).

Majowicz, S. E., Musto, J., Scallan, E., Angulo, F. J., Kirk, M., O'Brien, S. J., Jones, T. F., Fazil, A., & Hoekstra, R. M. 2010. The global burden of nontyphoidal *Salmonella* gastroenteritis. *Clin Infect Dis*, *50*(6), 882-889.

Masi, M., Pinet, E., & Pages, J. M. 2020. Complex response of the CpxAR two-component system to β-lactams on antibiotic resistance and envelope homeostasis in *Enterobacteriaceae*. *Antimicrob Agents Chemother*, *64*(6).

Masuda, N., Sakagawa, E., Ohya, S., Gotoh, N., Tsujimoto, H., & Nishino, T. 2000. Contribution of the MexX-MexY-OprM efflux system to intrinsic resistance in *Pseudomonas aeruginosa*. *Antimicrob Agents Chemother*, *44*(9), 2242-2246.

Medeiros, A. A., Obrien, T. F., Rosenberg, E. Y., & Nikaido, H. 1987. Loss of OmpC porin in a strain of *Salmonella* Typhimurium causes increased resistance to cephalosporins during therapy. *J Infect Dis*, *156*(5), 751-757.

Miao, E. A., Leaf, I. A., Treuting, P. M., Mao, D. P., Dors, M., Sarkar, A.,

Warren, S. E., Wewers, M. D., Aderem, A. 2010. Caspase-1-induced pyroptosis is an innate immune effector mechanism against intracellular bacteria. *Nat Immun*, *11*(12), 1136-U1194.

Mideros-Mora, C., Miguel-Romero, L., Felipe-Ruiz, A., Casino, P., & Marina, A. 2020. Revisiting the pH-gated conformational switch on the activities of HisKA-family histidine kinases. *Nat Commun*, *11*(1).

Mikheecheva, N. E., Zaychikova, M. V., Melerzanov, A. V., & Danilenko, V. N. 2017. A nonsynonymous SNP catalog of *Mycobacterium tuberculosis* virulence genes and its use for detecting new potentially virulent sublineages. *Genome Biol Evol*, *9*(4), 887-899.

Miller, J. H. 1972. Experiments in molecular genetics. *Cold Spring Harbor, NY*, Cold Spring Harbor Laboratory.

Mizuno, T. 1998. His-Asp phosphotransfer signal transduction. *J Biochem*, *123*(4), 555-563.

Mol, O., & Oudega, B. 1996. Molecular and structural aspects of fimbriae biosynthesis and assembly in *Escherichia coli*. *FEMS Microbiol Rev*, *19*(1), 25-52.

Munita, J. M., & Arias, C. A. 2016. Mechanisms of antibiotic resistance. *Microbiol Spectr*, *4*(2).

Neiger, M. R., Gonzalez, J. F., Gonzalez-Escobedo, G., Kuck, H., White, P., & Gunn, J. S. 2019. Pathoadaptive alteration of *Salmonella* biofilm formation in response to the gallbladder environment. *J Bacteriol*, *201*(14).

Norris, F. A., Wilson, M. P., Wallis, T. S., Galyov, E. E., & Majerus, P. W. 1998. SopB, a protein required for virulence of *Salmonella* Dublin, is an inositol phosphate phosphatase. *Proc Natl Acad Sci U S A*, *95*(24), 14057-14059.

Ohl, M. E., & Miller, S. I. 2001. *Salmonella*: A model for bacterial pathogenesis. *Annu Rev Med*, *52*, 259-274.

Ohno, H., & Hase, K. 2010. Glycoprotein 2 (GP2) Grabbing the $FimH^{+}$ bacteria into M cells for mucosal immunity. *Gut Microbes*, *1*(6), 407-410.

Page, A. J., Cummins, C. A., Hunt, M., Wong, V. K., Reuter, S., Holden, M. T. Fookes, M., Falush, D., Keane, J. A., & Parkhill, J. 2015. Roary: Rapid large-scale prokaryote pan genome analysis. *Bioinformatics*, *31*(22), 3691-3693.

Page, A. J., Taylor, B., Delaney, A. J., Soares, J., Seemann, T., Keane, J. A., & Harris, S. R. 2016. SNP-sites: rapid efficient extraction of SNPs from multi-FASTA alignments. *Microb Genom*, *2*(4).

Pages, J. M., James, C. E., & Winterhalter, M. 2008. The porin and the permeating antibiotic: A selective diffusion barrier in Gram-negative bacteria. *Nat Rev Microbiol*, *6*(12), 893-903.

Papp-Wallace, K. M., Nartea, M., Kehres, D. G., Porwollik, S., McClelland, M., Libby, S. J., Fang, F. C., & Maguire, M. E. 2008. The CorA Mg^{2+} channel is required for the virulence of *Salmonella enterica* serovar Typhimurium. *J Bacteriol*, *190*(19), 6517-6523.

Park, D. K., Lee, K. E., Baek, C. H., Kim, I. H., Kwon, J. H., Lee, W. K., Lee, K. H., Kim, B. S., Choi, S. H., & Kim, K. S. 2006. Cyclo(Phe-Pro) modulates the expression of *ompU* in *Vibrio* spp. *J Bacteriol*, *188*(6), 2214-2221.

Park, J. H., Jo, Y., Jang, S. Y., Kwon, H., Iriecurrency, Y., Parsek, M. R., Kim, M. H., & Choi, S. H. 2015. The *cabABC* operon essential for biofilm and rugose colony development in *Vibrio vulnificus*. *PLoS Pathog*, *11*(9).

Perez-Morales, D., Banda, M. M., Chau, N. Y. E., Salgado, H., Martinez-Flores, I., Ibarra, J. A., Ilyas, B., Coombes, B. K., & Bustamante, V. H. 2017. The transcriptional regulator SsrB is involved in a molecular switch controlling virulence lifestyles of *Salmonella*. *PLoS Pathog*, *13*(7).

Perkins, T. T., Davies, M. R., Klemm, E. J., Rowley, G., Wileman, T., James, K., Keane, T., Maskell, D., Hinton, J. C. D., Dougan, G., & Kingsley, R. A. 2013. ChIP-seq and transcriptome analysis of the OmpR regulon of *Salmonella enterica* serovars Typhi and Typhimurium reveals accessory genes implicated in host colonization. *Mol Microbiol*, *87*(3), 526-538.

Perkins, T. T., Kingsley, R. A., Fookes, M. C., Gardner, P. P., James, K. D., Yu, L., Assefa, S. A., He, M., Croucher, N. J., Pickard, D. J., Maskell, D. J., Parkhill, J., Choudhary, J., Thomson, N. R., & Dougan, G. 2009. A strand-specific RNA-Seq analysis of the transcriptome of the typhoid bacillus *Salmonella* Typhi. *PLoS Genet*, *5*(7), e1000569.

Philippe, N., Alcaraz, J. P., Coursange, E., Geiselmann, J., & Schneider, D. 2004. Improvement of pCVD442, a suicide plasmid for gene allele exchange in bacteria. *Plasmid*, *51*(3), 246-255.

Pontes, M. H., Lee, E. J., Choi, J., & Groisman, E. A. 2015. *Salmonella* promotes virulence by repressing cellulose production. *Proc Natl Acad Sci U S A, 112*(16), 5183-5188.

Poole, K. 2004. Resistance to β-lactam antibiotics. *Cell Mol Life Sci, 61*(17), 2200-2223.

Prehna, G., Li, Y. L., Stoynov, N., Okon, M., Vuckovic, M., McIntosh, L. P., Foster, L. J., Finlay, B. B., & Strynadka, N. C. J. 2012. The zinc regulated antivirulence pathway of *Salmonella* is a multiprotein immunoglobulin adhesion system. *J Biol Chem, 287*(39), 32324-32337.

Prigent-Combaret, C., Brombacher, E., Vidal, O., Ambert, A., Lejeune, P., Landini, P., & Dorel, C. 2001. Complex regulatory network controls initial adhesion and biofilm formation in *Escherichia coli* via regulation of the *csgD* gene. *J Bacteriol, 183*(24), 7213-7223.

Quinn, H. J., Cameron, A. D. S., & Dorman, C. J. 2014. Bacterial regulon evolution: Distinct responses and roles for the identical OmpR proteins of *Salmonella* Typhimurium and *Escherichia coli* in the acid stress response. *PLoS Genet, 10*(3).

Recht, M. I., & Puglisi, J. D. 2001. Aminoglycoside resistance with homogeneous and heterogeneous populations of antibiotic-resistant ribosomes. *Antimicrob Agents Chemother, 45*(9), 2414-2419.

Rehman, T., Yin, L. Z., Latif, M. B., Chen, J. H., Wang, K. Y., Geng, Y., Huang, X., Abaidullah, M., Guo, H., & Ouyang, P. 2019. Adhesive mechanism of different *Salmonella* fimbrial adhesins. *Microb Pathog, 137*.

Richter, M., & Rossello-Mora, R. 2009. Shifting the genomic gold standard for the prokaryotic species definition. *Proc Natl Acad Sci U S A, 106*(45), 19126-19131.

Romling, U. 2005. Characterization of the rdar morphotype, a multicellular behaviour in Enterobacteriaceae. *Cell Mol Life Sci, 62*(11), 1234-1246.

Romling, U., Rohde, M., Olsen, A., Normark, S., & Reinkoster, J. 2000. AgfD, the checkpoint of multicellular and aggregative behaviour in *Salmonella typhimurium* regulates at least two independent pathways. *Mol Microbiol, 36*(1), 10-23.

Rule, R., Mbelle, N., Sekyere, J. O., Kock, M., Hoosen, A., & Said, M. 2019. A rare case of colistin-resistant *Salmonella* Enteritidis meningitis in an HIV-

seropositive patient. *BMC Infect Dis*, *19*(1).

Scaltriti, E., Sassera, D., Comandatore, F., Morganti, M., Mandalari, C., Gaiarsa, S., Bandi, C., Zehender, G., Bolzoni, L., Casadei, G., & Pongolini, S. 2015. Differential single nucleotide polymorphism-based analysis of an outbreak caused by *Salmonella enterica* Serovar Manhattan reveals epidemiological details missed by standard pulsed-field gel electrophoresis. *J Clin Microbiol*, *53*(4), 1227-1238.

Seemann, T. 2014. Prokka: Rapid prokaryotic genome annotation. *Bioinformatics*, *30*(14), 2068-2069.

Serra, D. O., Richter, A. M., & Hengge, R. 2013. Cellulose as an architectural element in spatially structured *Escherichia coli* biofilms. *J Bacteriol*, *195*(24), 5540-5554.

Shea, J. E., Hensel, M., Gleeson, C., & Holden, D. W. 1996. Identification of a virulence locus encoding a second type III secretion system in *Salmonella typhimurium*. *Proc Natl Acad Sci U S A*, *93*(6), 2593-2597.

Sher, A. A., Mustafa, B. E., Grady, S. C., Gardiner, J. C., & Saeed, A. M. 2021. Outbreaks of foodborne *Salmonella enteritidis* in the United States between 1990 and 2015: An analysis of epidemiological and spatial-temporal trends. *International J Infect Dis*, *105*.

Sim, N. L., Kumar, P., Hu, J., Henikoff, S., Schneider, G., & Ng, P. C. 2012. SIFT web server: predicting effects of amino acid substitutions on proteins. *Nucleic Acids Res*, *40*(W1), W452-W457.

Simon, R., Priefer, U., & Puhler, A. 1983. A broad host range mobilization system for *in vivo* genetic engineering: Transposon mutagenesis in Gram-negative bacteria. *Biotechnology*, *1*(9), 784-791.

Slauch, J. M., Garrett, S., Jackson, D. E., & Silhavy, T. J. 1988. EnvZ functions through OmpR to control porin gene expression in *Escherichia coli* K-12. *J Bacteriol*, *170*(1), 439-441.

Snavely, M. D., Gravina, S. A., Cheung, T. T., Miller, C. G., & Maguire, M. E. 1991. Magnesium transport in *Salmonella typhimurium*. Regulation of *mgtA* and *mgtB* expression. *J Biol Chem*, *266*(2), 824-829.

Sokurenko, E. V., Hasty, D. L., & Dykhuizen, D. E. 1999. Pathoadaptive mutations: Gene loss and variation in bacterial pathogens. *Trends Microbiol*, *7*(5), 191-195.

Solano, C., Garcia, B., Valle, J., Berasain, C., Ghigo, J. M., Gamazo, C., & Lasa, I. 2002. Genetic analysis of *Salmonella enteritidis* biofilm formation: Critical role of cellulose. *Mol Microbiol*, *43*(3), 793-808.

Stabler, R. A., He, M., Dawson, L., Martin, M., Valiente, E., Corton, C., Lawley, T. D., Sebaihia, M., Quail, M. A., Rose, G., Gerding, D. N., Gibert, M., Popoff, M. R., Parkhill, J., Dougan, G., & Wren, B. W. 2009. Comparative genome and phenotypic analysis of *Clostridium difficile* 027 strains provides insight into the evolution of a hypervirulent bacterium. *Genome Biol*, *10*(9).

Stamatakis, A. 2006. RAxML-VI-HPC: Maximum likelihood-based phylogenetic analyses with thousands of taxa and mixed models. *Bioinformatics*, *22*(21), 2688-2690.

Stanaway, J. D., Reiner, R. C., Blacker, B. F., Goldberg, E. M., Khalil, I. A., Troeger, C. E., . . . Paratyphoid, G. T. 2019. The global burden of typhoid and paratyphoid fevers: A systematic analysis for the Global Burden of Disease Study 2017. *Lancet Infect Dis*, *19*(4), 369-381.

Steele-Mortimer, O. 2008. The *Salmonella*-containing vacuole - moving with the times. *Curr Opin Microbiol*, *11*(1), 38-45.

Theoret, J. R., Cooper, K. K., Zekarias, B., Roland, K. L., Law, B. F., Curtiss, R., & Joens, L. A. 2012. The *Campylobacter jejuni* Dps homologue is important for *in vitro* biofilm formation and cecal colonization of poultry and may serve as a protective antigen for vaccination. *Clin Vaccine Immunol*, *19*(9), 1426-1431.

Thomson, N. R., Clayton, D. J., Windhorst, D., Vernikos, G., Davidson, S., Churcher, C., Quail, M. A., Stevens, M., Jones, M. A., Watson, M., Barron, A., . . . & Parkhill, J. 2008. Comparative genome analysis of *Salmonella* Enteritidis PT4 and *Salmonella* Gallinarum 287/91 provides insights into evolutionary and host adaptation pathways. *Genome Res*, *18*(10), 1624-1637.

Tomomori, C., Tanaka, T., Dutta, R., Park, H. Y., Saha, S. K., Zhu, Y., Ishima, R., Liu, D., Tong, K. I., Kurokawa, H., Qian, H., Inouye, M., & Ikura, M. 1999. Solution structure of the homodimeric core domain of *Escherichia coli* histidine kinase EnvZ. *Nat Struct Biol*, *6*(8), 729-734.

Tsui, P., Huang, L., & Freundlich, M. 1991. Integration host factor binds specifically to multiple sites in the *ompB* promoter of *Escherichia coli* and

inhibits transcription. *J Bacteriol*, *173*(18), 5800-5807.

Tukel, C., Nishimori, J. H., Wilson, R. P., Winter, M. G., Keestra, A. M., van Putten, J. P. M., & Baumler, A. J. 2010. Toll-like receptors 1 and 2 cooperatively mediate immune responses to curli, a common amyloid from enterobacterial biofilms. *Cell Microbiol*, *12*(10), 1495-1505.

Uchiya, K., Barbieri, M. A., Funato, K., Shah, A. H., Stahl, P. D., & Groisman, E. A. 1999. A *Salmonella* virulence protein that inhibits cellular trafficking. *EMBO J*, *18*(14), 3924-3933.

Vergalli, J., Bodrenko, I. V., Masi, M., Moynie, L., Acosta-Gutierrez, S., Naismith, J. H., Davin-Regli, A., Ceccarelli, M., Berg, B., Winterhalter, M., & Pages, J. M. 2020. Porins and small-molecule translocation across the outer membrane of Gram-negative bacteria. *Nat Rev Microbiol*, *18*(3), 164-176.

Vescovi, E. G., Soncini, F. C., & Groisman, E. A. 1996. Mg^{2+} as an extracellular signal: Environmental regulation of *Salmonella* virulence. *Cell*, *84*(1), 165-174.

Wall, D. M., Nadeau, W. J., Pazos, M. A., Shi, H. N., Galyov, E. E., & McCormick, B. A. 2007. Identification of the *Salmonella enterica* serotype Typhimurium SipA domain responsible for inducing neutrophil recruitment across the intestinal epithelium. *Cell Microbiol*, *9*(9), 2299-2313.

Wang, L. C., Morgan, L. K., Godakumbura, P., Kenney, L. J., & Anand, G. S. 2012. The inner membrane histidine kinase EnvZ senses osmolality via helix-coil transitions in the cytoplasm. *EMBO J*, *31*(11), 2648-2659.

White, A. P., Gibson, D. L., Grassl, G. A., Kay, W. W., Finlay, B. B., Vallance, B. A., & Surette, M. G. 2008. Aggregation via the red, dry, and rough morphotype is not a virulence adaptation in *Salmonella enterica* serovar Typhimurium. *Infect Immun*, *76*(3), 1048-1058.

Winter, S. E., Winter, M. G., Godinez, I., Yang, H. J., Russmann, H., Andrews-Polymenis, H. L., & Baumler, A. J. 2010. A rapid change in virulence gene expression during the transition from the intestinal lumen into tissue promotes systemic dissemination of *Salmonella*. *PLoS Pathog*, *6*(8).

Worley, M. J., Ching, K. H. L., & Heffron, F. 2000. *Salmonella* SsrB activates a global regulon of horizontally acquired genes. *Mol Microbiol*, *36*(3), 749-761.

Xu, S. A., Zou, X., Sheng, X. M., Zhang, H. F., Mao, L. X., Du, H., Xu, H., & Huang, X. X. 2010. Expression of *fljB:z66* on a linear plasmid of *Salmonella*

enterica serovar Typhi is dependent on FliA and FlhDC and regulated by OmpR. *Brazilian J Microbiol*, *41*(3), 729-740.

Yang, L., Jelsbak, L., Marvig, R. L., Damkiaer, S., Workman, C. T., Rau, M. H., Hansen, S. K., Folkesson, A., Johansen, H. K., Ciofu, O., Hoiby, N., Sommer, M. O. A., & Molin, S. 2011. Evolutionary dynamics of bacteria in a human host environment. *Proc Natl Acad Sci U S A*, *108*(18), 7481-7486.

Yoshida, C. E., Kruczkiewicz, P., Laing, C. R., Lingohr, E. J., Gannon, V. P. J., Nash, J. H. E., & Taboada, E. N. 2016. The *Salmonella in silico* typing resource (SISTR): An open web-accessible tool for rapidly typing and subtyping draft *Salmonella* genome assemblies. *PLoS One*, *11*(1).

Young, M. D., Wakefield, M. J., Smyth, G. K., & Oshlack, A. 2010. Gene ontology analysis for RNA-seq: Accounting for selection bias. *Genome Biol*, *11*(2).

Yuan, J., Jin, F., Glatter, T., & Sourjik, V. 2017. Osmosensing by the bacterial PhoQ/PhoP two-component system. *Proc Natl Acad Sci U S A*, *114*(50), E10792-E10798.

Yuk, H. G., & Schneider, K. R. 2006. Adaptation of *Salmonella* spp. in juice stored under refrigerated and room temperature enhances acid resistance to simulated gastric fluid. *Food Microbiol*, *23*(7), 694-700.

국문초록

병원성 박테리아는 감염 주기 동안 다양한 환경 조건을 경험한다. 특정 환경에서 자연적으로 발생하는 유전적 돌연변이는 종종 박테리아의 생존 및 병원성을 향상시킨다. 본 연구는 식중독균인 살모넬라 엔테리티디스균이 갖고 있는 EnvZ/OmpR two-component system 의 감지단백질을 암호화하는 *envZ* 유전자에 발생한 특이적인 돌연변이의 기능을 밝혔다. 살모넬라 엔테리티디스균의 계통발생학적 분석을 통해 국내에서 분리된 FORC_075 와 FORC_078 을 포함하여 8 개의 균주들의 유전체 서열이 거의 동일하다는 것을 확인하였다. 하지만, FORC_075 의 생물막 및 적색의 건조하고 거친 (RDAR) 콜로니 형성 능력은 매우 손상되어, 8 개 균주 간에 표현형 차이가 발생하였다. 비교 유전체 분석을 통해 FORC_075 에만 발생한 SNP 중 하나가 *envZ* 유전자에 발생했다는 것을 확인하였다. 이 SNP 는 FORC_078 을 포함한 다른 균주가 갖고 있는 EnvZ 의 Pro248 을 FORC_075 가 갖고 있는 EnvZ 의 Leu248 로 치환시켰다. FORC_075 와 FORC_078 균주 사이의 *envZ* 유전자를 교환하여, *envZ* 유전자에 발생한 SNP 가 살모넬라 엔테리티디스균의 생물막 및 RDAR 콜로니 형성 능력에 중요한 역할을 한다는 것을 밝혔다. 생화학적 분석을 통해, *envZ* 유전자의 SNP 는 살모넬라 엔테리티디스균 내의 OmpR 인산화 수준을 증가시키며, OmpR 의 하위 유전자들의 발현 또한 변화시킨다는 것을 확인하였다.

표현형 분석을 통해 *envZ* 유전자의 SNP 는 살모넬라 엔테리티디스균의 운동성은 감소시키지만 인간 상피 세포와 쥐 대식 세포에 대한 부착과 침투 능력을 증가시키고 산 스트레스에 대한 생존력 또한 향상시킨다는 것을 확인하였다. 이러한 결과는 *envZ* 유전자에 자발적으로 발생한 SNP 가 살모넬라 엔테리티디스균의 표현형적 다양성에 기여하며 잠재적으로 생존 및 병원성을 향상시킬 수 있음을 시사한다. 한편, EnvZ/OmpR 은 작은 친수성 항생제의 주요 경로인 외막포린(OMP)인 OmpC 와 OmpF 의 발현을 조절한다는 것 외에는 항생제 내성에 대한 역할이 거의 알려져 있지 않다. 항생제 내성에 대한 EnvZ/OmpR 의 기능을 확인하기 위하여, 서로 다른 OmpR 인산화 수준을 보이는 두 개의 돌연변이 균주를 개발하였다. 높은 인산화 수준을 보이는 균주는 활성화된 EnvZ/OmpR 상태이며, 낮은 인산화 수준을 보이는 균주는 비활성화된 EnvZ/OmpR 상태를 의미한다. 흥미롭게도, 활성화된 EnvZ/OmpR 은 살모넬라 엔테리티디스균의 항생제 내성, 특히 베타-락탐계열 항생제에 대한 내성을 증가시켰다. 전사체 분석을 통해, 활성화된 EnvZ/OmpR 은 *ompC* 와 *ompF* 외에 SEN1522, SEN2875, *ompD*, *ompW* 와 같은 다양한 OMP 유전자들의 발현을 조절한다는 것을 새롭게 밝혔다. 생화학적 분석을 통해 OmpR 은 각 유전자의 상부에 직접 결합하여 SEN1522 와 SEN2875 의 발현을 활성화시키고 *ompD* 와 *ompW* 의 발현은 억제하여 OMP 조성을 조절한다는 것을 밝혔다. 특이적으로, 활성화된 EnvZ/OmpR 에 의해 세포 내 OmpR 수준이

증가하였을 때에만 4 개의 OMP 유전자들의 발현이 조절되었고, *ompD* 와 *ompW* 의 발현 억제는 OmpR 의 인산화 여부에 의존하지 않았다. 표현형 분석을 통해 OMP 유전자들 중 *ompD* 와 *ompF* 의 발현 감소가 EnvZ/OmpR 에 의해 매개되는 베타-락탐계열 항생제에 대한 내성을 결정한다는 것을 확인하였다. 놀랍게도 EnvZ/OmpR 은 외부 환경의 베타-락탐계열 항생제에 특이적으로 반응하여 살모넬라 엔테리티디스균의 생존을 향상시켰다. 이러한 결과는 EnvZ/OmpR 이 베타-락탐계열 항생제에 반응하여 OMP 조성을 조절하고 살모넬라 엔테리티디스균의 항생제 내성에 기여한다는 것을 시사한다. 결론적으로, 본 연구는 살모넬라 엔테리티디스균의 표현형적 다양성을 부여하는 *envZ* 유전자에 발생한 특이적인 유전적 변이와 활성화된 EnvZ/OmpR 이 항생제 내성에 기여하는 기작을 밝혔다.

핵심어: 살모넬라 엔테리티디스, EnvZ/OmpR two-component system, SNP, 표현형적 다양성, 병원성, 항생제 내성

학번: 2019-36715